TOLUENE METHYLATION WITH METHANOL OVER BI-POROUS ACIDIC AND BASIC ZEOLITE CATALYSTS: SYNTHESIS, CHARACTERIZATION AND KINETIC MODELING

BY

ALABI WAHAB OLAIYA

A Thesis Presented to the

DEANSHIP OF GRADUATE STUDIES

KING FAHD UNIVERSITY OF PETROLEUM & MINERALS

DHAHRAN, SAUDI ARABIA

In Partial Fulfillment of the
Requirements for the Degree of

MASTER OF SCIENCE

In

CHEMICAL ENGINEERING

MAY 2012

KING FAHD UNIVERSITY OF PETROLEUM & MINERALS

DHAHRAN 31261, SAUDI ARABIA

DEANSHIP OF GRADUATE STUDIES

This thesis, written by **ALABI WAHAB OLAIYA (g201002080)** under the direction of his thesis advisor and approved by his thesis committee, has been presented to and accepted by the Dean of Graduate Studies, in partial fulfillment of the requirements for the degree of **MASTER OF SCIENCE IN CHEMICAL ENGINEERING.**

Thesis Committee

27/5/12

Dr. Sulaiman .Alkhattaf (Advisor)

27/5/12

Dr. Abdullahi Alshammari (Member)

26/5/12

Dr. Nadhir A. H. Al Baghli (Member)

Dr. Usamah A. Al-Mubaiyedh
Department Chairman

Dr. Salam A. Zummo
Dean of Graduate Studies

3/6/12

Date

DEDICATION

This work is dedicated to Almighty ALLAH the most knowledgeable.

To Prophet Muhammad (saw) the light to the path of knowledge.

To my Sweetheart (my darling MUM) the first person to impact knowledge unto me.

To the Queen of my heart (Miss Oloyede Khairat) who taught me how to love.

To my Blood siblings (Fatai, Aminat and Habibat) for making me appreciate the value of knowledge and for taking care of my Mum through my days of acquiring knowledge.

To the Entire member of Alabi Family, Grand Children inclusive, without you, am just and entity.

To the entire person I had learned from, thanks for the patience in impacting me with knowledge.

To my deceased sister (Ashyaht), sorry for my absence during the last days of your life.

To my Lovely niece and nephew (HALEEMAH AND MALEEK), I love you and I will always do.

Lastly, to my unborn Children, I can't wait to see you, and I promise to love you and show you the affection and protection I got from the best Mum in the world (ALHAJA RUKAYAT AWERO).

ACKNOWLEDGEMENT

First and foremost I am grateful to Allah (SWT), the Lord of the worlds, for giving me life to accomplish this far. To Him belongs all praise in the Heavens and on Earth.

I am heartily grateful to my supervisor, Dr. Sulaiman Al-Khattaf, whose encouragement, guidance and support from the initial to the final level enabled me to develop an understanding of the subject. I would like to thank other members of my committee, Dr. Nahdir Al-Bagli and Dr. Abdullah Al-Shammari for their numerous contributions at all levels of the research project

I would be ungrateful not to mention Dr. A.Aitani and Dr. Nabil Al-Yassir for their numerous contributions of their expertise and assistance provided towards the completion of research project.

I thank Dr. Tope.B and Dr. Jermy for putting me through the catalysts synthesis for both the basic and acidic zeolites catalysts, respectively. For your patience and tolerance shown towards me, you are the best team I ever worked with. I would like to thank Mr. Mariano Gica who greatly helped out on the experimental work during the kinetic study.

To my Lovely Mum, Sorry I had to leave you for this long, but your thought is always with me and your place in my heart still remain as it was. I love you mum.

Fatai,Ameenat and Habibat,am glad I have you all, I don't know who could have understand me better in this world after you, I love you and I will always do.

Oloyede Khairat Adejoke,Hnm,am short of words, I will forever appreciate your patience towards me, even thou am still not perfect ,at least am improving. I doubt if any lady can cope with a troublesome guy like me. I love you and I will always do, you re-

define the word called love for me tanks so much. To the Oloyedes Family (ALHAJA SHIFAU AND ALHAJI SABIT), thanks for given birth to my queen.

Shina, Siraj, Hafeez, Hameed, Ibraheem, you are missed and I appreciate your support, you are the best friends one can ever have.

To Atanda Luqman andAdewunmi Ahmad, thanks for the support you gave towards the completion of my M.Sc Programme and Thesis.Its only ALLAH that can thank you enough.

My special appreciation goes to Emeritus Professor Hattori,I doubt if I can ever meet an industrious person like you. I will be eternally grateful for all you taught me.

I also want to offer my regards and appreciation to all of those who supported me in any respect during the completion of the project.

In conclusion, I recognize that this research would not have been possible without the financial assistance of KACST, the Center for Refining and Petrochemicals, King Fahd University ofPetroleum & Minerals Graduate Studies (Graduate Research Assistantship), and the Department of Chemical Engineering.

TABLE OF CONTENTS

LIST OF TABLES

LIST OF FIGURES

THESIS ABSTRACT

Name: **ALABI WAHAB OLAIYA**

Title of Study: **TOLUENE METHYLATION OVER BI-POROUS ACIDIC AND BASIC ZEOLITES: SYNTHESIS, CHARACTERIZATION AND KINETIC MODELING.**

Degree: **MASTER OF SCIENCE**

Major Field: **CHEMICAL ENGINEERING**

Date of Degree: **May, 2012.**

Toluene methylation with methanol was carried out over different bi-porous acidic composite HZSM-5/Almcm41 (ZM1, ZM2 and ZM3) and CsX modified basic catalysts. The porosity of the catalysts was adjusted through different degree of ZSM-5 dissolution via the top down approach. The textural properties of the composite catalysts were probed through various characterization techniques. The activity of the catalysts were compared with the parent ZSM-5 and MCM-41 with respect to toluene methylation and toluene disproportionation at different toluene to methanol molar feed ratios (6:1,3:1,1:1,1:3 and 1:6).

The meso porous catalysts(ZM3 and AlMCM-41) were less active, whereas ZM2 with 47% meso content showed the best catalytic activity with the highest mixed xylenes production and lowest toluene disproportion(measure through benzene formation) at all the molar feed ratio.

Kinetic study was carried out on ZM2, MOR/ZSM5 (composite mono porous) and HZSM-5 in a fluidized reactor at different temperatures and reaction time. Simplified power model was

developed to account for toluene conversion (methylation and disproportionation) and catalyst deactivation. The activation energy, reaction rate constant and catalyst deactivation were all estimated through the kinetic modeling.

For the basic catalyst, CsX was synthesized through ion exchange method, its basicity was increased by loading more Cs_2O and $ZrBO_3$ was also added to it (CsX) through mechanical mixing. The promoting effects of these additives were studied for side-chain methylation of toluene to styrene at different toluene to methanol molar feed ratio.$ZrBO_3$/CsX increases both toluene conversion and styrene selectivity while Cs_2O/CsX increases toluene conversion and reduces styrene selectivity.

THESIS ABSTRACT (ARABIC)

الملخص البحث

الاسم: ألابي وهاب أوليا

عنوان الدراسة: ألكلة التولوين مع الميثانول على حفازات زيولايتية حمضية ثنائية المسام وقاعدية: التحضير والتوصيف والنمذجة الحركية

الدرجة: الماجستير في العلوم

التخصص: هندسة كيميائية

تاريخ الدرجة: رجب 1433هـ (مايو 2012م)

أجريت تجارب ألكلة التولوين مع الميثانول باستخدام حفازات حمضية ثنائية المسام من النوع **HZSM-5/AlMCM41** (**ZM1**، **ZM2** و**ZM3**) وحفاز **CsX** القاعدي المعدل. ولقد تم تعديل مسامية الحفازات بدرجات مختلفة من انحلال **ZSM-5** باتباع طريقة من الأعلى إلى الأسفل. وتم تحديد الخواص التركيبية للحفازات بواسطة عدة تقنيات توصيف مختلفة. كما جريت مقارنة لنشاط الحفازات مع حفاز **ZSM-5** الأساسي و**MCM-41** بالنسبة لتفاعل ألكلة **(methylation)** التولوين وتفاعل عدم تناسبية (**disproportionation)** التولوين عند معدلات لقيم مختلفة من التولوين والميثانول: **(6:1; 3:1; 1:1; 1:3; 6:1).**

وأظهرت النتائج أن الحفازات ذات المسامات الكبيرة (**ZM3** و**AlMCM-41**) كانت الأقل من ناحية النشاط الحفزي، في حين أظهر حفاز **ZM2** ذات محتوى 47٪ من المسامات الكبيرة أفضل نشاط حفزي لإنتاج مزيج الزايلين وأدنى تفاعل عدم تناسبية التولوين (تم قياسه من خلال تشكل البنزين) عند جميع معدلات اللقيم.

وأجريت دراسة حركية التفاعل باستخدام حفازات **MOR/ZSM5** و**ZM2** (أحادي مركب المسامية) و**HZSM-5** في مفاعل مميع عند درجات حرارة وزمن تفاعلي مختلف. وتم تطوير نموذج حركي مبسط لحساب تحويل التولوين (تفاعلات الألكلة وعدم التناسبية) وفقدان نشاط الحفاز. وتم تقدير طاقة التنشيط الحفزي وثابت معدل التفاعل وفقدان نشاط الحفاز من خلال نمذجة حركية التفاعل.

وبالنسبة للحفاز القاعدي، فقد تم تحضير **CsX** بطريقة التبادل الأيوني وزيادة قاعديته بواسطة زيادة تحميل Cs_2O واضافة $ZrBO_3$ الى (**CsX**) من خلال الخلط الميكانيكي. وتمت دراسة التأثيرات الايجابية لهذه الاضافات في تفاعل ألكلة السلسلة الجانبية للتولوين إلى الستايرين عند معدلات مختلفة من لقيم

التولوين والميثانول. وأظهرت النتائج أن حفاز **$ZrBO_3$/CsX** يزيد كلاً من تحويل التولوين وانتقائية الستايرين بينما يزيد حفاز **Cs_2O/CsX** من تحويل التولوين ويقلل من انتقائية الستايرين.

CHAPTER ONE

INTRODUCTION

1.1 BACKGROUND INFORMATION ON TOLUENE METHYLATION

Toluene methylation is the addition of methyl to toluene to give xylenes as major product (using acidic catalyst), or styrene and ethyl benzene (using basic catalyst). Irrespective of the catalyst used, the products of toluene methylation are of great importance to the petrochemical industry.

Xylenes are aromatic compounds in which the two hydrogen atoms from the benzene ring are replaced with methyl groups. Xylenes are clear, colorless, sweet-smelling solution of three aromatic hydrocarbon isomers produced from crude oil through a process called reforming. Xylene consists of three distinct isomers: para-xylene, ortho-xylene and meta-xylene. As seen in Fig 1.1. the *ortho-*, *meta-*, and *para-* prefixes refer to which carbon atoms on the benzene ring the two methyl groups are attached [1].

The para-xylene is the most important isomer of xylenes and today's market for *para*-xylene is predominately directed towards the production of a variety of fibers, films, and resins. *para*-xylene is a key intermediate in the synthesis of purified tetraphthalic acid (PTA) and dimethyl terephthalate (DMT), both of which are used in the production of industrial plastics and polyesters. Specifically, PTA is used in the production of

polyethylene terephthalate (PET) bottle resins, a compound which is one of the most important polymers in the world [2]. Relatively smaller amounts of *para*-xylene are used as a solvent.

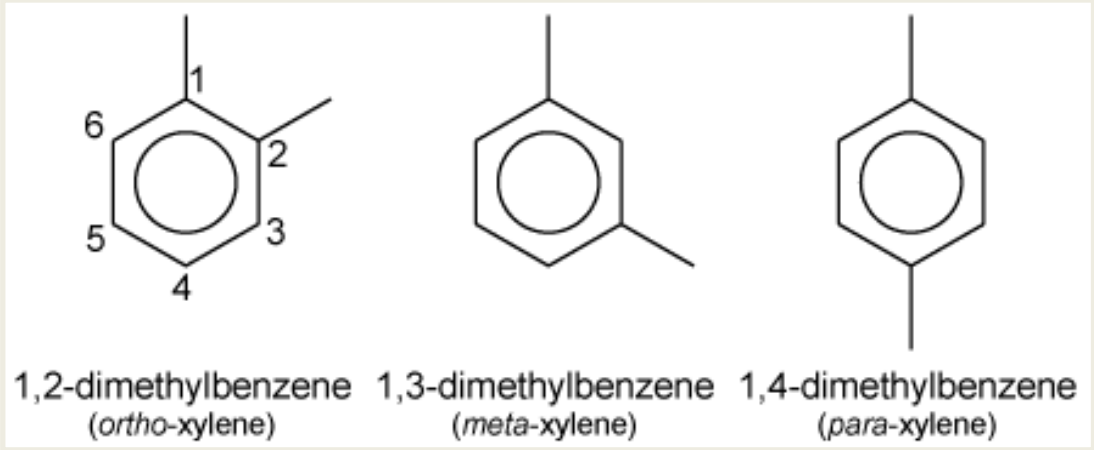

Fig 1.1: Isomers of xylene [1]

The majority of ortho-xylene is produced to make phthalic anhydride, an organic compound and plasticizer used to manufacture flexible polyvinyl chloride (PVC).The next most common use of ortho xylene is in the production of unsaturated polyester resins, thermosetting compounds that are molded as liquids and permanently cured under heat. The primary commercial application of these resins is to make fiberglass materials for the construction and marine industries [3].

Meta- xylene is used for the production of isophthalic acid (use for producing unsaturated polyester resins), methyl benzoate, isophthaloyl nitrile, and also can be used as raw material of pharmaceutical, dye, spice and color film purity.

Most of the products of xylene isomers have great benefits to our existence and they can be recycled. These products range from clothing materials, drinking bottles and medical applications.

The global demand for mixed xylenes has grown sharply over the last decade. The global demand in 2000 was 20.9 million tons. Global xylene capacity increased to 31.5 million tons in 2009. Much of the increase in demand for xylene came from the Asia Pacific region, and the same trend is expected to continue in the near future. Asia Pacific is expected to account for 81.5% of the global xylene demand in 2020. The global demand for xylene will grow and reach to 70.5 million tons in 2020 [4].Fig 1.2 shows the global demand for xylenes.While the global demand for para-xylene has been steadily increasing since 1999 and this growth is expected to continue over the next five to ten years (Figure 1.3). According to a 2007 market report performed by Yarns and Fibers Exchange, a textile market intelligence service, the global capacity of *para*-xylene was approximately 26 million tons per year [5]. Of the total *para*-xylene produced, *para*-xylene market demand was: 89% PTA, 10% DMT, and 1% others.

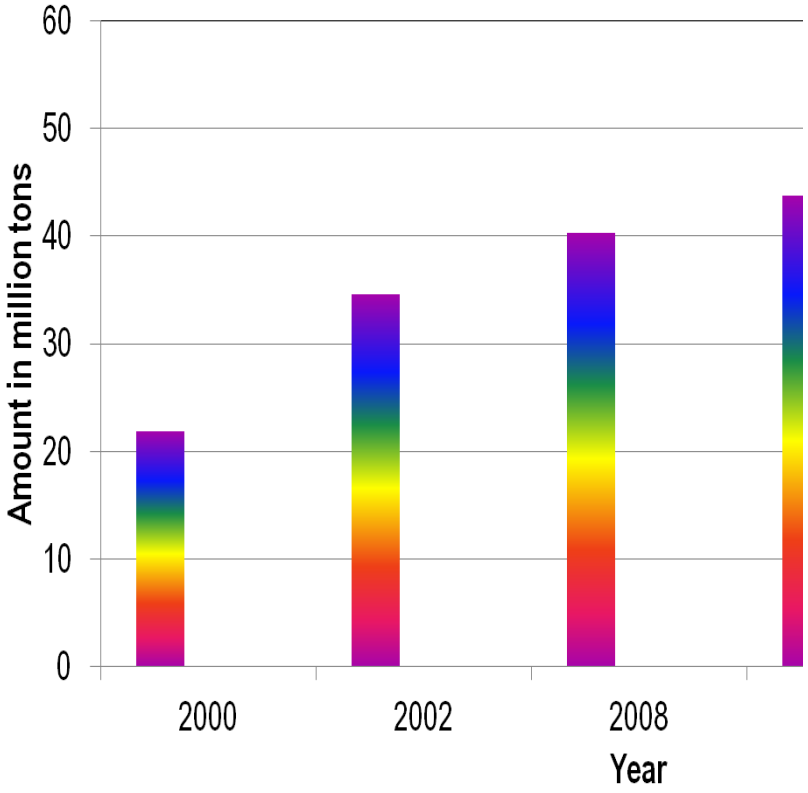

Fig 1.2: Global demand for xylene [4].

It is expected that the consumption of p*ara*-xylene to grow at an average rate of 7% per year over the next five years due to an increase in the use of PET in plastic bottles [6]. Growth in Asia is expected to be even higher, growing at a rate of 8.5% per year. The utilization rate of *para*-xylene over these five years is expected to remain constant at approximately 90% of the global capacity; however, due to a 6% increase per year in the global capacity of PET bottle production, the current production capability of *para*-xylene is far from adequate.

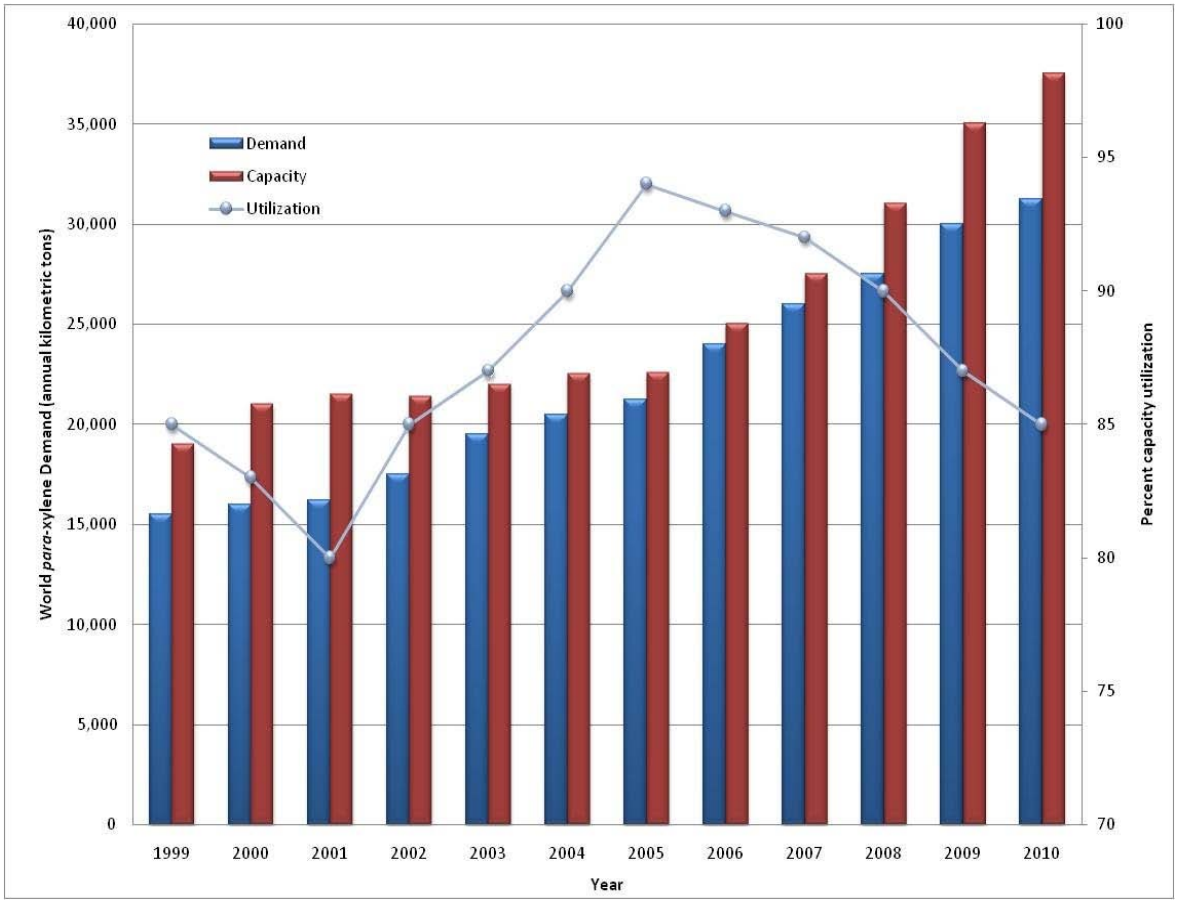

Fig 1.3: World *para*-xylene supply and demand balance, 1999-2010. *Para*-xylene demand is projected to increase at a rate of 7% per year while its utilization remains constant at approximately 90% [5].

1.2 Main Industrial Technologies for Xylene Production

Xylenes are produced industrially through one main process route namely; naphtha reforming and toluene disproportionation. The first process involves the reconstruction of low-octane hydrocarbons in the naphtha into more valuable high-octane gasoline components without changing the boiling point range. Naphtha and reformate are complex mixtures of paraffins, naphthenes, and aromatics in the $C_5 - C_{12}$ range. The reformation can either be thermal or catalytic. In most catalytic reforming processes, platinum is the active catalyst; it is deposited on the surface of some aluminum oxide carrier [7].

While in the disproportionation process, toluene is converted to equivalent volumes of benzene and xylenes.

1.2.1 Naphtha Reforming

This process route accounts for 72% of the total world para-xylene production [4]. In a typical reforming unit the naphtha charge is first passed over a catalyst bed in the presence of hydrogen to remove any sulfur impurities. The desulfurized feed is then mixed with hydrogen (about five molecules of hydrogen to one of hydrocarbon) and heated to a temperature of 500°–540°C.The gaseous mixture passes downward through catalyst pellets in a series of three or more reactor vessels. Early reactors were designed to operate at about 25 kilograms per square centimeter, but current units frequently operate at less than 7 kilograms per square centimeter (100 pounds per square inch). Because heat is absorbed in reforming reactions, the mixture must be reheated in intermediate furnaces between the reactors.

After leaving the final reactor, the product is condensed to a liquid, separated from the hydrogen stream, and passed to a fractionating column, where the light hydrocarbons produced in the reactors are removed by distillation. The reformate product is then available

for blending into gasoline without further treatment. The hydrogen leaving the product separator is compressed and returned to the reactor system [8].

A typical reforming process is depicted schematically in Fig 1.4.

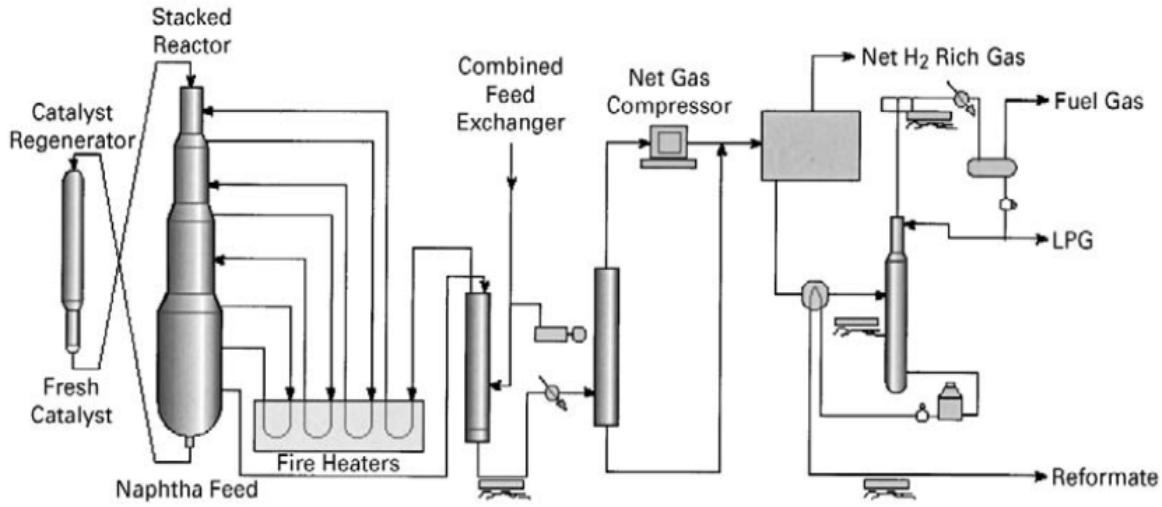

Fig 1.4: Schematic Diagram of UOP CCR Plat-forming Process [8].

1.2.2 Xylenes Production from Toluene Disproportionation or Transalkylation

About 25% of world para-Xylene is obtained from toluene disproportionation or transalkylation processes. In the disproportionation process, toluene is converted to equivalent volumes of benzene and xylenes, as shown in the equation that follows [9]:

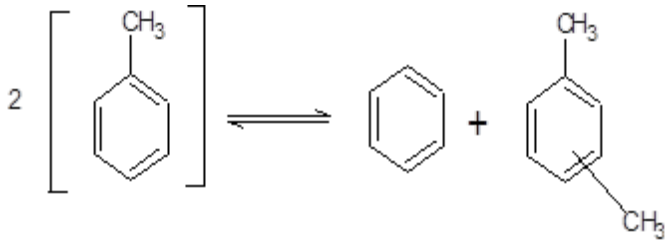

1.1

In transalkylation, the reaction is as follow;

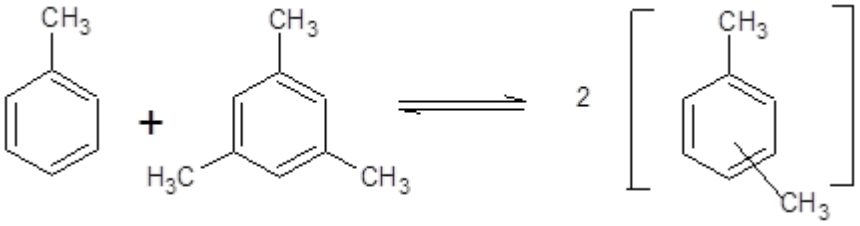

1.2

Many of the facilities that perform one of these processes can change mode to operate using the other process [9].

The toluene disproportionation/transalkylation method of producing xylenes is expensive when compared to the reforming process; however, it has two advantages. One is that no ethyl benzene is formed in the xylenes stream, so isomer isolation is less difficult. Second, no net hydrogen is consumed. An estimated 176 million kilograms (387 million pounds) of xylenes were produced by this method in 1988. The supply of xylenes from this source is estimated to reach about 244 million kilograms (538 million pounds) per year by 1993[10].

An example of a disproportionation/transalkylation process is illustrated in Figure 1.5 (Toray/UOP Tatoray Process). The use of a hydrogen atmosphere in this process, in addition

to the type of catalyst employed, allows several months of operation before catalyst regeneration is required.

1.3 Xylene Production from toluene and methanol

The ring chain alkylation of toluene with methanol is a potential alternative technology to xylene production. The conventional process converts toluene to *para*-xylene (and its isomers) in the presence of methanol over a heated catalyst bed of ZSM-5 zeolite. The process follows the following highly exothermic reaction:

$$C_7H_8 + CH_3OH \rightarrow C_8H_{10} + H_2O \qquad (1.3)$$

An equilibrium mixture of 23% *para*-, 51% *meta*-, and 26% *ortho*- xylene is produced. An oxide-modified ZSM-5 catalyst is commonly used to improve the selectivity towards *para*- xylene. Further methods for improving the selectivity of *para*-xylene include operating at higher temperatures (550 – 606°C) which promotes catalyst coking. As the catalyst becomes coked, active sites on the catalyst are blocked leaving a smaller amount of sites for *para*-xylene to become isomerized. Although the selectivity to p*ara*-xylene is improved, a decrease in the available active sites on the catalyst causes a decrease in the overall conversion of toluene. This indicates a clear trade-off between *para*-xylene selectivity and toluene conversion [11].

Unfortunately, there are a number of technical hurdles for toluene methylation to be commercially successful and improvements are needed. Among these are fast catalyst deactivation and low methanol selectivity. Fig 1.6 shows a proposed block diagram for toluene methylation [12].

.

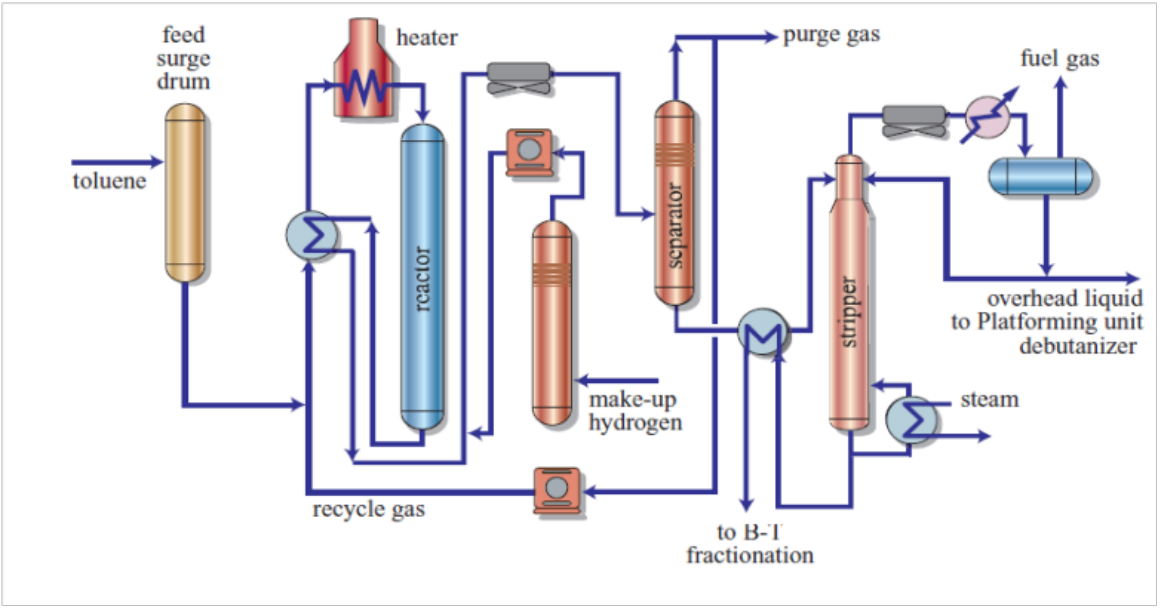

Fig 1.5: Toray/UOP Tatoray disproportionation/transalkylation process [8].

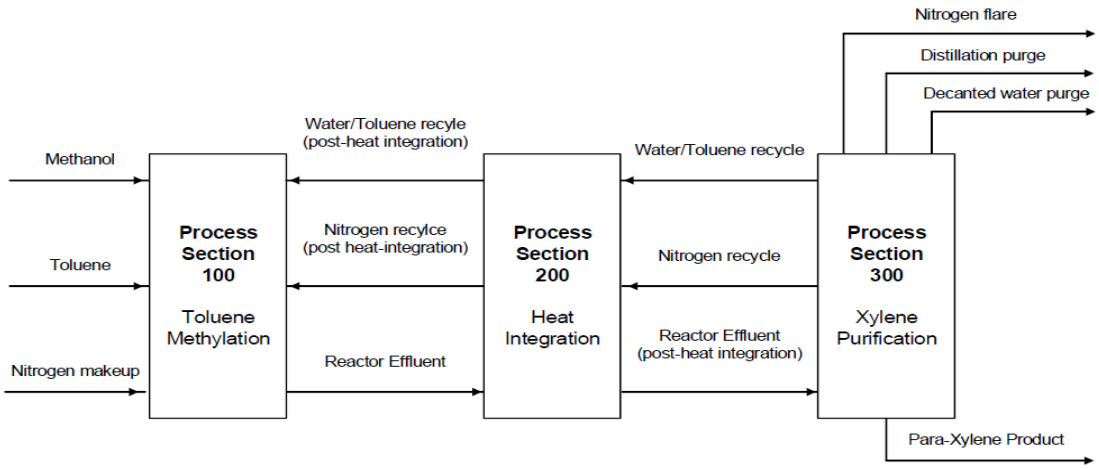

Fig 1.6: A proposed block diagram for toluene methylation [12].

1.4 Cost Analysis of xylene Feed Stock from Toluene Disproportionation and Methylation

The price of materials required for xylene production from the two processes is given below;

MATERIAL	PRICE($/TONNE) as of December,2011
Methanol	**400**
Toluene	**900**
Xylene	**1400**

a) For Toluene Disproportionation:

$2C_7H_6 \rightarrow C_6H_6 + C_8H_{10}$ 1.4

1.735 tonne toluene → 1tonne xylene

Thus, $1,561.5 is required as feed cost to produce 1 tonne of xylene from toluene disproportionation

b) For Toluene Methylation:

$C_7H_6 + CH_3OH \rightarrow C_8H_{10} + H_2O$ 1.5

0.87 tonne TOLUENE + 0.3021 tonne METHANOL → 1 tonne of XYLENE

Thus, $903 is required as feed cost to produce xylene from toluene methylation.

From this we can see that the present cost of materials makes xylene production from toluene methylation a feasible process.

1.5 Styrene Background Studies.

Styrene is one of the most important monomers in modern petrochemical industry. The market has grown from around 20 million tons in 2000 to around 28 million tons in 2010 [13]. However, prior to World War II, the styrene

industry, which uses ethyl benzene as a starting material was relatively insignificant. The tremendous demand for synthetic styrene – butadiene rubber (SBR) during the war prompted accelerated technology improvements and capacity expansion. The styrene process was developed in the 1930s by BASF (Germany) and Dow Chemical (USA) and this effort have led to the construction of several large-scale factories, and styrene production became a significant industry.

Styrene is a basic building block in making a variety of materials, most recognizable is polystyrene. Other materials include acrylonitrile-butadiene styrene (ABS) plastic, styrene-acrylonitrile (SAN) plastic, styrene-butadiene rubber (SBR), unsaturated polyester resins and expanded polystyrene foam (EPS). These materials can further be transformed to produce variety of products across a wide range of industries as there is no direct end use for styrene. Products made from styrene are of high performance, durable, safety, value and high quality [13]. Many of these products offer very good insulation qualities and the ability to be recycled. These products range from packaging materials to a myriad of consumer electronics, construction, transportation and medical applications. The global styrene capacity in 2008 is 26million tons per year. The global demand of the styrene is shown in Figure 1.7a. While global distribution of styrene consumption by product is shown in Figure 1.7b [14].

Figure 1.7a: Global styrene demand and capacity[14].

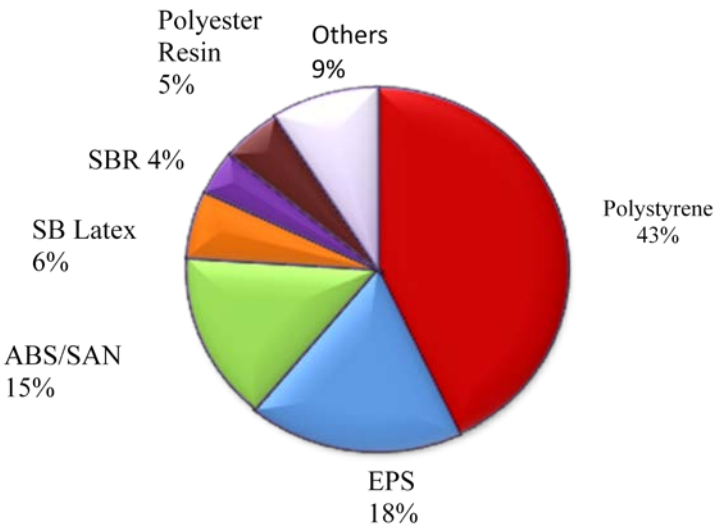

.

Fig 1.7b:Global styrene Consumption 2008[14].

1.6. Main Industrial Technologies for styrene production

Industrially, styrene is produced through two main routes: dehydrogenation of ethyl benzene(EB) and co-production with propylene oxide in a process known as SM/PO (Styrene Monomer/Propylene Oxide) or POSM. Both routes use ethyl benzene as the intermediate, EB is first made by the catalytic alkylation of benzene with ethylene, using either aluminum chloride or, more recently, zeolite catalysts [15]. Ethyl benzene and styrene units are almost always installed together with matching capacities because nearly all of the ethyl benzene produced commercially is converted to styrene. Alkylation is exothermic and dehydrogenation is endothermic, as a result energy economy in a typical ethyl benzene-styrene complex is achieved by integrating the energy flows of the two units.

1.6.1. Catalytic Dehydrogenation of Ethyl benzene

This route accounts for 90% of the total world production. Dehydrogenation of ethyl benzene can be run industrially using either multiple bed adiabatic or tubular isothermal reactors in which the reactants are passed over the catalyst bed employing radial or axial flow. In this process, EB is dehydrogenated to styrene in the presence of potassium promoted iron oxide catalyst and a super-heated steam was fed to supply the heat of endothermic dehydrogenation and further to suppress the coking. Formations of by-products are suppressed by reducing the partial pressure of the reaction. Typical conversions up to 69%, styrene selectivity of more than 97 mol% and a styrene monomer purity of 99.85 wt% are achieved. Flow scheme of a typical Lummus/UOP adiabatic ethyl benzene dehydrogenation plant is shown in Figure 1.8.

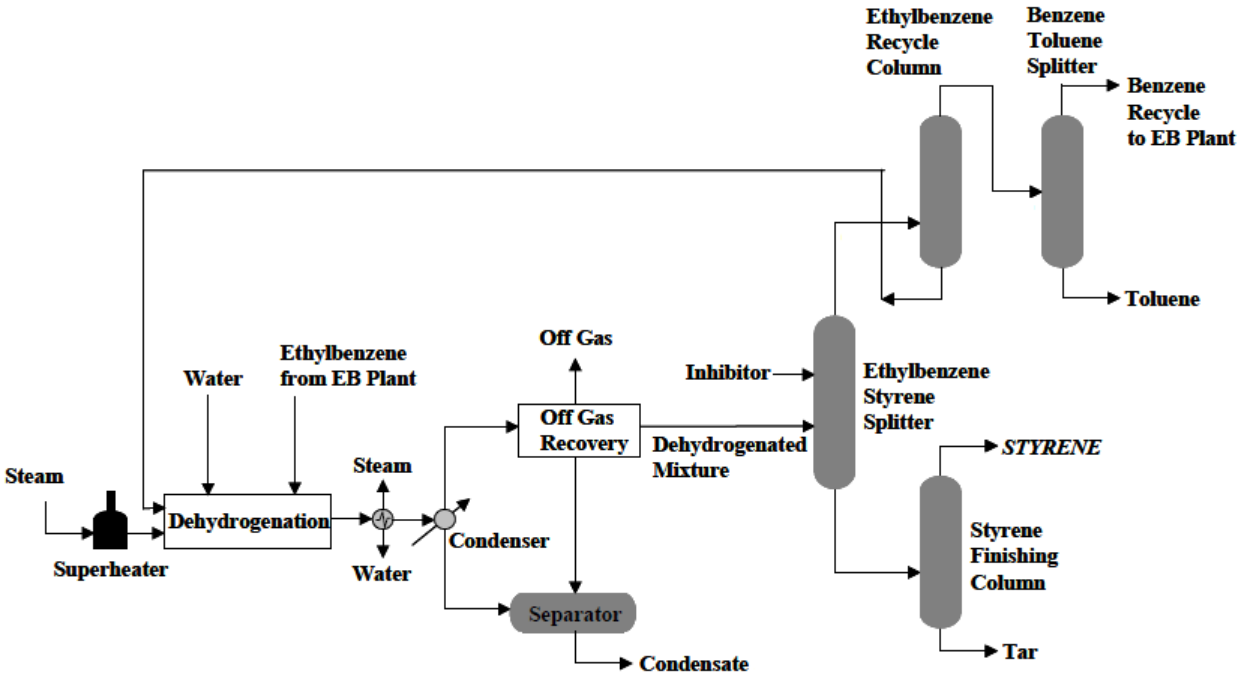

Figure 1.8: Lummus/UOP Classic SM process of adiabatic ethyl benzene dehydrogenation plant [16].

1.6.2. Styrene and Propylene Oxide (SMPO) Process

This process was discovered in the 1970's by Halcon and improved by Royal Dutch Shell [17]. The coproduction of propylene oxide (PO) and styrene (SM) route is complex and capital-intensive in comparison to dehydrogenation of ethyl benzene. The process includes three reaction steps: oxidation of ethyl benzene to ethyl benzene hydro peroxide (EBHP), epoxidation of ethyl benzene hydro peroxide (EBHP) with propylene to form α-phenyl ethanol and propylene oxide, and dehydration of α-phenyl ethanol to styrene.

$$C_6H_5{-}CH_2CH_3 + O_2 \rightarrow C_6H_2CH_2O_2H \quad (1.6)$$

$$C_6H_5{-}CH_2CH_2O_2H + CH_3 \rightarrow C_6H_5{-}CH_2OH + CH_3CHCH_2O \quad (1.7)$$

$$C_6H_5{-}CH_2CH_2OH \rightarrow C_6H_5{-}CH{=}CH_2 + H_2O \quad (1.8)$$

Fig 1.9 shows a flow diagram for SMPO process.

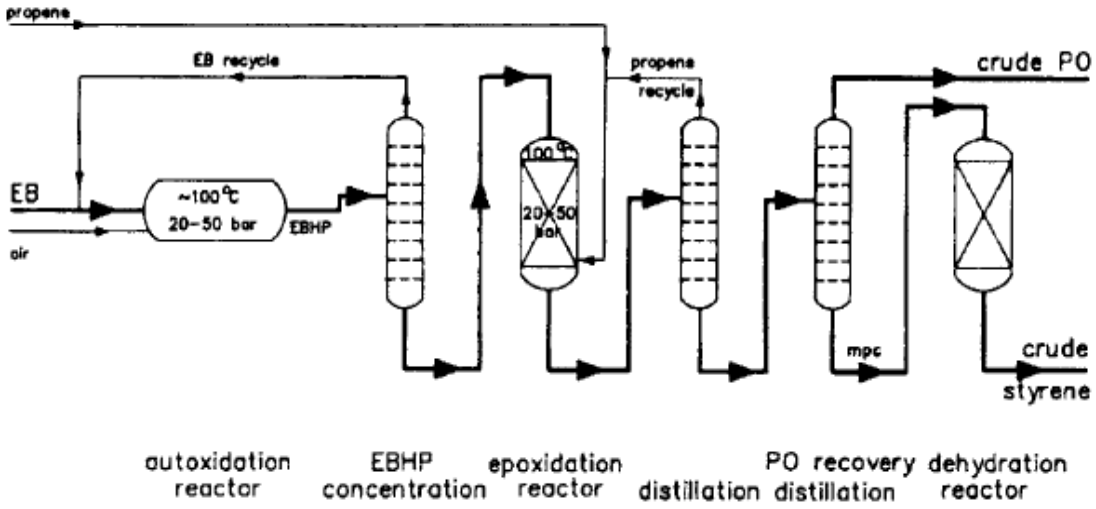

Figure 1.9: Simplified flow diagram of the SMPO process [18].

1.7. Styrene Production from Methanol and Toluene

The side chain alkylation of toluene with methanol is a potential alternative technology to produce styrene. Direct side alkylation of toluene over basic zeolites is an interesting reaction, considering the industrial importance of its products, especially ethyl benzene and styrene [19]. It is generally accepted that zeolites with some basicity catalyze side-chain alkylation to styrene which is subsequently hydrogenated to ethyl benzene while those which compose of acid sites accomplish only ring alkylation. Styrene monomer production via alkylation of toluene occurs in gas phase at 420 °C,

4-7 bar with the presence of zeolite X and Y catalyst. The reactions occur in two parallel reactions that produce styrene and ethyl benzene. The raw material being used are liquid toluene and liquid methanol that are preheated to 420 °C before enter the reactor. The catalyst used in this process has high styrene selectivity so that the styrene yield could reach 85%. This process has been claimed to be economically attractive offering the advantage of lower raw material cost compared with the traditional process [20].

Other processes for the production of styrene are: side-chain chlorination of ethyl benzene, styrene extraction from pyrolysis gasoline (Toray's STEX process) and oxidative conversion of ethyl benzene to a-phenyl ethanol via acetophenone and subsequent dehydration of the alcohol [21].

1.8 Cost Analysis of Feed Stock for Styrene Production from Toluene Methylation

From the reaction equation;

$$C_6H_5CH_3 + CH_3OH \rightarrow C_6H_5CH{=}CH_2 + H_2O + H_2 \qquad 1.9$$

0.885 tonne Toluene + 0.3076 tonne Methanol ⟹ 1 tonne of Styrene.

MATERIAL	**PRICE ($/TONNE) as of December, 2011.**
Methanol	**400**
Toluene	**900**
Styrene	**1400**

Thus, $919.5 is required as feed cost to produce styrene from toluene methylation

1.9. Motivation

Research and development of new catalysts, reactor design, and process routes have been continuously pursued to achieve process improvement. Recently a number of patent work has been done on both the catalyst modification and process development, and such work has evidently enabled the development of new much energy-saving catalytic process, to decrease the cost unit of raw materials and finally to enhance the production capability.

A research team at the University of Pennsylvania in 2009 worked on a project that investigated the economic and environmental feasibility of converting 180,000 tons/yr of toluene to p*ara*-xylene using a steamless reactor. The methylation reactor was designed to reproduce operating conditions that yield 99.9% *para*-xylene selectivity and a 100% single-pass methanol conversion. Conserving resources is prioritized through extensive recycling of reactants and through introduction of an intricate heat exchanger network that capitalizes upon the high exothermic nature of the reaction. The Total

Capital Investment for the process was $63,170,900 with a projected Net Present Value in 15 years of $60,468,500 and an Investor's Rate of Return of 28.80%. In light of the economic profitability of the process and the projected increase in demand for *para*-xylene, it is recommended that the design be considered for further implementation [12]. Not forgetting that the success of this investigation will depend on the development of new catalyst or modifying the existing ones.

While for side chain alkylation, research is still on-going for a good process design to optimize the process.

1.10 Thesis Objectives

The main objectives of this work are of two-folds;

i) To develop highly efficient acid and basic catalysts for toluene methylation to xylenes and styrene respectively, and

ii) Kinetic studies of the reaction. The detailed specific objectives are as follows:

1.10.1. Synthesis of Acid Catalyst for Toluene Methylation to Xylenes

i. Synthesis of bi-porous composite HZSM-5 and ALMCM41 catalysts with different Mesoporosities.

ii. Study the effect of catalysts mesoporosities on both toluene conversion and xylenes yield.

iii. Examine the effect of toluene: methanol molar feed ratio on the activity of the catalysts.

iv. Study the effect of bi porosity on both toluene disproportionation and methylation.

v. Compare the activities of the composite catalysts with the individual parent catalysts.

vi. Determination of the physico-chemical properties of the catalysts through some characterization techniques.

1.10.2 Synthesis of Base Catalyst for Toluene Methylation to Styrene

i. Synthesis of Cs-X zeolites catalyst through ion exchange method.

ii. Study the effect of different amount of Cs_2O loading on the activity of Cs-X.

iii. Inspect the effect of borate on the activity of Cs-X.

iv. Inspect the effect of Zirconium borate (ZrB) loading on the activity of Cs-X.

v. Effect of ZrB loading on the catalytic activity of Cs_2O/CsX.

vi. Compare the catalytic activities of Cs-X, Cs_2O/Cs-X and ZrB/Cs2O/CsX.

vii. Examine the effect of toluene: methanol (molar feed ratio) on the activity of the catalysts.

viii. Determination of the physico-chemical properties of the catalysts through some characterization techniques.

1.10.3 Catalysts Test Performance

The prepared catalysts' activity and selectivity will be determined for the toluene methylation process. Fixed bed reactor will be used for the catalytic test for a time on stream of 75mins and reaction temperature 410°C which is the supposed optimum temperature that has been established for the reaction.

1.10.4 Kinetic Modeling

Key to any process development is the availability of important design parameters such as the activation energy of the reaction, rate constants, etc. This will involve the following:

i. Proposition of a possible reaction models

ii. Fitting experimental data into the proposed models to check the suitability of the models

iii. Determination of kinetic parameters; apparent activation energies, apparent reaction rate constants.

1.11 Thesis Write up Overview

- **Chapter 2** presents a literature review on toluene methylation on both acid and base catalysts. An overview of its reaction mechanism is given, catalyst composition and deactivation. Challenges facing the commercial catalyst used for EB dehydrogenation process are discussed, and what has been done so far in terms of catalysts development to tackle these challenges. Overview of the kinetic studies of the reactions involved is also reviewed.
- **Chapter 3** deals with the experimental section. Description of the equipment used for the experimental set-up is given as well as the procedures adopted. This chapter also explains catalyst synthesis, characterization and evaluation.
- **Chapter 4** focuses on the results of the experimental work using acidic zeolite catalysts. Discussions of the effects of different amount of meso-porosity loading on catalyst activity and selectivity towards the desired product route are given in details. The effect of molar feed ratio of toluene to methanol on toluene conversion and xylenes selectivity are discussed also.
- **Chapter 5** Kinetic modeling of the reaction over all the catalysts are presented. Starting from the model formulation to the estimation of kinetic parameters using non-linear regression analysis.
- **Chapter 6** gives the experimental results of the reaction using basic zeolite catalysts. The promoting effects of $ZrBO_3$ and CS_2O additives are discussed, as well as the effect of toluene to methanol molar feed ratio on the catalyst activity and product selectivity.

- **Chapter 7** presentes the Conclusions and Recommendations for the work done.

CHAPTER TWO

LITERATURE REVIEW

2.1 Introduction

The alkylation of toluene with methanol is an important and interesting reaction due to the diversity of the type of catalysts used. The reaction can proceed either on acid or base catalyst.

For acid catalyzed toluene methylation, the methylation takes place at the ring producing xylenes mixture (major product), benzene and trimethyl benzene. In the process of toluene methylation with methanol, there are other reactions taking place; toluene disproportionation, further alkylation of xylenes with methanol and methanol conversion to hydrocarbons at high temperature [22].

Thus benzene formation comes from toluene disproportionation, while trimethyl benzene results from further alkylation of toluene.

Toluene disproportionation to benzene and xylenes may take place over zeolites with strong acidity at high temperatures. Compared to toluene, methanol is more reactive over acid catalysts forming water and gaseous hydrocarbons [22].

The equations below show the different reactions taking place during toluene methylation process;

Toluene methylation (main reaction),

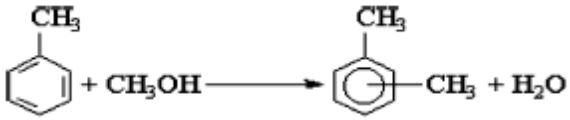

(2.1)

Other reactions;

Toluene disproportionation;

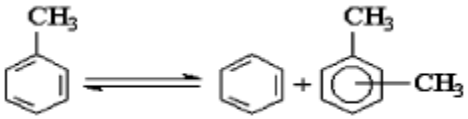

(2.2)

Alkylation of xylene;

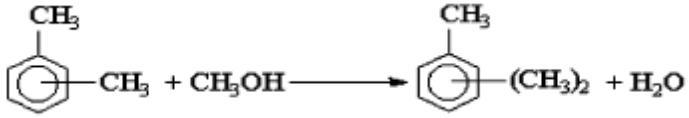

(2.3)

Methanol decomposition;

$$CH_3OH \rightarrow C_nH_{2n} + nH_2O \qquad (2.4)$$

The methylation of toluene with methanol reaction is highly exothermic and a thermodynamic equilibrium exists between the isomers of xylene formed. At thermodynamic equilibrium ,the composition of the isomers are 23% *para*-, 51% *meta*-, and 26% *ortho*- xylene. ZSM-5-type zeolite has shown good catalytic ability towards the selectivity of xylene during toluene methylation and oxide-modified ZSM-5 catalyst has been used to improve the selectivity towards *para*-xylene. Further methods for improving the selectivity of *para*-xylene include operating at higher temperatures (550 – 605°C) which promotes catalyst coking [23]. Thus, the reaction is usually carried out between a temperature of 400 and 450^{o}C.

The selectivity to xylene isomers partially originates from the catalyst's specific pore size, which imposes steric limitations on the guest molecules [24].Large pore zeolites such as

mordenite, the para selectivity is less pronounced [25].Not only the structure of the zeolite but also its chemical composition (e.g. Al content) influences the selectivity. The para selectivity over large pore zeolites is slightly enhanced when the strength of the acid sites increases [26].

In general, the observed selectivity can be attributed to a combination of differences in :(i) diffusivity, (ii) adsorption behavior, and (iii) intrinsic reaction rate of the xylene isomers [27].

For base catalyzed toluene methylation reaction, the methylation takes place at the side of the ring, thus the process is called side-chain toluene methylation. The main products of the reaction are styrene and ethylbenzene.

Since high selectivities to styrene and ethyl benzene in the alkylation with methanol of toluene performed over moderately basic X zeolites with a low Si/Al ratio has been reported [28] (see Scheme 2.1a). The side-chain methylation reaction of toluene has received a lot of attention, since it has theoretical potential as a novel route to styrene. This process is thermodynamically nearly zero, when the rates are properly balanced: methanol dehydrogenation yielding formaldehyde is endothermic while the reaction of toluene and formaldehyde is exothermic [29].

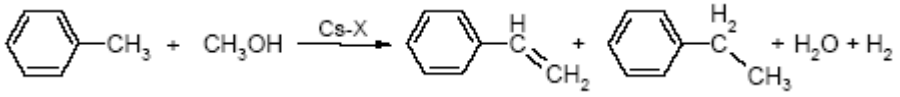

(2.5)

Scheme 2.1a: Reaction Scheme for toluene methylation over basic catalyst.

High styrene selectivity at 425^{o}C was only obtained with cations with a small electrostatic potential at the ion-exchangeable site, i.e., Cs+ and Rb+ [30]. The high styrene selectivity of these materials was related to a formed formaldehyde intermediate,

resulting from the dehydrogenation of methanol [31, 32]. Methanol dehydrogenation was claimed to be the result of the presence of strong basic, framework oxygen, sites with weak Lewis acidic centers (the cation) in the zeolite pores. Up to now, the dehydrogenation mechanism over these type of materials remains a mystery.

The use of formaldehyde as alkylating species increased the alkylation activity and the styrene selectivity [31-33]. Recently, it was shown that not only methanol or formaldehyde can alkylate toluene on the side chain. Dimethoxy carbonate was used as alternative methylating agent with high styrene selectivity [34], whereas the use of isopropanol as toluene alkylating agent yielded isobutyl benzene [35].

Scheme 2.1b shows toluene-methanol reaction network over acid –base catalyst at a glance.

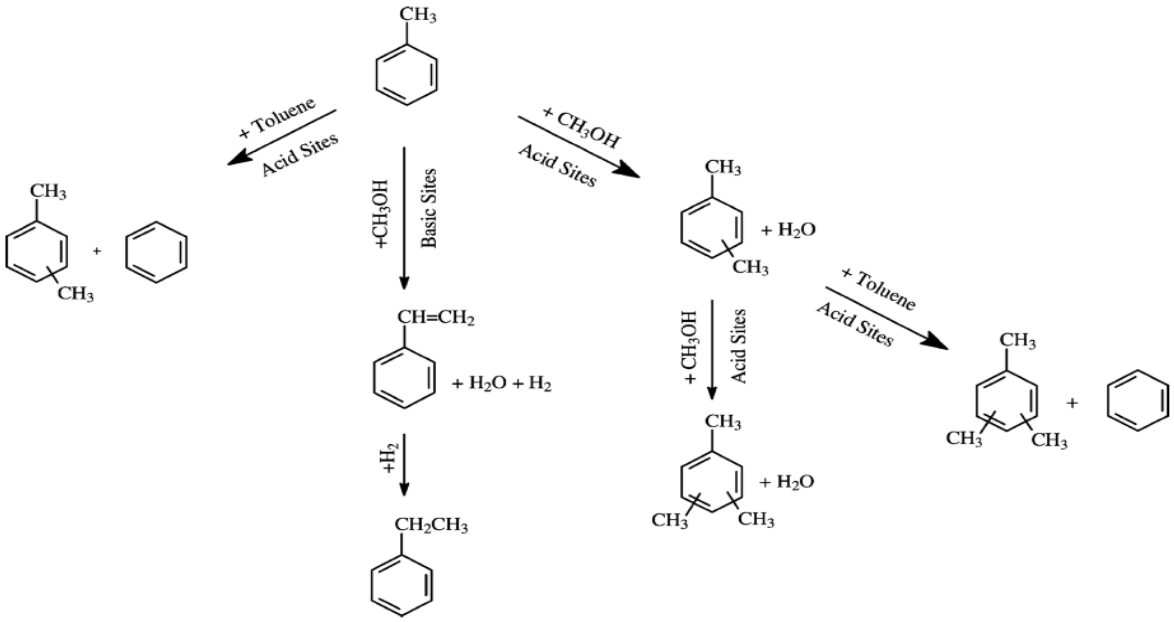

Scheme 2.1b: Toluene-methanol reaction network over acid –base catalyst at a glance.

2.2 Toluene Methylation with Methanol

2.2.1 Side-Chain Methylation of Toluene with Methanol

After Sidorenko et al. [28] have reported high selectivities of styrene and ethyl benzene in the methylation of toluene performed over moderately basic X zeolites with low Si/Al ratio, many catalysts have been tested, either by modification of zeolites X or Y, or some other catalysts.

Yashima et al. [31] reported that methylation of toluene over Li-X, Li-Y zeolites yield xylenes, over Na, K, Rb, Cs-X and Y zeolites, styrene and ethyl benzene were observed. X zeolite is more active than Y zeolite over K-X, Rb-Y, and HCl promoted xylenes and inhibited side-chain alkylation. Aniline inhibited xylenes production and promoted side-chain alkylation and the active sites for the catalyst were basic. From these facts, the importance of basic sites in the side-chain alkylation over zeolites was stressed. The basicity of K-X and K-Y was confirmed by the color change of adsorbed indicators, cresol red and thymolphthalein.

Cu, Ag deposited on Cs exchanged and B doped zeolite 13X were reported to favor side alkylation using hydrogen as carrier gas and non-washed Cs-X is better than washed Cs-X. H_2 carrier increased conversion and ethyl benzene yield under the reaction of 400^0C Tol/MeOH = 5 /1[36].

Binary zeolites: KX/KY, KX, KM, KZSM-5 showed much higher activity than separate zeolites and H_3BO_3, KOH modification improved selectivity to styrene. Stating that acid-base cooperation is needed for the reaction [37].

Unilad et al. [38] confirmed the works carried out by earlier researchers and stated that the addition of certain inorganic compounds such as phosphoric acid or boric acid to ion-exchange solution improved the selectivity for the side-chain alkylation. The borate-promoted Cs-X zeolite was the most favorable catalyst and a selectivity of >50% to styrene(SM) and EB on the methanol basis. High selectivity over Cs-X was suggested to

be due to the adsorption of a toluene molecule between two or more large cations in an overcrowded super-cage of X-zeolite in such a way that (1) an electrostatic potential at the molecule was higher than expected; (2) only the methyl group was exposed for alkylation; (3) because of the strong interaction of cations with aromatic molecules. It was also suggested that incorporation of borate in the super-cage slow down the decomposition of formaldehyde, which was a real alkylating agent.

Wieland et al. [35] confirmed the positive effect of boron addition to Cs-X on the side-chain alkylation reaction and it was suggested that the primary effect of boron addition was to reduce the decomposition of intermediate formaldehyde to carbon monoxide, without inhibiting the sites active for alkylation, by poisoning some of the strongly basic sites.

In another Study,Wieland et al. [34] studied alkali-exchanged zeolites (X, Y, L, and Beta) and alkali-impregnated mesoporous alumina as catalysts for toluene alkylation with methanol. At 407–417 ºC and atmospheric pressure, highly basic, alkali-exchanged zeolites X and Y were found active for toluene alkylation but primarily decomposed methanol to CO. Cs-exchanged zeolites L and Beta were also active alkylation catalysts but required higher temperatures to attain similar aromatic yields. Very little CO was produced over the L and Beta based catalysts. Results suggested that variations in particle size of Y zeolite did not affect methanol decomposition and alkali-exchanged X and Y zeolites adsorbed much higher amounts of CO_2 than Cs-L and Cs-Beta zeolites. Mesoporous alumina modified with Cs and B was inactive for toluene alkylation but decomposed methanol to CO. They also found that Cs-L is a unique catalyst for side-

chain alkylation of toluene. The yield at 487 ºC over Cs-L was similar to that over boron-promoted Cs-Y at 410 ºC, but Cs-L catalyst did not produced substantial amount of CO.

Itoh et al. determined through the quantum chemical calculation that, though the presence of basic sites is indispensable for side-chain alkylation, specific configurations of acidic sites and basic sites promote the alkylation [32]. Actually, Rb-X with a small amount of Li^+ ions showed a higher activity than Rb-X for side-chain alkylation of *p*-xylene [39, 40]. It was shown that Li-Rb-X has slightly stronger acid sites than Rb-X. Incorporation of Li^+ ions also suppressed the decomposition of formic acid intermediate.

Methanol dehydrogenation ability and the toluene side-chain methylation selectivity are directly proportional to the basicity of alkali metal cation exchanged zeolites and the proximity of acid-base sites and the zeolite basicity is related to the Si/Al ratio and the topology of the zeolite. Introduction of metal oxide clusters into the zeolite pores increase the zeolite basicity and thus promote the side-chain methylation of toluene [41-43]. Nevertheless, substantial amounts of methanol are decomposed to carbon monoxide over such strong basic material.

Boron impregnated Cs^+ exchanged X zeolites decreased the alkylation activity slightly, compared to Cs-X [44-47] and this may have increased acidity of the catalyst upon impregnation with boron. In another study, boron impregnation exhibited an increasing effect on the toluene alkylation selectivity and activity compared to CsO impregnated Cs-X zeolites, since it increased the dehydrogenation abilities for methanol [41]. It was found out that incorporation of boron produced $B_2Cs_2O_4$ species inside the zeolite channels, resulting in a lower overall basic strength of the CsO cluster. In the presence of H_2, high

yields of EB were found, due to in-situ hydrogenation of SM, while under Ar or N_2, high yields of SM are obtained.

It was illustrated that Cs^+ exchanged X zeolite decomposed MeOH to CO [41] in the presence of hydrogen which reduced the formation of coke and thus increased the catalyst lifetime. It was reported that dual catalysts comprising Fe-Mo oxide deposited over Cs^+ exchanged zeolites were found active at 325 ºC [46], while single Cs^+ exchanged catalysts exhibit catalytic activities only at temperatures higher than 375 ºC. This may be due to the concerted interaction of the Cs^+ exchanged zeolite and Fe-Mo oxide with toluene. Fe-Mo oxide deposited over Cs^+ exchanged zeolite increased both SM yield and selectivity significantly as compared to Cs^+ exchanged zeolite at reaction temperature 425 ºC. Using this dual catalyst, styrene/ethyl benzene ratio was increased by a factor of 4.5.

2.2.2 Ring Methylation of Toluene with Methanol

The old alkylation process uses AlCl3, [48, 49] which is corrosive and associated with tedious disposal problems. Synthetic zeolites have attracted attention as alkylation catalysts owing to their higher acidity, freedom from corrosive substances, potential for regeneration, easy separation from reaction Products and elimination of problems associated with disposal of spent catalyst [50].

The study of toluene methylation over acid catalysts to produce xylenes has been done particularly over zeolite or zeolite-type catalyst. In particular, ZSM-5-type zeolite, zeolite Beta and silica alumino phosphate (SAPO) catalysts have been used for this process.

ZSM-5-type catalyst was found to give xylene products containing significantly greater amounts of p-xylene than the thermodynamic concentration. This is due to the shape

selectivity of the catalyst. A significantly higher amount of p-xylene can be obtained in toluene methylation reaction if the catalyst has shape selective properties. Shape selective properties can be obtained in modified zeolite catalysts by narrowing zeolite pore opening size, inactivation of the external surface of the zeolite or controlling zeolite acidity [51]. So most toluene methylation with methanol work has been done over HZSM-5 modified catalyst.

Kaeding et. al [52], modified ZSM-5 catalyst by incorporating 5% phosphorus through impregnation with a solution of diphenylphosphinous acid in toluene. The modified ZSM-5 catalyst showed toluene methylation activity with 84-90% para isomer in the xylene product. In another procedure, a catalyst was modified by incorporating 8.51% phosphorus from an aqueous phosphoric acid reagent. The catalyst showed p-xylene selectivity as high as 97% at a temperature of 450^{o}C, however, the catalyst showed a decreasing activity within hours due to coke deposition.

Aboul-Gheit et al. [53] synthesized a set of catalysts containing different Pt contents (0.2, 0.4 and 0.6%) supported on H-ZSM-5 or H-mordenite (H-M) zeolites. Toluene disproportionation and methylation were studied on these catalysts. Both reactions were more accelerated using HZSM-5 containing catalysts than H-M containing catalysts. The yield of xylenes, and in particular para-xylene, was significantly influenced by the yield of trimethylbenzenes (TMBs) in product. The selectivities for para-, ortho- and meta-xylenes production were found largely dependent on the Pt content in the catalysts, particularly when supported on H-ZSM5-zeolite. However, using Pt/H-M catalysts, these selectivities were not strictly controlled by Pt content in the catalysts.

A mixture of xylenes was obtained as the main reaction products: 69% and 74% of xylenes for the Al- and GaAl–PILC (pillared clays) catalysts, respectively, at 573 K. Trimethylbenzenes (1,2,4- and 1,2,3-isomers) were also found (31% and 26% for the Al and GaAl catalysts, respectively, at 573 K) when catalytic activity and selectivity of montmorillonite pillared with Al_{13} and $GaAl_{12}$ polyoxycations were investigated at temperatures between 573 K and 673 K for the gas-phase micro catalytic alkylation of toluene with methanol. The isomer distribution followed the order *o*>*p*>*m* for both catalysts, since there are no shape-selective effects, due to the pore system of pillared clays [54].

Zhu et al. [22] worked extensively on toluene methylation with methanol and toluene disproportionation with variety of zeolites, including MOR, MCM-22, SAPO-34, SAPO-11, SAPO-5 and ZSM-5 with different SiO2/Al2O3 ratio, for catalyzing toluene alkylation with methanol to produce xylene. The catalytic activity of zeolite for the toluene alkylation was approximately proportional to the number of its mid-strength acidic sites, except for SAPO-34 with small channels and MOR with strong acidity.

Moreover, the acidic sites for catalyzing toluene alkylation were weaker in strength than those for catalyzing toluene disproportionation, but slightly stronger than those for catalyzing the reaction of methanol to hydrocarbons. On the other hand, zeolites with 12-membered ring channels may lead to the further alkylation of xylene and the rapid deactivation by coking. Zeolites with 8-membered ring channels restrict toluene alkylation, only favorable for forming non-aromatic hydrocarbons. As a result, zeolites with 10-membered ring channels and mid-strength acidity show high catalytic selectivity and activity for methylation of toluene.

The reactivity for the toluene alkylation is approximately linear with the number of mid-strength acidic sites. Toluene disproportionation, corresponding to the formation of benzene, becomes severer with increasing strong Bronsted acid sites As a result, ZSM-5 (SAR 136), SAPO-11 and MCM-22 have >70% selectivity of toluene alkylation to xylene and >30% single-pass toluene conversion, and their stability are significantly improved than MOR zeolite.

Zeolite catalysts, having layered structure of ZSM-5 or borosilicate core covered with a silicalite shell (double structured catalyst), prepared by hydrothermal crystallization of silicalite in the presence of ZSM-5 or borosilicate seeds showed considerably higher *para*-selectivity compared to ZSM-5 in toluene alkylation reactions, but had slightly lower activity. The former showed higher *Para*-selectivity at the same conversion level. This result suggests that *para*-selectivity could be enhanced by selectively inactivating the external acid sites without changing the pore mouth size [55].

Odedairo et al [56] investigated an array of zeolites with varying channel structural design and acidity for toluene methylation with methanol, together with toluene disproportionation, using fluidized-bed and fixed-bed reactors. The conversions of toluene in the methylation and disproportionation reactions in the fixed-bed reactor were higher than those in the fluidized-bed reactor over the zeolite based catalysts at similar reaction conditions. The unique pore architecture of zeolite TNU-9, with 10-ring channel systems, being slightly larger zeolite compared with ZSM-5, can offer new opportunities for toluene disproportionation, as well as for toluene methylation. The medium pore zeolite TNU-9 was found to possess the highest conversion in toluene disproportionation as compared with other zeolite based catalysts under study. In toluene methylation, the highest toluene conversion was achieved with mordenite based catalyst (MOR-A), while

the xylene selectivity follows the order: ZSM-5 > TNU-9 > MOR-A > SSZ-33 > MOR-B. This order indicates that xylene selectivity is directly related to the size of channels from medium to large pore zeolites.

2.3 Catalyst Deactivation

Catalyst deactivation is the loss in the catalyst activity of the course of reaction. For toluene methylation with methanol over zeolite catalysts, catalyst deactivation has been attributed to the deposition of coke which poisons the active site of the catalyst.

Acid sites of zeolites play a vital role in coke formation, being severe on strong acid sites which promote condensation of olefins and aromatics which are potential coke precursors [57]. The large pores provide the room for forming polynuclear aromatics [22].

Ramakrishna et al [58] reported the effect of carrier gas (H_2 and N_2) on the deactivation of catalyst during methylation of toluene with methanol. Time-on-stream studies were carried out on H-ZSM-5 catalyst under constant contact time (30g of catalyst/mol-h), temperature (400^oC) and feed ratio (toluene: methanol (3:1)) using both the gases independently. Catalyst deactivation was more rapid in N2 atmosphere as compared with H_2 atmosphere. To account for this kind of behavior, one can assume either a difference in coke distribution or a difference in the nature of gaseous atmosphere.

Mass spectrum studies by Minachev et al [59] revealed rapid deactivation of the catalyst due to coke deposition on the outer surface of the catalyst. Further, they observed that the coke deposited under the nitrogen atmosphere consisted of higher molecular weight compounds than the coke deposited under the hydrogen atmosphere.

Carbonium ions were found to be the intermediates for coking [60]. It is believed that a zeolite which has very strong acid sites is capable of activating molecular hydrogen to enable it to reduce the concentration of adsorbed carbonium ion species on the catalyst

surface, thus minimizing the coke formation [60]. It has been recommended that low contact time with catalyst will reduces coke formation and increases Para xylenes selectivity [61].

2.4 Reaction Mechanism

2.4.1 Reaction Mechanism for Ring Alkylation of Toluene with Methanol

Partially exchanged zeolites are known to be very active catalysts for the ring alkylation of toluene with methanol. This high reactivity towards ring methylation is attributed to the presence of residual Brönsted acid sites inside the zeolite pores and is thought to proceed as found for fully exchanged H+ zeolites [62]. The reaction mechanism for the formation of xylenes over acidic zeolites was studied using infrared [63], NMR [64] and molecular modeling techniques [65-67]. The reaction scheme is presented in Scheme 2.4.1a, while the reaction mechanism is presented in scheme 2.4.1b

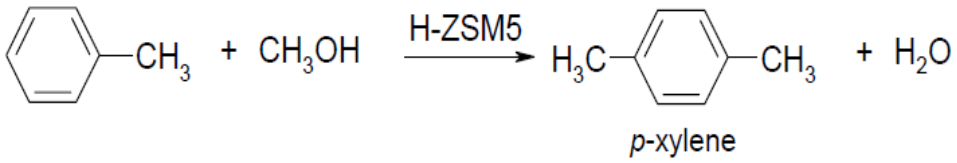

2.6

Scheme 2.4.1a: Reaction scheme for Ring Alkylation of Toluene with Methanol.

The general accepted idea for the reaction shown in Scheme 2.4.1a is that methanol adsorbs on a Brönsted acid site (Scheme 2.4.1b step 1). This interaction of methanol with a Brönsted acid site leads to the formation of a surface methoxy group, also called a methyl carbonium ion (CH_3^+) and water (Scheme 2.4.1b: step 2). CH_3^+ (an electrophilic agent)is stabilized by the zeolite-O^- and reacts subsequently with the aromatic ring (Scheme 2.4.1b: step 3 and4), whereby the remaining zeolite-O- group abstracts a leaving proton of the toluene ring, recreating the starting Brönsted acid site

(Scheme 2.4.1b: step 5). The formation of surface methoxy groups is also concluded to be the reactive species for the methanol to gasoline (MTG) process [68].

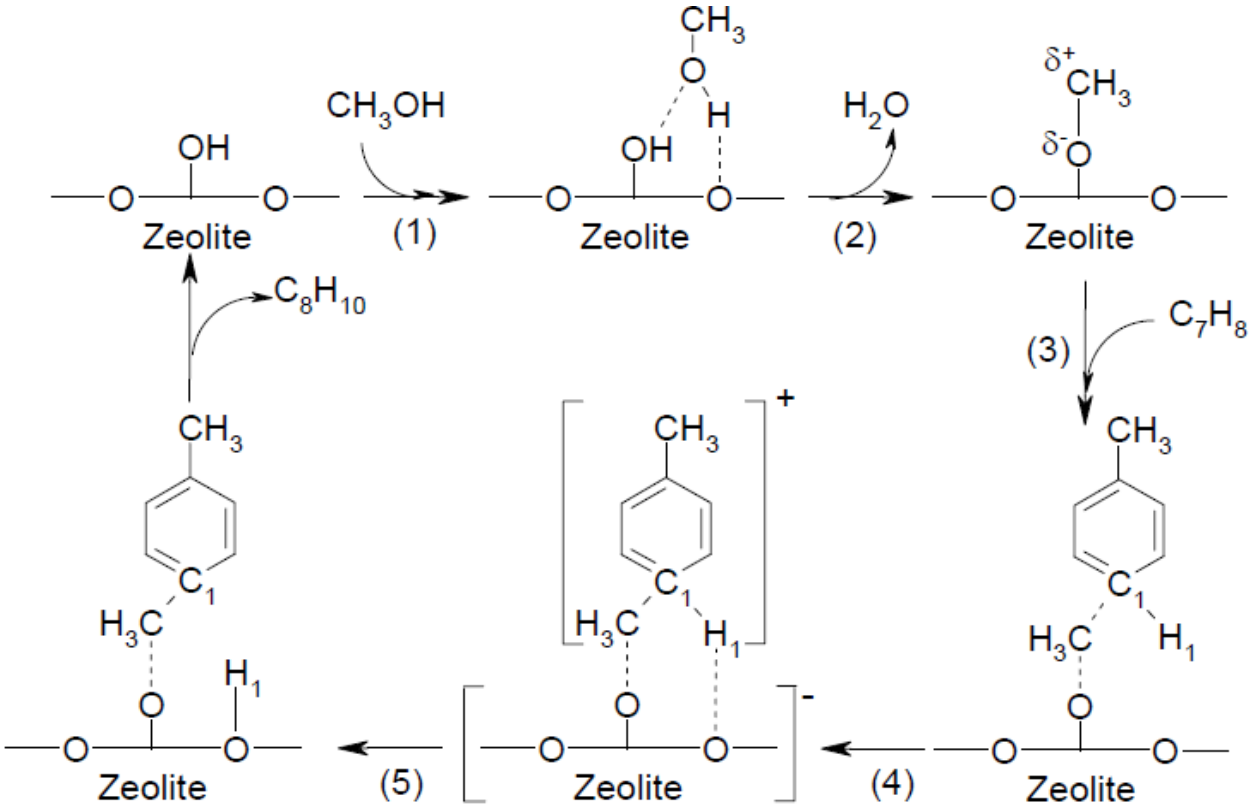

Scheme 2.4.1b: Reaction Mechanism of Ring Alkylation of Toluene with Methanol.

Sidorenko and Galich [62] proposed the formation of a methylene biradical ($:CH_2$) as the reactive methylating species. They opposed the idea of a CH_3+ ion being the ring alkylating species in the methylation of toluene, since the CH_3+ ion was shown to be extremely stable, prohibiting its reaction with the toluene ring. The reason for this was not very clear [62]. A methylene biradical species is also claimed as alternative in the MTG process [68].

Gas phase analysis has shown that during the alkylation of toluene with methanol over acidic ZSM-5 zeolites, besides para-xylene, also ortho- and meta-xylenes are formed within the pores of ZSM-5.The existence of large cavities with an average diameter of 9 Å, formed by intersecting straight and sinusoidal channels, are thought to facilitate their formation. It was believed that since the pore size of ZSM-5 is approximately 5.6 Å (the size of a benzene molecule), the diffusion of these bulky xylenes isomers (o- and m-xylene) out of the zeolite pores is limited; experiments had shown that the diffusion rate of p-xylene was three orders of magnitude higher than of the other xylene isomers [69]. However, in situ I.R. experiments of the catalyst under working conditions suggest that in addition to the rate of product diffusion, a subtle balance between the intrinsic slow rate of alkylation and the high rate of isomerization exists, which determines the observed selectivity in combination to the diffusion rate of the different xylene isomers [70], as will be explained now in more detail.

2.4.2 Reaction Mechanism for Side alkylation of Toluene with Methanol.

Mechanistic study done by numerous research groups have resulted in many different reaction mechanisms explaining the observed side-chain alkylation selectivity in the methylation of toluene with methanol. Most reaction mechanisms [30, 33, 71, and 35] are based on the mechanism proposed by Itoh *et al.* [32], which resembles an aldol type condensation as shown in scheme 2.4.2 Interaction of toluene with a basic and an acidic site was claimed, i.e., a zeolite framework oxygen and an extra framework Lewis cation, respectively, yielding a highly activated methyl group, whereas formaldehyde only interacts with a Lewis acid site. The interaction of toluene with the basic framework oxygens increases the reactivity of the side chain (the side chain becomes negatively polarised), whereas simultaneous interaction with an acid site stabilizes the toluene

molecule [32]. When toluene is adsorbed only on an acid site, the benzene ring is highly activated towards ring-alkylation. The concerted zeolitic acid-base interaction with toluene needed during side-chain alkylation was shown also by molecular modeling [72] and *in situ* poisoning of Cs-X catalysts during the methylation of toluene with an acid or base [73]. Co-feeding of the reactant mixture (toluene and methanol) with a basic compound (pyridine, *2,3*-dimethyl pyridine or butyl amine) resulted in a sharp catalyst deactivation [73]. After acetic acid submission to the feed also a sharp catalyst deactivation was observed [73]. These results indicate that a cooperative action of acid-base pairs is needed for the side chain alkylation.

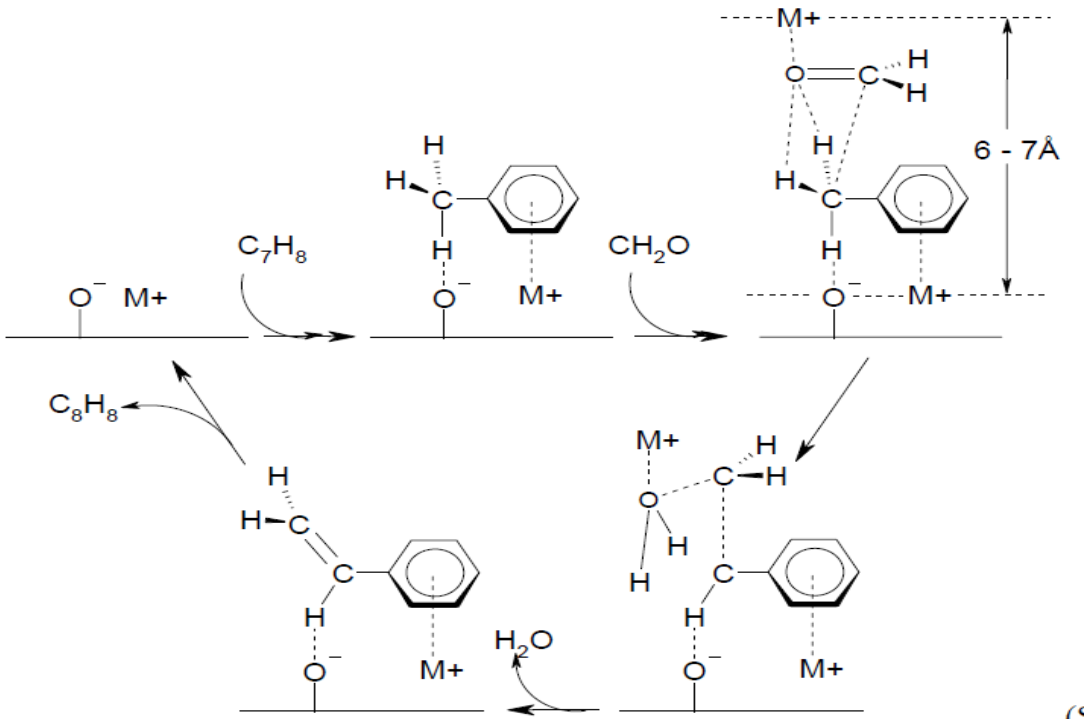

Scheme 2.4.2 Mechanism for Side-Chain Methylation of Toluene with Methanol

Many modifications of the side-chain alkylation reaction mechanism have been proposed.Instead of formaldehyde as alkylating intermediate, a unidentate formate resulting from formaldehyde oxidation was proposed by King and Garces [74].

Lacroix *et al.* [35] and Garces *et al.* [75] have proposed proton abstraction from toluene yielding a phenylcarbanion, which is subsequently alkylated by formaldehyde.

Garces *et al.* [75] claimed a redox mechanism that involves alkali metal vapors formed *in situ* during the alkylation. These alkali metal vapors are formed by the reduction of alkali metal oxides, which result from the decomposition of metal carbonates during the activation inside the zeolite pores.

However, this is highly unlikely if one considers the stability of alkali oxide and hydroxide clusters. It was proposed that the high selectivity towards styrene and ethyl benzene could also be the result of the presence of Cs+ cations in the zeolite pores, which sterically hinder the formation of the transition states that lead to the products of ring alkylation [76]. NMR experiments showed inhibition of the toluene mobility in the pores of Cs-X [76].

The activation of methanol and the dehydrogenation mechanism yielding formaldehyde by basic zeolites and its reaction in the alkylation of toluene towards styrene over basic zeolites is still a matter of debate. However, from the previous discussions it becomes clear that a subtle balance between methanol (activation and) dehydrogenation, toluene activation and zeolite structure is needed, when yielding styrene (and ethyl benzene).

2.5 Catalyst Preparation

Improvement of xylene production and styrene production from toluene methylation of methanol using acid and base catalyst, respectively, includes development of high selectivity catalyst and reactor design. The presence of several consecutive reactions is responsible for the typical trade-off between conversion and selectivity to the desired product. Therefore, the main challenges in the area of catalyst development for toluene methylation with methanol are the development of

catalysts which:

i. Stabilize the active species

ii. Possess high surface area

iii. Minimize coke formation and catalyst deactivation

iv. Minimize unwanted and undesired products and reactions, and

v. Active and selective towards increased xylenes (acid catalyst) and styrene (base catalyst).

For our study on ring alkylation of toluene with methanol, HZSM-5 zeolite was modified with different degree of meso porous ALMCM41 (Bi porous), vary the molar feed ratio of toluene to methanol, we were able to overcome some of the challenges stated above.

And for the side alkylation of toluene with methanol, the CsX catalyst was modified with different composition of Cs_2O, metal borate, and optimization of reaction condition to improve both the selectivity and conversion of styrene and toluene respectively.

CHAPTER THREE

EXPERIMENTAL SECTION

3.1 Experimental Set-up

The experimental runs for toluene methylation with methanol using acid and basic catalysts were carried out in a fully integrated, discrete, micro-processor controlled fixed-bed continuous flow reactor system (Model # 401C-0286, Autoclave Engineers, USA). The system consists of one tubular stainless steel reactor (0.312 I.D.×0.562 O.D.×6") attached with stainless steel one-zone furnace assembly through reactor furnace wall thermo well. The catalyst sample (400 mg) was packed inside the reactor and the reactor was pre-reduced (agitated) with flowing nitrogen (0.1 MPa) at 450^{o}C for 2 h. After which the temperature of the reactor was reduced to 410^{o}C which is the experimental (optimum) temperature. The flow rate of reactant feed and N_2 was maintained at 0.12 ml/min and 40 ml/min, using high pressure feeding pump (Series III Digital HPLC Pump, Autoclave Engineers), and smart mass flow controller (Model # 5850S/BC, Brooks), respectively. Each of the catalyst was run on a various feed ratio composition of toluene: methanol (ranging from 6:1 to 1:6) in order to study the effect of molar feed ratio on toluene conversion and product selectivity.The products were analyzed by online gas chromatograph (Agilent Technologies, Model # 6890N). The products were identified by

comparison with authentic samples. A schematic diagram of the reaction set up is shown in Figure 3.1a

The best acid catalyst for the ring alkylation was then modeled using the riser simulator reactor.The reactor was connected to a vacuum box through a four-port valve. The products were removed from the riser simulator at the end of the pre-set reaction period. A time/actuator assembly linked to the feed injection system controlled the four-port valve. The vacuum system was connected to a manually operated six-port sampling valve. This sampling valve was connected on-line to the gas chromatograph (Agilent Chromatograph Model 6890N) . Furthermore, the riser simulator reactor and the vacuum box were equipped with pressure transducers to monitor the pressure during and after the reaction periods. Both the reactor and the vacuum system were supplied by separated heating systems and both were well insulated.

The feed injecting system includes a gas tight syringe connected to switches to control the timer/actuator assembly on the four port valve and the data acquisition system. The data acquisition system allowed monitoring the change of pressure with time from both the reactor and vacuum pump box. A four-port valve, controlled by a timer/actuator assembly, was linked to the injection system. A vacuum system was also connected to the manually operated six port sampling valve which allows for sampling injections into the gas chromatograph. Both, the reactor and the vacuum system are located in temperature controlled ovens. Connections between components are accomplished using heated and well insulated lines. The unit was also equipped with two pressure transducers which allowed for continuous pressure monitoring during the reaction and post-reaction evacuation periods. A schematic diagram of the experimental setup is given in Figure 3.1b

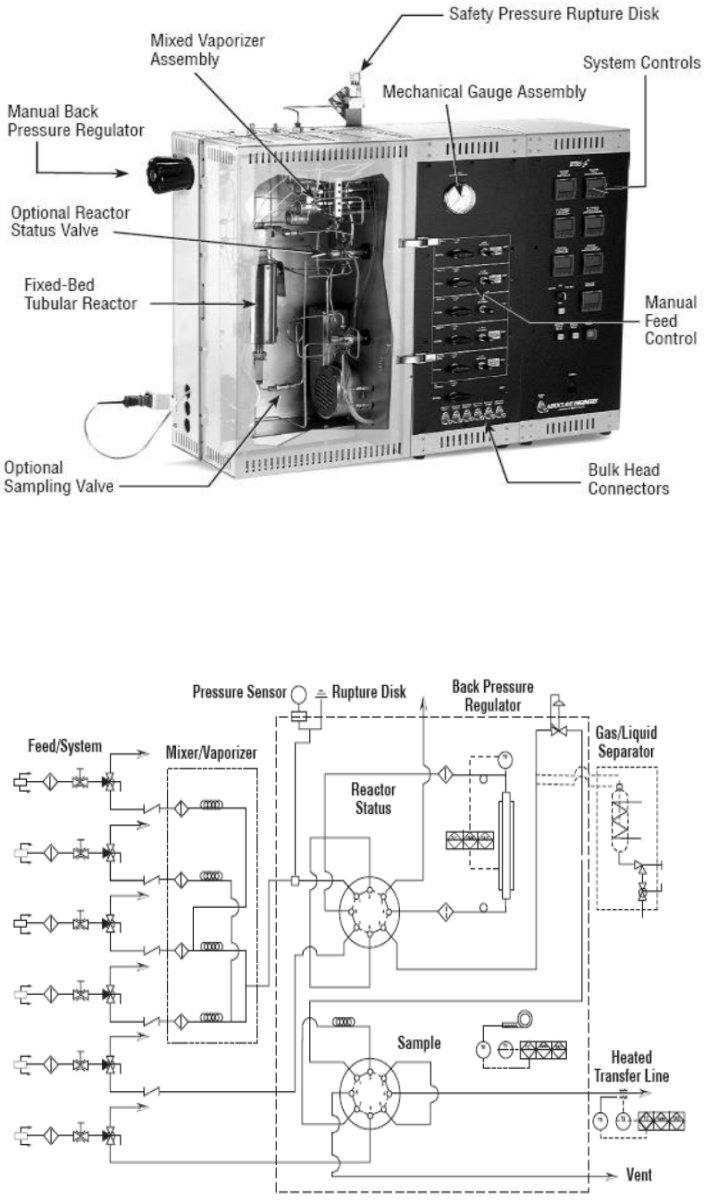

Figure 3.1a: Pictorial and Schematic diagram of a fixed bed reaction system

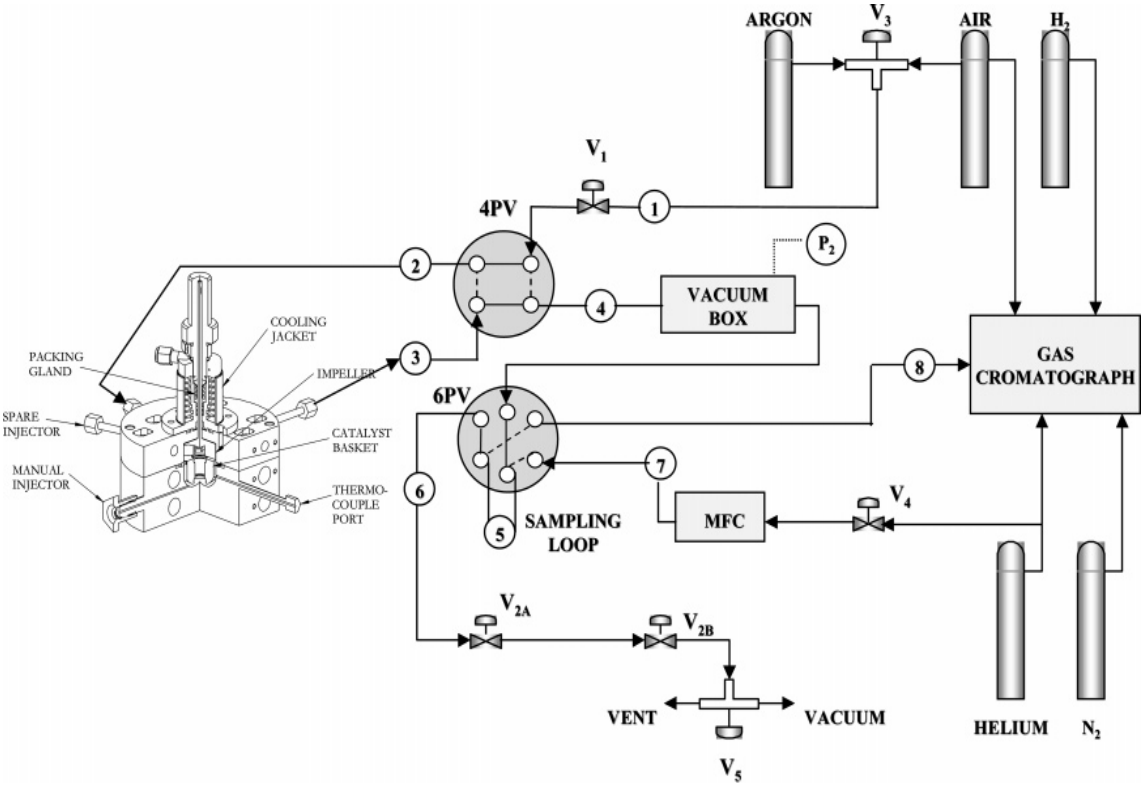

Figure 3.1b: Schematic diagram of the riser simulator experimental set-up

3.1.2 Riser Simulator

This novel reactor was invented by de Lasa [77] and it was designed to provide high gas phase circulation rates as well as intense catalyst mixing. In this respect, perfect mixing with the absence of coke profiles and gas channeling can be obtained with all catalyst particles being exposed to the same reaction environment. As mentioned by Pruski et. al. [78], good fluidization is achieved under typical riser conditions and using shaft spinning rates close to 7600 rpm.

The riser simulator can be used for several purposes: a) to test industrial catalysts at commercial conditions [79], b) to carry out kinetic and modeling studies for certain reactions, c) to develop adsorption studies [78], d) to use the data of this unit for assessing the enthalpy of cracking reactions. The riser simulator consists of two outer shells, the lower section and the upper section, which allow one to load or to unload the catalyst easily. The reactor was designed in such a way that an annular space is created between the outer portion of the basket and the inner part of the reactor shell. A metallic gasket seals the two chambers with an impeller located in the upper section. A packing gland assembly and a cooling jacket surrounding the shaft provide support for the impeller. Upon rotation of the shaft, gas is forced outward from the center of the impeller toward the walls. This creates a lower pressure in the center region of the impeller, thus inducing flow of gas upward through the catalyst chamber from the bottom of the reactor annular region where the pressure is slightly higher. The impeller provides a fluidized bed of catalyst particles as well as intense gas mixing inside the reactor. A schematic diagram of the riser simulator is shown in Figure 3.2

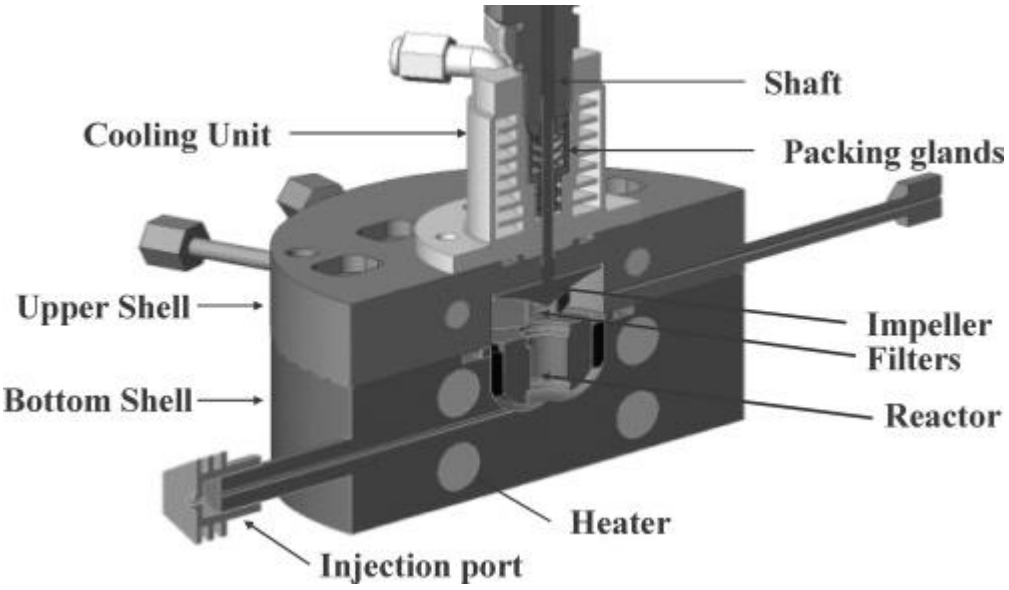

Figure 3.2a: Schematic diagram of the Riser simulator

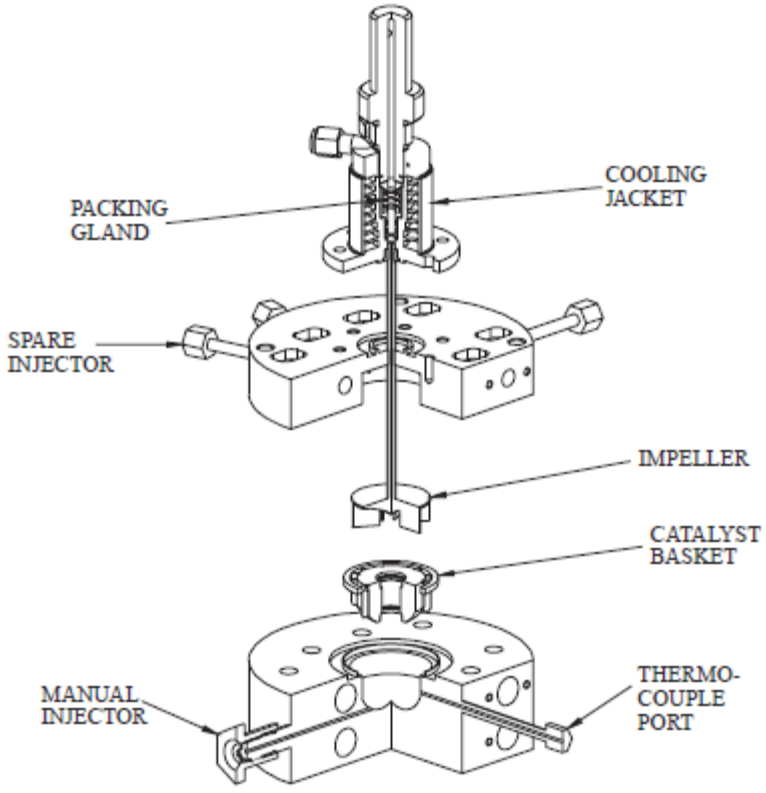

Figure 3.2b: Cross section of the riser simulator displaying the unit components.

3.1.3 Gas Chromatography (GC) System

The quantitative analysis of the reaction products were carried out online using an Agilent GC equipped with Flame Ionization Detector FID (Agilent Chromatograph Model 6890N), equipped with an HP-INNOWAX capillary column (Polyethylene glycol (PEG)) (length 60 m x internal diameter 0.32 mm x film thickness 0.50μm). Helium is used as the carrier gas, while air and hydrogen gases are used for the FID detector. Furthermore, liquid nitrogen is used to facilitate the initial cryogenic operation of the GC temperature program. The liquid nitrogen cools the GC oven to -30 °C. The flow of liquid nitrogen is administered by a solenoid valve actuated from the GC's internal oven temperature controller. The integrator allows strip chart recording as well as integration of the GC detector signal. The integrator is connected to the GC via a HPIL instrument network cabling system. Figure 3.3 shows a schematic diagram of the gas chromatography.

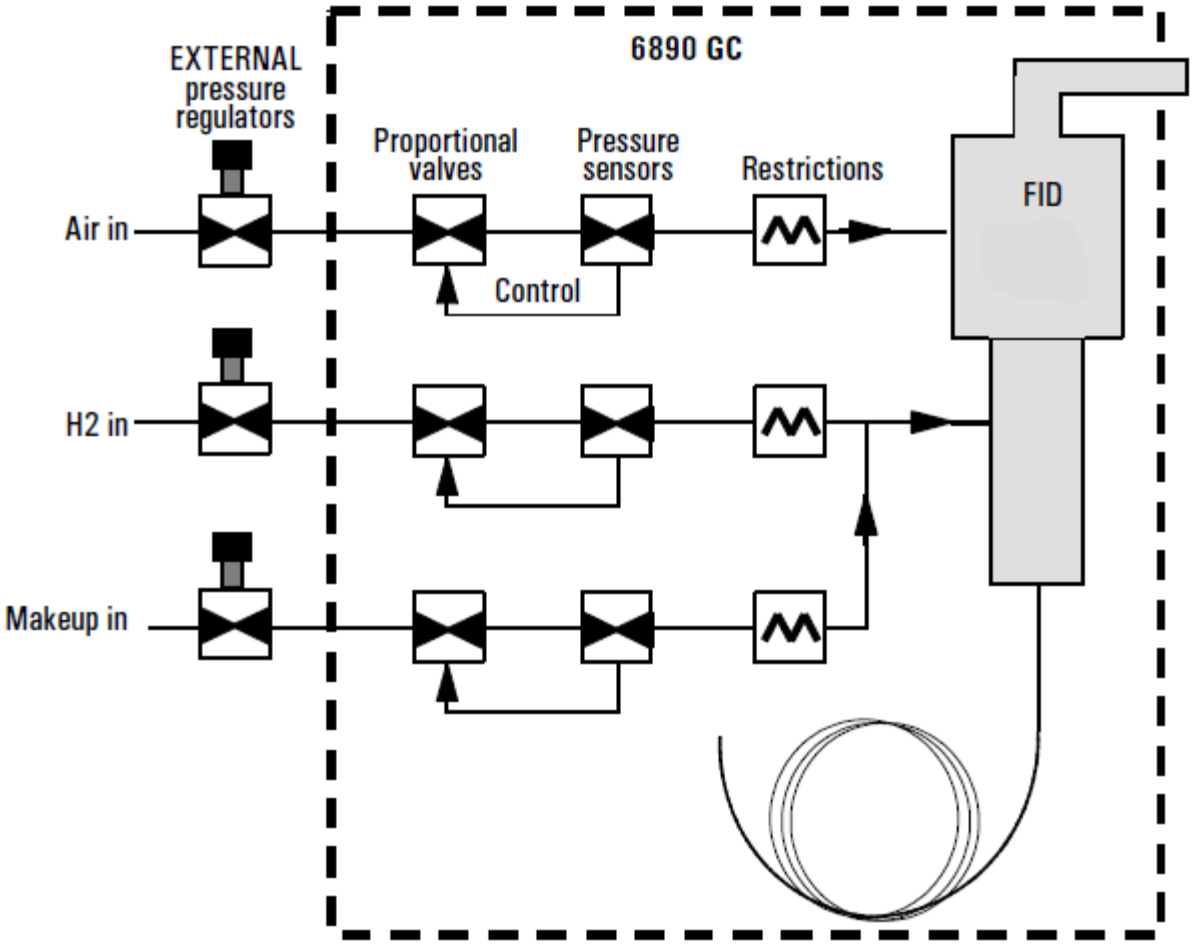

Figure 3.3: Schematic diagram of the gas chromatography.

3.2 EXPERIMENTAL PROCEDURE

3.2.1 Materials

All the precursors used in the synthesis of catalysts were obtained from different chemical companies. HZSM-5, NaX, CsOH were obtained from Tosoh Corporation Company,Junsei Chemicals and Kanto Chemicals Corporations, respectively.ALMCM41 was synthesized, while the chemical methanol (99.9%) and toluene (99.9%) were supplied by Sigma –Aldrich Company.

3.2.2 Catalyst Preparation

3.2.2.1 Synthesis of composite bi porous HZSM-5/ALMCM4 (ZM-1, ZM-2 and ZM-3) composite catalysts

ZM-1 and ZM-2 Catalysts were prepared by disintegrating 2g of ZSM-5 using 0.2M and 0.7M NaOH solution respectively. Disintegration was achieved by gradual heating at 100 °C for 24 hr in the presence of 4.5wt% cetyltrimethylammonium bromide (CTAB). Then the mixture was pH adjusted, aged at 100 °C for 24 h. The product was filtered, dried and calcined. ZM-3 was synthesized in a similar fashion, but during zeolite disintegration, the solution was stirred vigorously at 100^{o}C for 2hrs.Al-MCM-41 was synthesized according to the recipe of Beck et al. [80].

3.2.2.2 Synthesis of CsX, Cs20/CsX, and Metal borates/CsX

NaX was ion-exchanged with Cs^{+} (CsOH). The NaX has Si/Al ratio of 1.24 and surface area of 527 m^2/g. Into 200 ml of an aqueous solution of 16.8g cesium hydroxide (0.5 *M*), 30 g of NaX was immersed, and stirred for ca. 8 h. The slurry was filtered with Buchner funnel. The filtered cake was again immersed in a 200 ml of the aqueous solution of the 16.8g cesium hydroxide (0.5 *M*) and stirred ca. 8h.The immersion and filtration procedures were repeated three more time (total 5 times). The resulting slurry

was filtered, washed with a small amount (10ml) of water, and dried in an oven at 120^{o}C. The sample was then divided into two parts; One was calcined at 480^{o}C in air for 4 h (heating rate 10^{0}C/min) to be named as (Cs-X) and the other part was immersed in a 10 ml aqueous solution containing 0.5g CsOH in H_2O, and dried again in an oven at 120^{o}C and calcined at 480^{o}C in air for 4 h (heating rate 10^{0}C/min) to be named as (Cs_2O/CsX).

Metal borates/CsX catalyst was prepared by mechanical mixing of the metal borates with the above CsX in the desired amount of loading 5%, 10% and 15%(to know the effect of metal borates on the catalysts activity),followed by calcination in air at temperatures of 480^{o}C.

3.2.3 Catalyst Characterization.

A comprehensive catalyst characterization was done to determine the physico-chemical properties of the synthesized catalysts. The following characterization techniques were employed:

i. BET Surface Area and pore size distribution

The textural properties were characterized by N2 adsorption measurements at 77 K, using Quantachrome Autosorb 1-C analyzer. Samples were outgassed at 220 °C under vacuum (10-5 Torr) for 3 hours before N_2 physisorption. The BET surface areas were determined from the adsorption data in the relative pressure (P/P_0) range from 0.02 - 0.3, assuming a value of 0.164 nm2 for the cross-section of the N2 molecule.

ii. X-ray Diffraction (XRD)

XRD was use to determine the degree of crystallinity and meso porosity of the catalysts. Low- and high- angle X-ray diffraction patterns were recorded

on a Rigaku Miniflex II XRD powder diffraction system using CuKa radiation (lKa1 = 1.54051Å, 30Kv and 15mA). The XRD patterns were recorded in the static scanning mode from 1.2 - 60° (2q) at a detector angular speed of 2 °/min and step size of 0.02°.

iii. Fourier Transform Infrared Spectroscopy

Transmission FTIR spectra of adsorbed pyridine were recorded for all the catalysts using Nicolet FTIR spectrometer (Magna 500 model) in order to determine the nature of acid sites (that is, Brönsted and Lewis acid sites). The samples in the form of a self-supporting wafer (50 - 60 mg in weight and 20 mm in diameter) were obtained by compressing a uniform layer of zeolite powder. The wafer was then placed in an infrared vacuum cell equipped with KBr windows (Makuhari Rikagaku Garasu Inc.), and pretreated under vacuum at 450 C for 2 hours. The pretreated wafer was then contacted with pyridine vapor at 150 ºC for 5 min. followed by evacuation at 150 °C for 2 hours. The IR cell was cooled down to ambient temperature and placed in an IR beam compartment while under vacuum and transmission spectra were recorded. Desorption of pyridine was also carried out at 300 - 500 °C.

iv. Scanning Electron Microscopy (SEM) images and Electron Diffraction SEM (EDSEM)

SEM and EDSEM mappings were performed on selected sample to determine the morphology. These images were recorded using FE-SEM Nova NanoSEM 230.

v. Transmission Electron Microscopy (TEM)

TEM images were obtained with a FEI Titan electron microscope operated at 300 kV to determine the pore ordering and structural morphology of the zeolite.

vi. Thermo Gravimetric Analysis (TGA)

TGA was performed using a TA Instrument SDT Q 600 TGA analyzer to determine the level of mesoporosity of the bi-porous acidic zeolite catalysts.

vii. CO_2 Adsorption FT-IR Test

This was carried out on the catalysts to determine the nature and strength of basic sites of the catalysts.

3.3. GC Calibration

The calibration of the GC used in determining the product composition of the methylation of toluene reaction was done as explained in the following sections.

3.3.1. Determination of Retention Time for the Different Compounds

The retention times of all compounds of interest in this work were determined by analyzing pure samples of each of the compounds in the GC in turns. Table 3.1 shows the different compounds and their corresponding retention times. These retention times were used to identify each component of the reaction products.

Table 3.1: Retention time of different Compounds in the GC.

GC Conditions;

Flow rate of carrier gas (Helium):20ml/min

Oven Temperature: Programmed from 40^{o}C to 250^{o}C in 25mins

Compounds	Retention Time (min)
Gaseous Hydro carbon	3.019-3.45
Benzene	8.607
Ethyl benzene	13.114
Styrene	15.807
Toluene	11.217
Para-Xylene	13.300
Ortho-Xylene	14.500
Meta-Xylene	13.500
1,2,3 Tri methyl benzene	16.990-17.000
1,3,5 Tri methyl benzene	15.570
1,2,4 Tri methyl benzene	16.200
Tetra methyl benzene	18.000-18.2000

Retention Time may vary slightly with operating conditions.

3.3.2. Correlating GC response and actual weight percentage of each compound

In calibrating the GC, standard samples of different compositions containing ethyl benzene and the main reaction products (styrene, benzene, toluene) were prepared. The composition of the prepared samples were carefully chosen to reflect all the possible product compositions (obtained from preliminary experimental runs) under the different reaction conditions to be investigated. 0.2µl of the first sample was then injected into the GC and the GC responses (area %) for each of the components in sample were obtained. The sample procedure was repeated for all the other samples.

3.4. Catalysts Evaluation

Toluene methylation with methanol was carried out over the synthesized Bi porous catalysts (ZM1, ZM2 and ZM3), and the basic catalysts (CsX, Cs_20/CsX and $ZrB0_3$/CsX) in order to test their catalytic activity. All catalysts were evaluated at reaction temperatures of 410^OC. For each reaction temperature, experimental runs was repeated at least twice to enhance the reproducibility of the data,

3.4.1 Testing Procedure

For the experiments carried out in the fixed-bed reactor, the catalysts testing procedure is as described in Section 3.1.However, for the kinetic modeling done with the riser, the testing procedure involves charging the reactor with 0.8g of catalyst previously crushed and sieved to a particle size of ~ 60 µm diameter. The catalyst/reactant ratio was 5 (weight of catalyst = 0.81 g, weight of reactant injected = 0.162 g). The system is then sealed and tested for any pressure leaks by monitoring the pressure changes in the system.

Furthermore, the reactor is heated to the desired reaction temperature. The vacuum box is also heated to around 250^{O}C and evacuated to around 0.5 psi to prevent any condensation of hydrocarbons inside the box. The heating of the riser simulator is conducted under continuous flow of inert gases (argon) and the process usually takes few hours until thermal equilibrium is finally attained.

Meanwhile, before the initial experimental run, the catalyst is activated for 15 minutes at 620^{O}C with air. The temperature controller is set to the desired reaction temperature likewise the timer is set to the desired reaction time. At this point the GC is started and set to the desired conditions.

Once the reactor and the GC have reached their desired operating conditions, 200µl of the feed stock is injected directly into the reactor via a loaded syringe while the impeller is rotating at a speed of 6000rpm. After the reaction, the four port valve opens immediately ensuring that the reaction is terminated and the entire product stream sent online to the gas chromatograph via the pre-heated vacuum box chamber. The products were then analyzed in the gas chromatograph .After each experimental run, the catalyst is regenerated at condition similar to the initial activation.

3.5 Conversion and Selectivity Definition

The Conversion and Selectivity are defined as follows;

Methanol Conv. = {1 – (moles methanol recovered/moles of methanol fed)} X 100 (3.1)

Toluene Conv. = {1 – (moles Toluene in products/moles of Toluene fed)} X 100 (3.2)

EB.Select. = {Ethyl benzene yield/(Ethyl benzene yield + styrene yield)}X 100 (3.3)

Styrene Sel.= {Styrene yield/ (Ethyl benzene yield + styrene yield X 100 (3.4)

Styrene Yield={Toluene Conv.X Styrene sel./(total hydrocarbon products)} X 100 (3.5)

Xylenes Yield={Toluene Conv. X Xylenes sel./(total hydrocarbon products)} X 100 (3.6)

Para-xylene selectivity = {Para xylene Yield/Xylenes Yield} X 100 (3.7)

CHAPTER FOUR

RESULTS AND DISCUSSIONS OF ACID CATALYST

4.1 Catalyst Characterization Results (Physico Chemical properties)

4.1.1 XRD *and BET*

The XRD patterns of AlMCM-41, ZSM-5 and ZSM-5/MCM-41 composites are shown in Figure 4.1A. The textural properties are presented in Table 4.1. AlMCM-41 shows well resolved peaks typical to that of MCM-41 structure [81]. ZM-1 treated with 0.2M NaOH showed the transformation of zeolitic phase into bi-porous phase. The mesoporous content was determined to be 19wt. %. ZM-2 obtained using 0.7M NaOH show an enhanced meso content of 47wt. %. The XRD pattern of ZM-3, which contained fragments of ZSM-5, showed a pure meso phase.

The N_2 adsorption isotherm for composites shown in Figure 4.1B show an intermediate between type IV and I with H4 hysteresis loop indicating the coexistence of micro and meso pores [82]. The results presented in Table 4.1 show that the textural properties of composite zeolite change markedly leading to an intermediate BET surface area and increase in pore volume compared with parent catalysts. An increase in total pore volume signals the interconnection between mesoporous fragments and ZSM-5 structure.

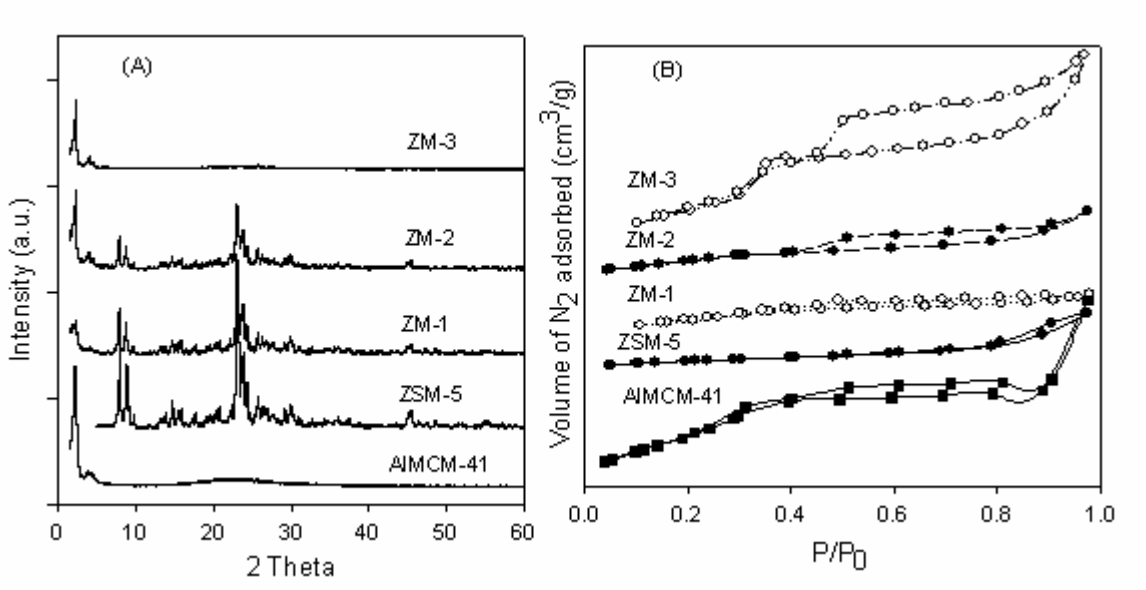

Figure 4.1: A) XRD Patterns for AlMCM-41, ZSM-5 and Composite Catalysts. B) BET for AlMCM-41, ZSM-5 and Composite Catalysts.

Table 4.1: Textural Properties of Catalysts.

Samples	Si/Al ratio	$d_{spacing}$ (nm)	a_0[a] (nm)	SA[b] (m2/g)	PD[c] (nm)	MPV[d] (cm3/g)	TPV[e] (cm3/g)
AlMCM-41	39	4.06	4.68	661	4.4	0.1	0.73
ZSM-5	13.5	3.85	-	284	-	0.16	0.29
ZM-1	8.5	3.85	4.45	404	2.5	0.18	0.35
ZM-2	12	4.06	4.68	468	2.4	0.18	0.25
ZM-3	13	3.86	4.45	527	2.2	-	0.72

[a]Unit cell; [b]Surface area; [c]Pore diameter; [d]Micropore volume; [e]Total pore volume.

4.1.2 FT-IR and TGA Results

Figure 4.2 shows the FT-IR spectra for calcined AlMCM-41, ZSM-5, and ZSM-5/MCM-41 composites. The absorption bands at 1201, 1082 and 777 cm^{-1} represent various stretching vibration of SiO_4 tetrahedron [83]. AlMCM-41 clearly shows no band at 550– 600 cm^{-1}, which is characteristic of zeolite subunits present in ZSM-5. Conversely, ZSM-5/MCM-41 composites ZM-1, ZM-2 and ZM-3 clearly show the presence of five membered rings ~551 cm^{-1}, whose intensity decrease with decreased ZSM-5 content.

The TGA analysis of composites showed characteristics decomposition of templates in three steps between 150^{o}C to 350^{o}C [84] (Table 4.2). ZM-1 (0.2M) showed a mass loss with comparatively low amount organics occluded in the composite (5.08%) but as the alkalinity increased to 0.7M (ZM-2), a higher consumption of surfactant occurs (~13.99%). The presence of large amount of surfactant in ZM-3 (26.34%) indicates the meso character similar to AlMCM-41 (27.74%).

4.1.3 TEM Result

The pore ordering and structural morphology of ZM-2 composite was analyzed with TEM (Figure 4.3). The image of ZM-2 shows that ZSM-5 forms a well aligned composite formation lying perpendicularly with the MCM-41 layers that are stationed with a well-ordered pore structures.

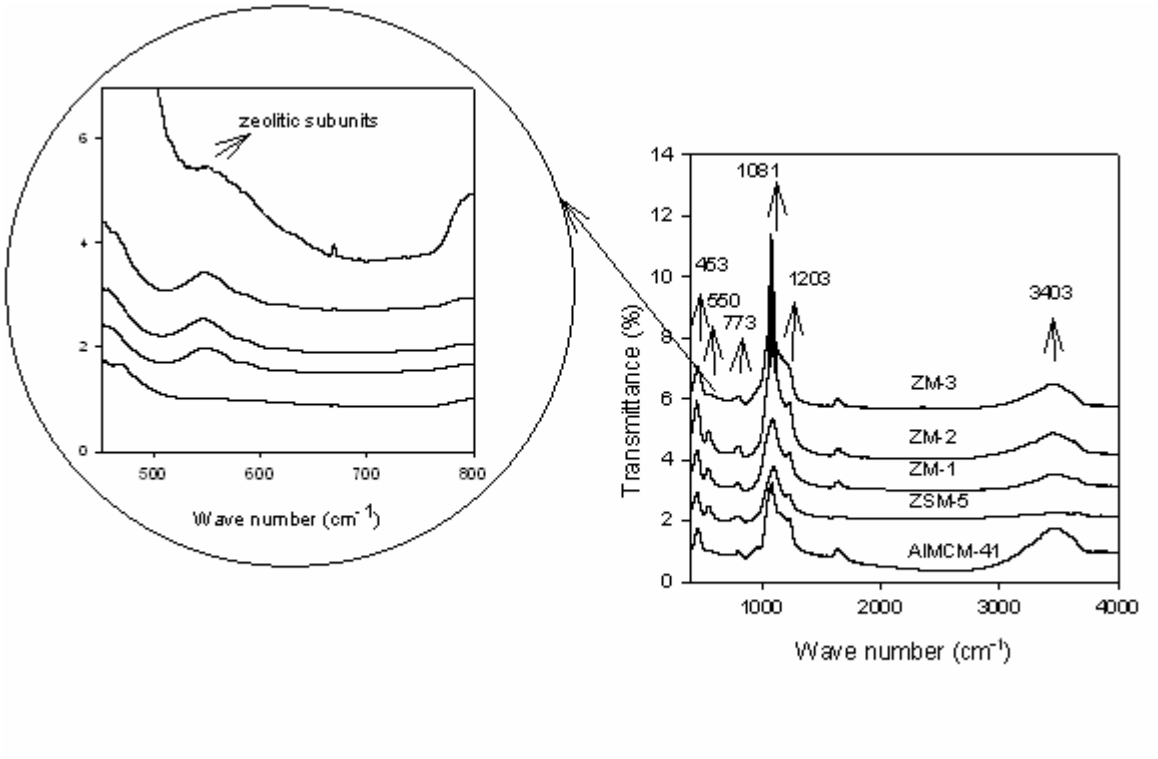

Figure 4.2: FT-IR spectra for AlMCM-41, ZSM-5 and the Composite Catalysts.

Table 4.2: TGA for the Synthesized Catalysts.

Sample	25-120 ^{o}C (%)	150 -350 ^{o}C (%)	380 – 800 ^{o}C (%)	Total Mass loss (%)
ZM-1	4.26	5.08	7.56	19.04
ZM-2	3.41	13.99	7.26	27.41
ZM-3	4.09	26.34	7.28	41.80
MCM-41	4.57	27.74	7.84	43.98

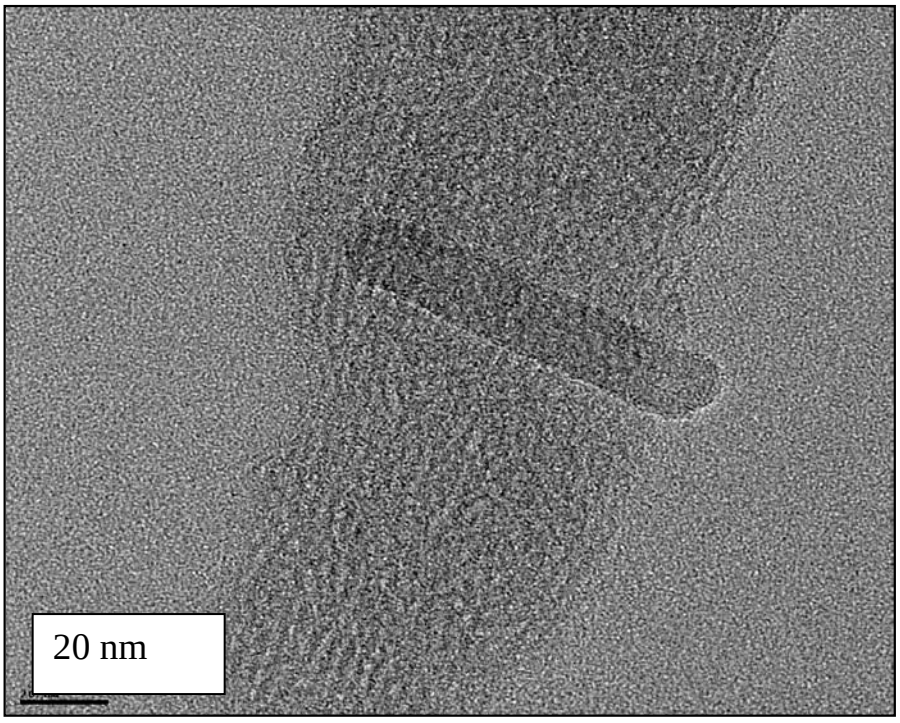

Figure 4.3: TEM micrograph for ZM-2

4.1.4 Pyridine FT-IR spectra

The amount of Lewis and Brønsted acid sites of AlMCM-41, ZSM-5, and ZSM-5/MCM-41 composites evacuated at 150^{o}C and 400^{o}C are presented in Table 4.3. AlMCM-41 contains a high amount of three-coordinated lattice Al standing for its Lewis acidity [85]. The Brønsted acidity of ZSM-5 is found to be highest, while ZM-3 showed highest Lewis acid site. The concentration of Brønsted sites at 150^{o}C decreased in the following order: ZSM-5 > ZM-2 (0.67) ~ ZM-1 (0.69) > MCM-41 (2.71)> ZSM-13 (10.24). These results substantiate that ZSM-5/MCM-41 samples have a unique acidity that can be attributed due the presence of zeolitic species in the meso structural framework of the samples.

Table 4.3: Acidic Properties of Catalysts.

Samples	150 ^{o}C mmol pyridine/g			400 ^{o}C mmol pyridine/g		
	B	L	L/B	B	L	L/B
AlMCM-41	0.1952	0.5302	2.71	0.0921	0.1588	1.72
ZSM-5	0.4497	0.2093	0.46	0.3296	0.1305	0.30
ZM-1	0.3919	0.2697	0.69	0.3286	0.1178	0.35
ZM-2	0.3541	0.2380	0.67	0.2658	0.1448	0.54
ZM-3	0.0711	0.7284	10.24	0.0374	0.4225	11.29

B = Bronsted acid site, L= Lewis acid sites.

4.2 Catalytic Activity

The results of the catalytic activity of the catalysts for toluene methylation over different feed ratios of toluene to methanol (6:1, 3:1, 1:1, 1:3, and 1:6) are shown in Table 4.4. The major reaction products observed were gases, benzene, xylene isomers (p-xylene, m-xylene and o-xylene), trimethyl benzenes and tetra methylbenzenes. The conversion of toluene increased over tested catalysts with toluene to methanol feed ratio of 6:1, 3:1 and 1:1. However, increasing methanol feed ratio to 1:3 and 1:6 decreased the conversion over mesoporous catalysts (AlMCM-41 and ZM-3) due to the very low active sites available for methylation. The biporous composites (ZM-1 and ZM-2) exhibited high toluene methylation compared to ZSM-5. In the case of ZSM-5, an intermediate activity was observed with maximum conversion of toluene of 47.74% at 1:6, whereas biporous composites in particular ZM-2 showed high toluene conversion of 54%. The observed high methylation of composites can be attributed to moderately strong acid sites and to the structural modifications. Toluene alkylation is reported to occur through chemisorptions of methanol on acidic sites, to form methoxonium ions, which can further react with weakly adsorbed toluene [86]. Since toluene conversion at the catalyst surface is diffusionally controlled, an interconnected pore between ZSM-5 and MCM-41 of composite is expected to allow more diffusion resulting in more toluene conversion.

The effect of feed ratio on mixed xylenes from methylation and benzene formation from disproportionation were examined. For a feed ratio of 6:1 (toluene: methanol) up to 1:1, there was an increase in mixed xylenes production for all catalysts with composite catalyst having the highest production. The mesoporous ZM-3 and MCM-41 showed a decrease in xylenes formation beyond the feed ratio of 1:1. A high methylation over bi-porous catalyst ZM-2 and ZM-1 compared to ZSM-5 and mesoporous catalyst (ZM-3 and

AlMCM-41) might be due to optimum L/B ratio leading to high xylenes production (Table 4.3). This is further supported by the moderate modification of the catalyst pore diameter that increased the contact area of reactants in adjusted diffusional path.

Figure 4.4(A-D) shows a comparison of product distribution over active catalysts ZSM-5, ZM-1, and ZM-2 at conversion level of 11%, 20%, 40%, 50%, 52% at toluene to methanol molar ratio of 6:1, 3:1, 1:1, 1:3, 1:6, respectively. The formation of benzene from toluene disproportionation and xylenes through methylation for each of the catalyst at various toluene to methanol ratio is in the order; 6:1>3:1>1:1>1:3>1:6. For all catalysts at all feed composition, the formation of benzene through toluene disproportionation is of the order; HZSM-5 > ZM-1 > ZM-2 (Figure 4A). The reactivity of toluene disproportionation, corresponding to the amount of benzene produced, increases with the acidic strength of zeolites [22]. In the present study, ZM-3 showed the highest Lewis to Brønsted (L/B) ratio, whereas ZSM-5 displayed the lowest L/B ratio. In line with acidity, at high toluene feed ratio, the excess toluene at catalyst active site of ZSM-5 undergoes disproportionation to form more benzene. In the case of composites, formation of benzene over ZM-1 in spite of similar L/B ratio of ZM-2 can be explained to the presence of high amount of ZSM-5 content that eventually increased the acidic strength (Table 4.3). Whereas for feed ratio with excess methanol, high methylation of reactants and further methylation of products occur to give xylenes, TMB and TeMB. Correspondingly, formation of more hydrocarbon gases occurs due to the decomposition of excess methanol that could not involve in methylation.

The selectivity to the mixed xylenes over different catalysts at feed ratios of 6:1, 3:1, 1:1, 1:3, 1:6, follow the order: ZM-2 > ZM-1 > ZSM-5. Comparatively, ZM-2 with intermediate acidic sites showed a good selectivity towards xylenes formation (Figure

4.4B). The lower selectivity of xylenes observed over ZM-1 is attributed to the rate of byproducts formation (TMBs and tetra methylbenzenes), thereby decreasing the selectivity toward xylenes (Figure 4.4 (C and D). The para-xylene selectivity in toluene methylation over ZSM-5, ZM-1, and ZM-2 is of the order; HZSM-5 > ZM-1 >ZM-2. The medium pore zeolite ZSM-5 with 10 membered ring channels showed higher Para selectivity as compared with composite zeolites. Among the composites, ZM-1 with more ZSM-5 character showed high para selectivity. It is therefore important for ZSM-5 to be preserved in the composite for high para selectivity.

Table 4.4: Toluene methylation over ZSM-5, ALMCM-41 and Composites at 410°C

Toluene: Methanol (molar ratio)	Samples	Toluene Conv(%)	gases	Benzene	p-Xylene	m-Xylene	o-Xylene	Total Xylenes	TMBs	TeMBs
(6:1)	ZSM-5	10.48	0.22	0.70	2.50	4.15	1.55	8.21	1.21	0.22
	ZM-1	10.57	0.18	0.51	2.39	4.11	1.58	8.08	1.52	0.28
	ZM-2	10.91	0.02	0.15	2.58	4.89	2.06	9.53	1.07	0.12
	ZM-3	9.38	0.00	0.00	3.92	2.9	2.38	9.20	0.18	0.00
	MCM-41	0.98	0.00	0.00	0.25	0.21	0.52	0.98	0.00	0.00
(3:1)	ZSM-5	16.43	0.99	0.63	4.21	6.00	2.23	12.45	2.12	0.24
	ZM-1	17.33	0.55	0.25	3.75	6.41	2.66	12.82	2.93	0.79
	ZM-2	19.63	0.24	0.12	3.93	7.81	3.44	15.18	3.39	0.68
	ZM-3	9.77	0.27	0.00	3.17	2.56	2.84	8.57	0.78	0.14
	MCM-41	2.03	0.24	0.00	0.46	0.39	0.93	1.78	0.00	0.00
(1:1)	ZSM-5	33.63	3.00	0.50	8.13	10.16	4.62	22.91	5.86	1.36
	ZM-1	36.06	2.37	0.15	7.43	11.62	5.05	24.10	7.31	2.13
	ZM-2	39.51	1.00	0.05	7.98	15.30	6.68	29.96	7.10	1.40
	ZM-3	28.20	1.73	0.00	8.49	6.91	6.02	21.42	3.50	1.54
	MCM-41	5.82	1.39	0.00	0.98	0.82	2.15	3.95	0.36	0.10
(1:3)	ZSM-5	46.98	11.26	0.23	8.74	13.93	5.09	27.77	6.10	1.62
	ZM-1	46.49	10.00	0.14	9.67	10.53	4.79	25.00	8.94	2.41
	ZM-2	47.08	10.40	0.00	10.25	8.91	7.65	26.82	7.75	2.11
	ZM-3	14.35	5.78	0.00	2.59	2.08	2.79	7.47	0.90	0.20
	MCM-41	2.15	0.00	0.00	0.48	0.41	1.07	1.98	0.10	0.07
(1:6)	ZSM-5	47.74	13.00	0.21	12.63	9.14	4.24	26.01	6.55	1.96
	ZM-1	49.17	10.19	0.10	13.06	9.69	4.73	27.48	8.19	3.20
	ZM-2	54.00	7.58	0.00	12.58	12.37	7.44	32.40	10.91	3.09
	ZM-3	8.76	0.00	0.00	2.98	2.35	2.90	8.23	1.08	0.00
	MCM-41	1.52	0.00	0.00	0.31	0.25	0.65	1.21	0.30	0.00

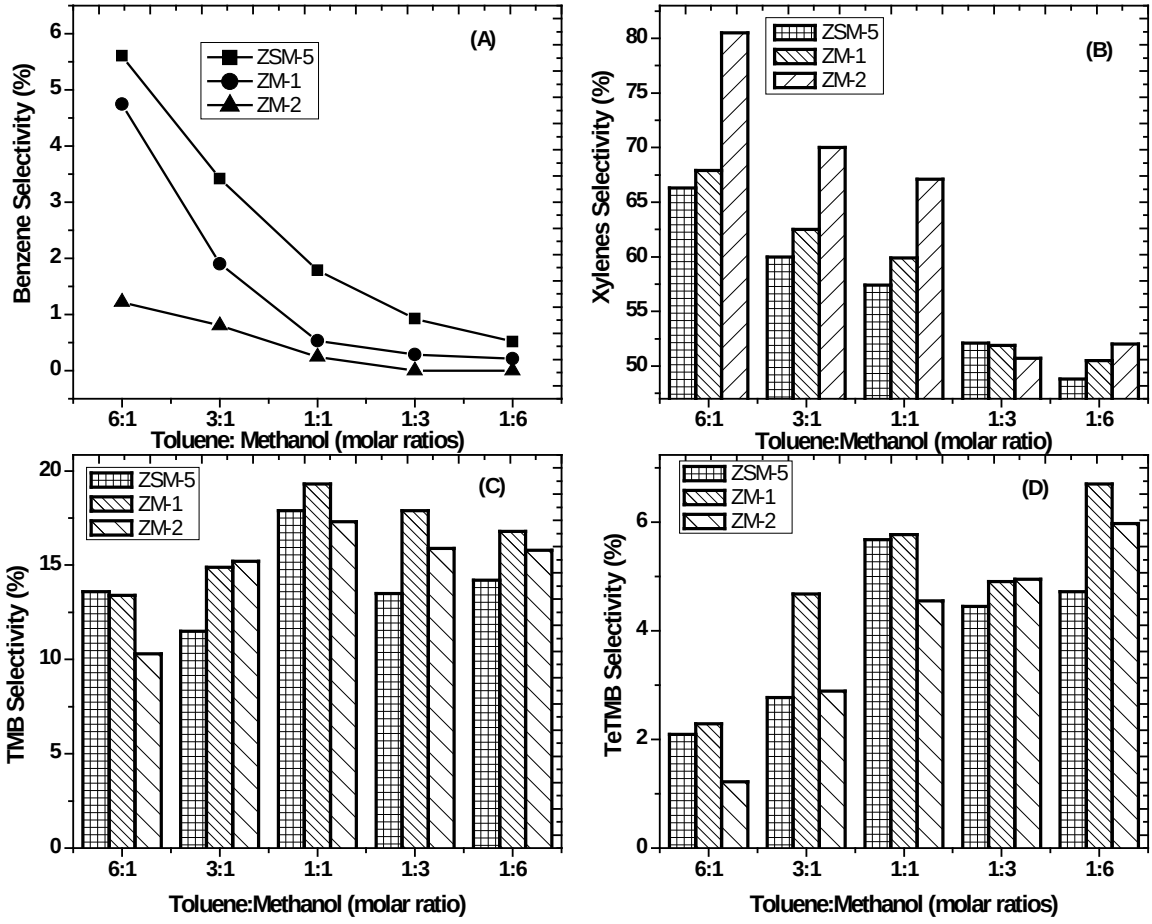

Figure 4.4: A) Benzene selectivity over ZSM-5, ZM-1, and ZM-2.B) Xylenes selectivity over ZSM-5, ZM-1, and ZM-2.C) TMB Selectivity over ZSM-5, ZM-1, and ZM-2.D) TeTMB selectivity ZSM-5, ZM-1, and ZM-2. At constant conversion of 11%, 20%, 40%, 50%, and 52% with different feed ratios at reaction temperature of 410 ^{o}C.

CHAPTER FIVE

KINETIC MODELING OF RING METHYLATION OF TOLUENE

5.1 Kinetic Study

Kinetic study of toluene ring methylation with methanol was carried over three catalysts; ZM-2 (bi-porous catalyst that gave the highest methylation among the synthesized catalysts), MOR/ZSM-5(mono micro porous) and HZSM-5(micro porous) using the riser simulator described in Chapter three. Based on the results obtained, a simplified power law kinetic model consisting of three reactions was developed to account for the transformation of toluene. Catalyst deactivation was also accounted for using both time-on-stream and reactant conversion decay functions.

5.2 Catalysts Used.

The calcined HZSM-5 with Si/Al ratio of 13.5 and surface area of 284 m^2/g was obtained from CATAL, UK. The uncalcined proton form of mordenite with Si/Al ratio of 18.3 and surface area of 364 m^2/g was obtained from Tosoh Chemicals, Japan. The calcined form of mordenite was then physically mixed with HZSM-5 in 1:1 ratio to form MOR/ZSM-5 catalysts. While the synthesis method for ZM-2 was as described in Section 3.2.2.

5.3 Catalysts Characterization

The catalysts were subjected to three characterization methods namely; XRD, BET surface area measurement and pyridine FT-IR .The testing procedure and purpose was as described in Section 3.2.3.

5.4 Catalytic Testing

The catalytic ability of the catalysts (ZM-2, MOR/ZSM-5 and HZSM-5) to ring methylation of toluene was tested in the riser simulator with the experimental procedure described in Section 3.4.1.Experimental runs were made at temperatures 300, 350 and 400^{o}C at the time interval of 3 – 20s.

5.5 Results and Discussions

5.5.1 Catalysts characterization results

5.5.1.1 Textural and structural properties

X-ray diffraction patterns of HZSM-5, MOR/ZSM-5 and ZM-2 are shown in Figure 5.1. Figure 5.1a is typical of HZSM-5; hence the zeolite structure is crystalline. ZM-2 (Figure 5.1c) shows a remarkable reduction in the peak intensities similar to HZSM-5 but with appearance of new peak at very low 2θ angle, which is a characteristic of mesoporous material. Diffraction patterns observed on MOR/ZSM-5 (Figure 5.1b) depicts combined characteristics of individual component of the composite structure as the peaks are characteristics of both mordenite and HZSM-5 structures. Therefore, it is expected that both HZSM-5 and MOR/ZSM-5 are more crystalline than ZM-2.

The BET surface areas were determined from the adsorption data. All catalysts exhibit large surface areas (> 280 m^2/g) as given in Table 5.1.

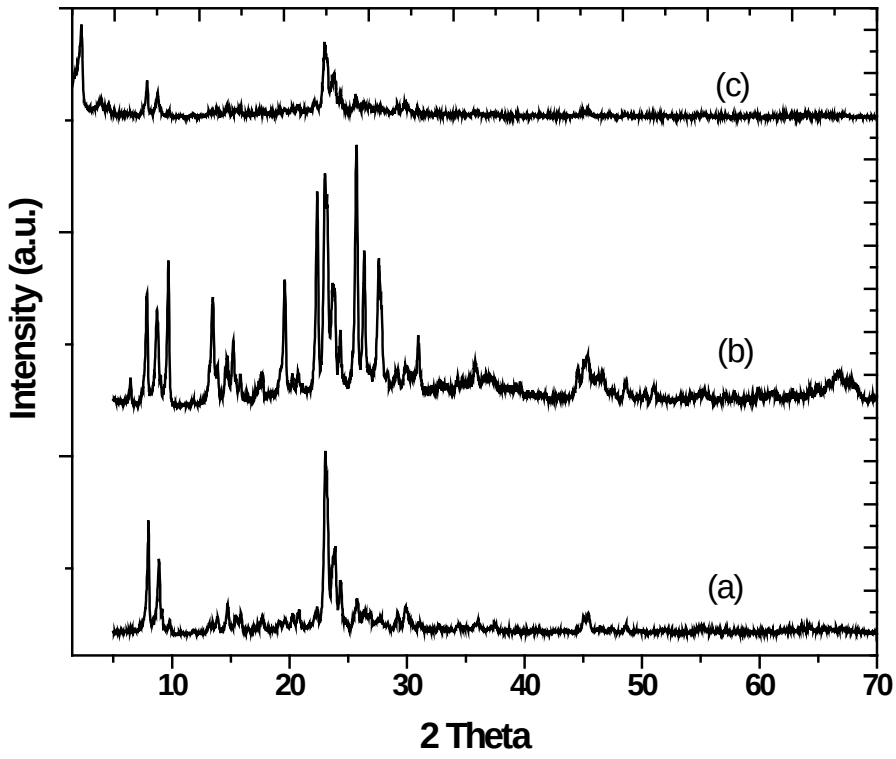

Figure 5.1: XRD pattern of zeolites: a) HZSM-5, b) MOR/ZSM-5, c) ZM-2

Table 5.1: Physicochemical and acid properties of the three zeolites samples

Samples	Si/Al ratio	Surface Area (m^2/g)	Brønsted acid sites (mmol/g)		Lewis acid sites (mmol/g)		L/B ratio (400 °C)
			150 °C	400 °C	150 °C	400 °C	
ZSM-5	13.5	284	0.4497	0.3296	0.2093	0.1305	0.40
MOR/ZSM-5	22	364	0.5381	0.4278	0.0447	0.0321	0.08
ZM-2	12	468	0.3541	0.2658	0.2380	0.1448	0.54

L=Lewis acid sites; B= Brønsted acid sites

5.5.1.2 Acid properties

The acid properties of zeolites are important in determining the catalytic activity and product selectivity for any catalyzed reaction. Acidic measurement was achieved by pyridine adsorption with FTIR. The spectra of the samples are shown in Figure 5.2. The recorded spectra after desorption at 150 °C shows distinguishable IR bands which are similar for all samples. The absorption peak at 1450 cm^{-1} is assigned to the C-C stretching of coordinately bonded pyridine on the Lewis acid sites while the peak at 1540 cm^{-1} is attributed to the C-C stretching vibration of pyridinium ion formed by interaction with Brønsted acid sites [86]. The peak at 1490 cm^{-1} has been attributed to the interaction of both types of acid sites with pyridine [87, 88]. Furthermore, the peak at 1620 cm^{-1} has been referred to as Lewis acid sites generated by extra framework aluminium species [89]. A weak band of Brønsted acid sites is observed at 1640cm^{-1}. The concentrations of Brønsted and Lewis acid sites were calculated from the integral intensities of individual bands characteristic of pyridine on Brønsted acid sites at 1550 cm^{-1} and band of pyridine on Lewis acid sites at 1445 cm^{-1}, with their respective molar absorption coefficient of $\varepsilon(B) = 1.67\pm0.1 cm\mu mol^{-1}$ and $\varepsilon(L) = 2.22\pm0.11 cm\mu mol^{-1}$ [90]. The amount of both Brønsted and Lewis acid sites expressed as mmol of acid sites per unit weight present on all the zeolite samples are given in Table 5. 1.

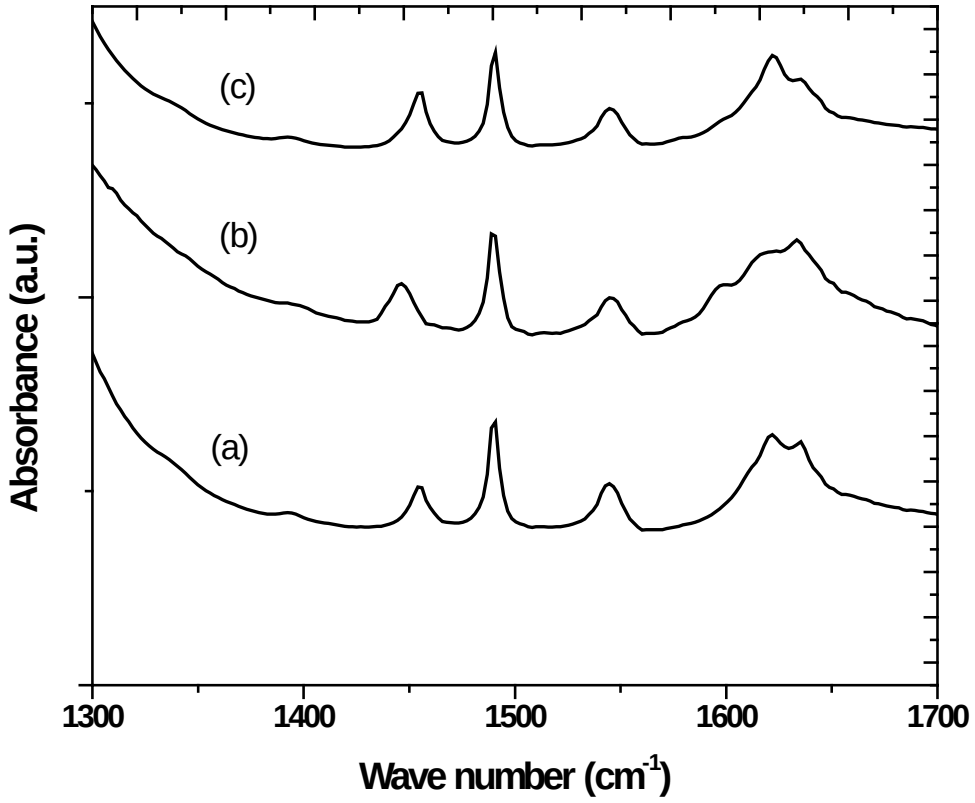

Figure 5.2: Pyridine IR spectra of desorbed samples at 150 °C: a) ZSM-5, b) MOR/ZSM-5, c) ZM-2.

5.5.2 Catalytic activity

The effect of reaction conditions (time and temperature) on the activity of the catalyst samples is presented in Figures 5.3 (A-C). As expected, toluene conversion increased with both temperature and time over all the catalysts. However for MOR/ZSM-5 (Figure 5.3B), at temperature above 350 °C there was no significant increase in toluene conversion. This may be attributed to an increase in methanol decomposition to hydrocarbon [58,91]. The products yield are presented in Tables 5.2 – 5.4. Yields typically increased as the temperature was raised. The presence of xylenes and benzene in the product mixture indicates that both alkylation and disproportionation reaction occurs concurrently. Likewise the presence of considerable amount of TMBs in the product stream signifies secondary alkylation of xylenes and transalkylation reaction. Comparison of the catalytic performance of the catalyst samples is shown in Figure 5.4. At all reaction temperatures, conversion was found to be highest for MOR/ZSM-5 relative to both HZSM-5 and ZM-2 (Figure 5.4A). Maximum toluene conversion of approximately 31%, 32 and 39% was achieved on HZSM-5, ZM-2 and MOR/ZSM-5 respectively at 400 °C and 20s reaction time. Furthermore, the catalysts selectivity were compared at a fixed toluene conversion of 25% (Figure 5.4B). Xylene yield of approximately 15.8% was achieved on both HZSM-5 and ZM-2. This value is more than that (~11%) on MOR/ZSM-5. On the other hand, benzene yield is approximately 6.2% on MOR/ZSM-5, a value which is at least 1.5 times greater than obtained on the other two catalysts. It is thus observed that toluene disproportionation on MOR/ZSM-5 contributes to a large extent to its high toluene conversion relative to the two other catalysts. Even though HZSM-5 and ZM-2 exhibit similar catalytic performance in the yield of xylene, a difference is noted in the yield of benzene and TMB on both catalysts. For

disproportionation reaction, higher benzene yield is achieved on HZSM-5. On HZSM-5 the ratio of benzene/TMB yield is around 2.5 while the same ratio on ZM-2 is almost unity. It can be deduced that toluene disproportionation is least favored on ZM-2 and follows the order MOR/ZSM-5 > HZSM-5 > ZM-2 while toluene methylation is the reverse (ZM-2 > HZSM-5 > MOR/ZSM-5).

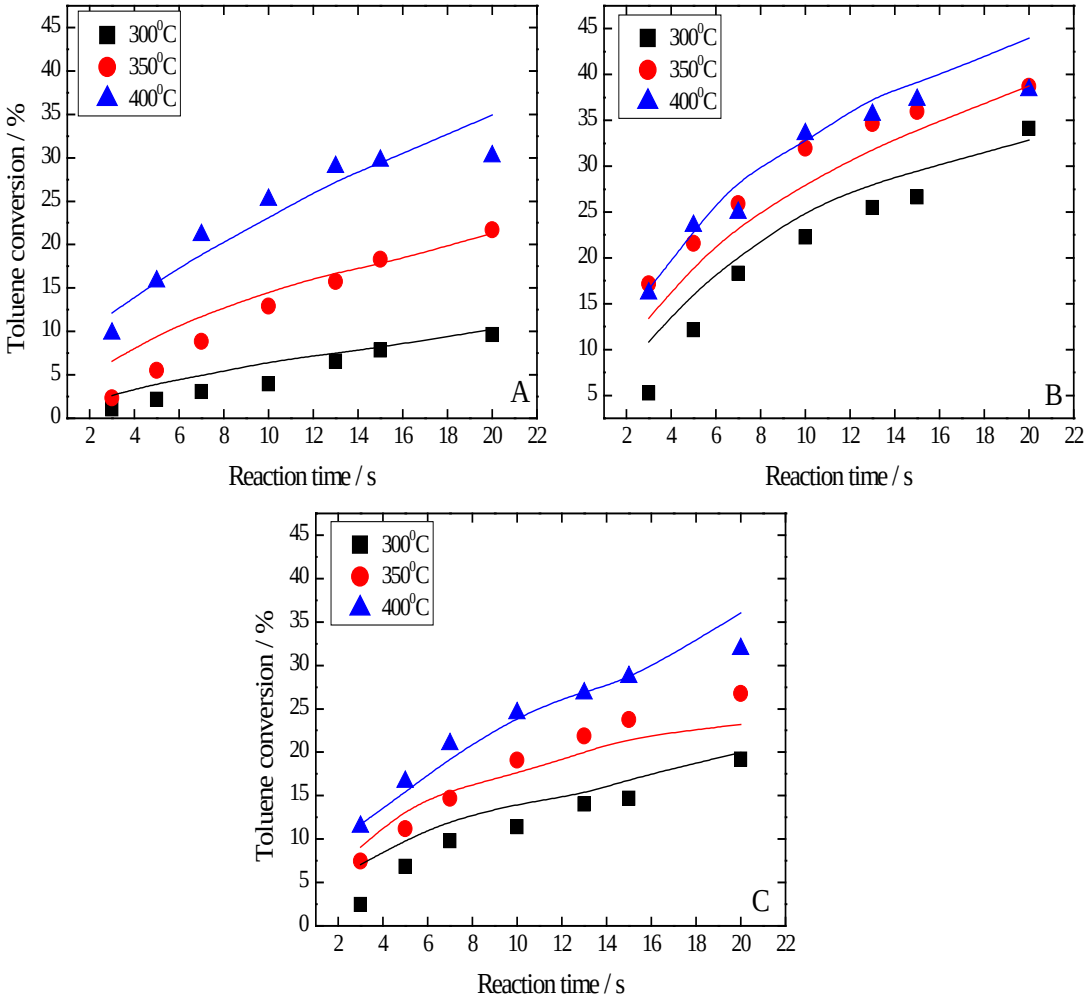

Figure 5.3: Catalytic activity of A) HZSM-5, b) MOR/ZSM-5, c) ZM-2. Reaction conditions: temperature = 300 – 400 °C, reaction time = 3 – 20 s, Toluene/MeOH molar ratio = 1:1

Table 5.2: Product distribution of toluene alkylation with methanol (Toluene/MeOH ratio = 1:1) on HZSM-5

Reaction time (s)	Toluene Conv. (%)	Yield (%)						
		Gas	Benzene	*p*-xylene	*m*-xylene	*o*-xylene	Total xylene	[a]TMBs
300 °C								
3	1.07	0.38	0.34	0.82	0.78	0.30	1.90	0.28
5	2.18	0.40	0.65	1.24	1.70	0.52	2.46	0.32
7	3.05	1.28	0.83	1.82	2.14	0.81	4.77	0.41
10	3.97	1.40	0.86	2.16	2.46	0.96	5.58	0.45
13	6.54	1.59	1.15	2.57	3.12	1.22	6.91	0.52
15	7.85	1.74	1.27	2.76	3.48	1.36	7.60	0.55
20	9.65	1.85	1.37	3.05	4.00	1.58	8.63	0.63
350 °C								
3	2.35	0.95	0.75	1.28	1.73	0.65	3.66	0.36
5	5.48	1.38	1.07	1.87	2.64	1.00	5.51	0.45
7	8.84	1.75	1.60	2.36	3.58	1.39	7.33	0.61
10	12.92	2.17	1.94	2.94	4.55	1.77	9.26	0.74
13	15.76	2.48	2.32	3.37	5.39	2.13	10.89	0.88
15	18.30	2.76	2.50	3.73	6.07	2.42	12.22	0.96
20	21.67	3.14	3.34	4.05	6.98	2.83	13.86	1.27
400 °C								
3	9.76	1.74	1.78	2.11	3.51	1.38	7.00	0.52
5	15.73	2.54	2.51	3.13	5.38	2.11	10.62	0.68
7	21.09	3.20	3.01	3.86	6.88	2.69	13.43	0.76
10	25.15	3.45	3.82	4.22	8.07	3.29	15.58	0.99
13	28.92	3.66	4.31	4.82	9.32	3.83	17.97	1.11
15	29.63	3.78	4.73	4.90	9.75	4.08	18.73	1.17
20	30.14	3.88	5.29	5.06	9.86	4.08	19.00	1.44

[a]TMB – all isomers of TMB, catalys/feed ratio = 5

Table 5.3: Product distribution of toluene alkylation with methanol (Toluene/MeOH ratio = 1:1) on MOR/ZSM-5

Reaction time (s)	Toluene Conv. (%)	Yield (%)						
		Gas	Benzene	*p*-xylene	*m*-xylene	*o*-xylene	Total xylene	[a]TMBs
300 °C								
3	5.26	0.60	2.46	1.08	2.22	0.95	4.25	1.03
5	12.12	0.85	3.63	1.80	3.76	1.59	7.14	1.73
7	18.31	1.81	4.76	2.42	4.99	2.10	9.51	1.92
10	22.25	2.19	5.67	2.79	5.85	2.47	11.11	2.37
13	25.47	2.23	6.44	3.35	6.98	2.92	13.25	2.64
15	26.61	2.67	6.64	3.58	7.26	3.06	13.90	2.70
20	34.13	3.83	8.88	4.14	8.76	3.67	16.57	3.33
350 °C								
3	17.17	1.94	4.47	2.03	4.34	1.90	8.27	1.88
5	21.55	2.32	5.38	2.57	5.56	2.40	10.53	2.25
7	25.91	3.11	6.67	3.02	6.47	2.80	12.29	2.54
10	31.97	3.75	7.64	3.79	5.25	3.50	12.54	3.19
13	34.65	4.22	8.82	4.02	8.57	3.70	16.29	3.25
15	35.98	4.33	8.69	4.26	9.02	3.91	17.19	3.42
20	38.72	4.84	10.19	4.50	9.71	4.19	18.40	3.90
400 °C								
3	16.10	2.19	4.33	1.83	3.92	1.77	7.52	1.78
5	23.48	2.95	5.78	2.64	5.67	2.56	10.87	2.49
7	24.87	3.45	6.37	2.70	5.77	2.60	11.07	2.36
10	33.47	4.25	8.01	3.80	8.15	3.65	15.60	3.31
13	35.60	4.81	8.81	3.95	8.50	3.86	16.31	3.53
15	37.25	5.19	9.02	4.32	9.24	4.16	17.72	3.74
20	38.27	5.39	10.03	4.28	9.24	4.09	17.61	3.76

[a]TMB – all isomers of TMB, catalyst/feed ratio = 5

Table 5.4: Product distribution of toluene alkylation with methanol (toluene/MeOH ratio = 1:1) on ZM-2

Reaction time (s)	Toluene Conv. (%)	Yield (%)						
		Gas	Benzene	*p*-xylene	*m*-xylene	*o*-xylene	Total xylene	[a]TMBs
300 °C								
3	2.45	0.78	0.31	1.50	2.03	0.99	4.52	0.57
5	6.83	1.26	0.44	2.15	3.21	1.45	6.81	0.80
7	9.80	1.50	0.50	2.60	3.92	1.79	8.31	0.99
10	11.38	1.71	0.52	3.14	4.37	2.20	9.71	1.18
13	14.02	1.85	0.54	3.50	5.17	2.51	11.18	1.39
15	14.66	1.89	0.62	3.44	5.37	2.53	11.34	1.46
20	19.17	2.37	0.81	3.75	6.63	2.91	13.29	1.77
350 °C								
3	7.44	1.18	0.53	1.87	3.35	1.38	6.60	0.87
5	11.16	1.55	0.73	2.41	4.37	1.82	8.60	1.07
7	14.68	1.94	0.79	2.94	5.41	2.25	10.60	1.28
10	19.10	2.31	1.03	3.50	6.75	2.83	13.08	1.59
13	21.86	2.55	1.14	3.85	7.46	3.14	14.45	1.80
15	23.73	2.68	1.29	3.94	7.84	3.32	15.10	1.95
20	26.74	3.00	1.55	4.32	8.86	3.78	16.96	2.26
400 °C								
3	11.43	1.56	0.79	2.26	4.34	1.82	8.42	1.04
5	16.55	2.07	1.04	2.99	5.85	2.46	11.30	1.36
7	20.91	2.47	1.30	3.63	7.40	3.07	14.10	1.75
10	24.50	2.82	1.79	3.95	8.15	3.54	15.64	1.86
13	26.74	2.87	2.03	4.31	8.93	3.90	17.14	2.02
15	28.62	3.12	2.42	4.63	9.75	4.28	18.66	2.21
20	31.88	3.19	2.64	4.85	10.29	4.59	19.73	2.41

[a]TMB – all isomers of TMB, catalyst/feed ratio = 5

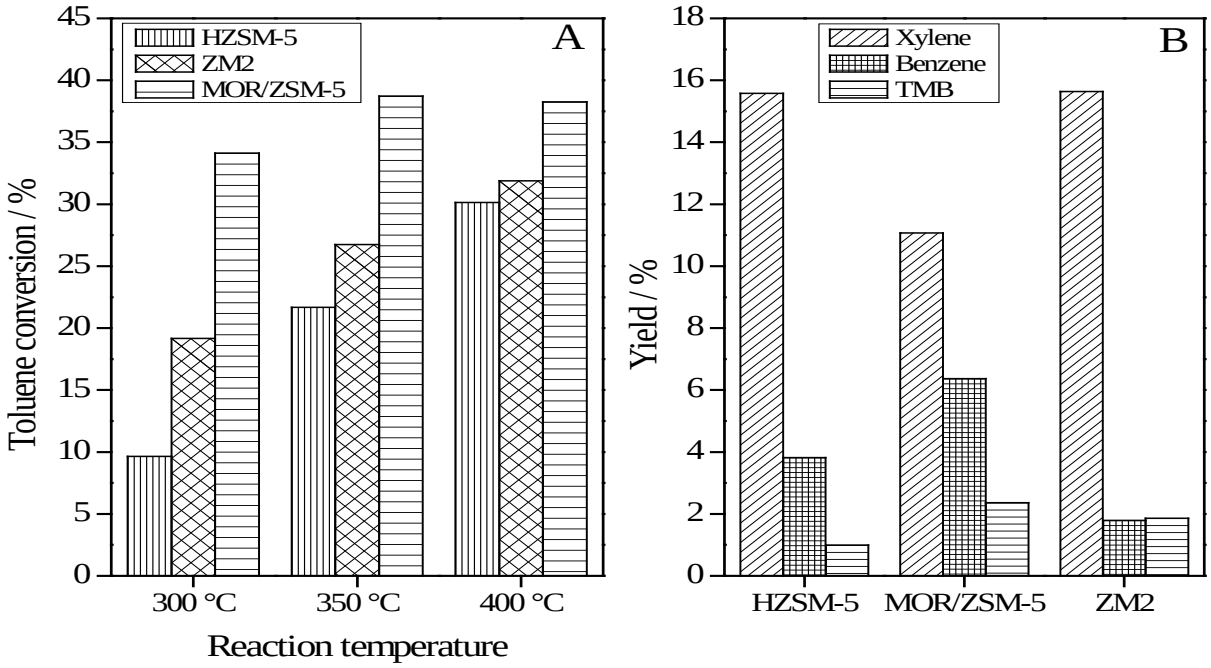

Figure 5.4: Comparison of catalytic activity on the three catalysts: A) toluene conversion as a function of temperature at 20 s; B) product yield at constant toluene conversion of 25%

5.5.3 Xylene yield and selectivity

Figure 5.5 shows the dependence of xylene yield on toluene conversion which exhibits a linear relationship. This trend is expected because both the methylation and disproportionation of toluene account for xylene produced. The proportion of xylene produced by either reaction can be estimated from the stoichiometry ratio of benzene and xylene from disproportionation reaction. Benzene in the product stream is produced only via toluene disproportionation reaction, therefore, corresponding xylene yield by disproportionation reaction (X_{disp}) can be determined. Subsequently, amount of xylene yield from alkylation of toluene with methanol (X_{meth}) is obtained by subtracting X_{disp} from the total xylene produce X_{tot} ($X_{tot =}. X_{disp} + X_{meth}$).

A comparison of X_{disp} and X_{meth} on the three catalysts is shown in Figure 5.6 at 400 °C for 20 s reaction time. It is clearly evident from this igure that ZM-2 is the most active for alkylation of toluene with methanol to form xylene. Figure 5.7 shows the trend of xylene and benzene selectivity for the alkylation reaction at 20s reaction time. Xylene selectivities of approximately 71%, 64% and 49% are achieved on ZM-2, HZSM-5 and MOR/ZSM-5 respectively for reaction temperature of 400 °C. Xylene selectivity shows no dependence on temperature except for HSZM-5 which shows an initial decrease from 300 °C to 350 °C and maintains a constant value afterwards. Similar to selectivity of xylene over MOR/ZSM-5, benzene selectivity is equally independent of temperature. On the other hand, both HZSM-5 and ZM-2 shows a linear dependence of benzene selectivity with temperature. Thus, it can be inferred that increase in temperature enhances decomposition of some methanol from the surface of HZSM-5 and ZM-2 catalysts. This creates empty sites which are occupied by toluene adsorbates for subsequent disproportionation reaction to benzene.

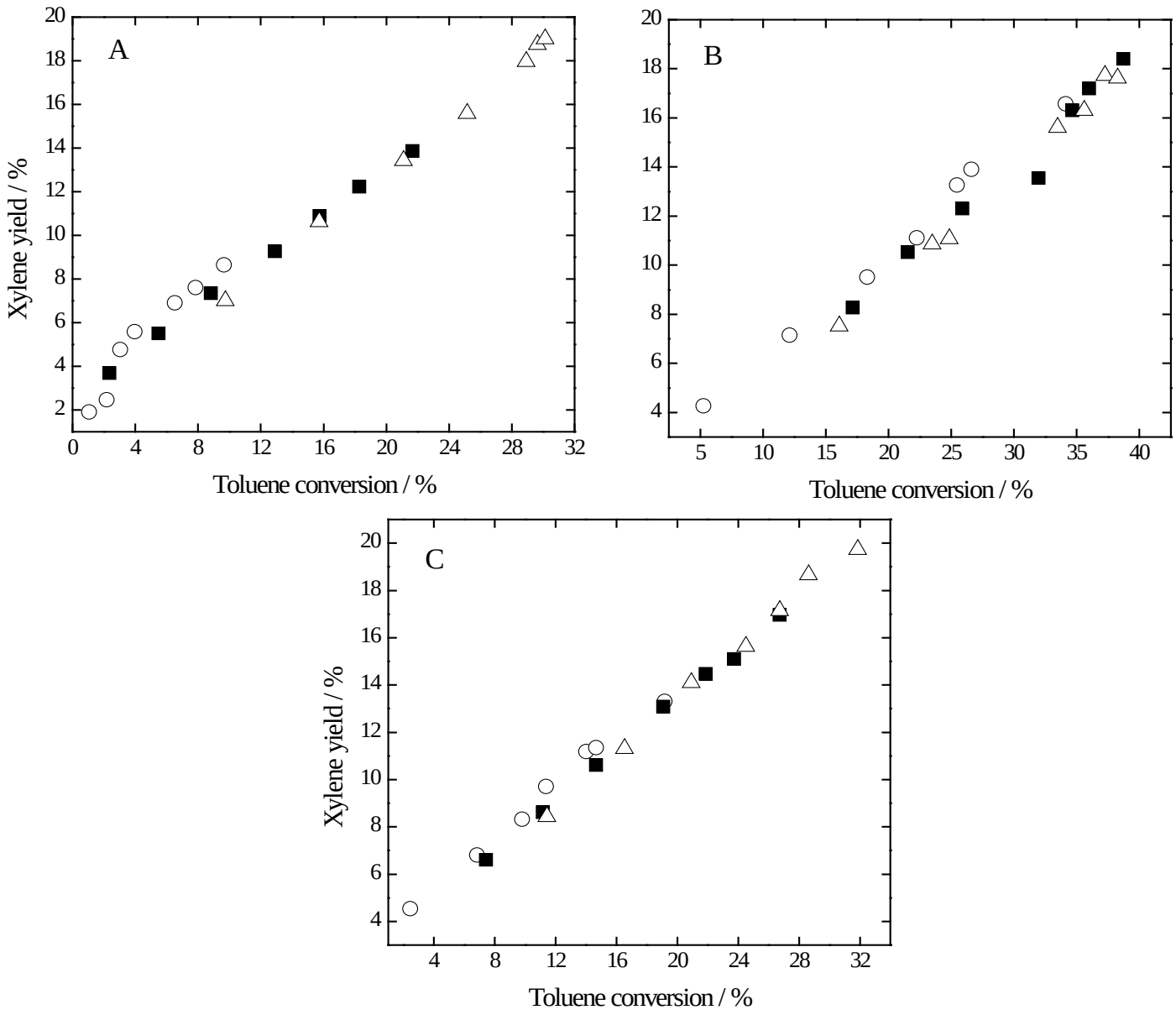

Figure 5.5: Dependence of xylene yield on toluene conversion for: A) HZSM-5, B) MOR/ZSM-5, C) ZM-2 at reaction temperatures (○) 300 °C, (■) 350 °C, (Δ) 400 °C

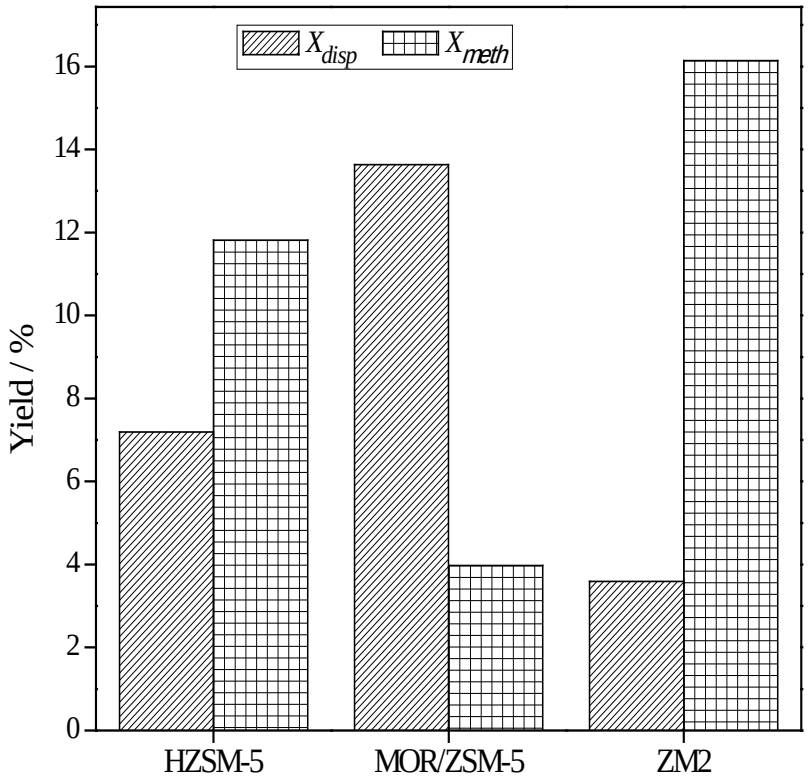

Figure 5.6: Comparison of xylene produced via methylation and disproportionation reactions on the catalyst samples at 400 °C for 20 s reaction time.

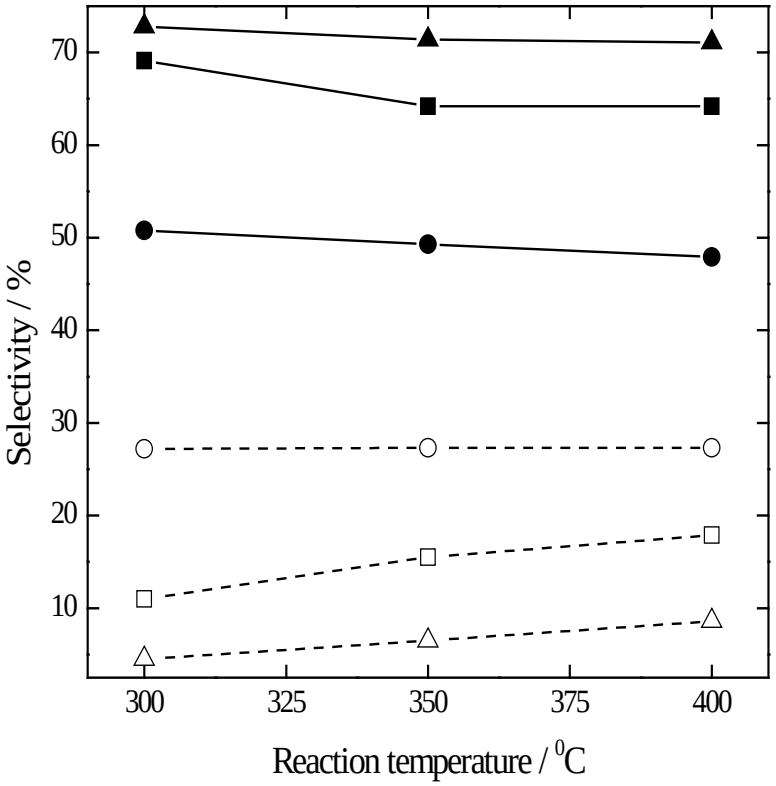

Figure 5.7: Xylene and benzene selectivity as a function of reaction temperature at 20 s over: (■, □) HZSM-5, (●, ○) MOR/ZSM-5, (▲, Δ) ZM-2. Full line and closed data – xylene selectivity; dash line and open data – benzene selectivity.

5.5.4 Acidity and Pore Structure

From the Py-IR, all the catalyst samples exhibited similar distribution of both acid site types as characterized by identified bands. MOR/ZSM-5 catalyst has predominantly brønsted acid sites and showed lowest Lewis to Brønsted (L/B) acid sites ratio (0.08), while HZSM-5 displayed intermediate L/B ratio of 0.40. ZM-2 has the highest L/B ratio (0.54) due to enhancement of lewis acid sites with corresponding decrease of the Bronsted acid sites. The variation of acid sites of these zeolites can be attributed to its preparation method and conditions as was identified by Zhu et. al. [22]. Essentially, toluene disproportionation has been reported to be favored over zeolites with strong acidity [22]. MOR/ZSM-5 has the most concentration of Brønsted acid sites which can be said to constitute the strong acid sites that catalyze disproportionation reaction of toluene as evident by the yield of benzene on the catalyst. Therefore, it can be concluded that activity of the catalyst samples towards toluene disproportionation is proportional to the number of strong Brønsted acid sites [22]. The ability of ZM-2 to preferentially catalyze the alkylation of toluene with methanol to form xylene can possibly be linked to the simultaneous presence of almost equal proportion of acid sites of both types. This is similar to the catalyst possessing medium-strength acidity which has been reported to show high catalytic activity and selectivity for toluene alkylation with methanol [22].

Pore channel configuration of the zeolite samples is another factor influencing their catalytic activity. Structure of HZSM-5 was slightly modified by incorporating mordenite (MOR/ZSM-5) and MCM-41 (ZM-2) to investigate on how possibly xylene yield can be enhanced through toluene methylation. Modernite is a large pore zeolite possessing unidirectional channel systems which are formed by 12 oxygen atom rings. This gives access to large molecules and accommodates the formation of bulky transition states

which precedes toluene disproportionation [92]. In the case of ZM-2, HZSM-5 (in the composite) are assembled onto the walls of MCM-41 which affords both reactants (toluene and methanol) easier access to the active sites due to the presence of meso pores. It can be said that in the presence of high catalytic surface covered by the alkylating agent, the rate of toluene alkylation is expected to proceed faster than toluene disproportionation. This assumption is supported by the work of Mikkelsen et al. [93] who reported an increase in toluene conversion upon addition of methanol and concluded that methylation of toluene proceeded faster than its disproportionation. ZM-2 has high degree of meso porosity compared to the other two zeolites which are basically micro-crystalline, and possess very high surface area. Therefore, a combination of meso porous structure with acidic properties of ZSM-5 could be promising for use as solid acid catalysts for xylene production through alkylation reaction.

5.6 Reaction Kinetics and Modeling

The purpose of this was to develop a simplified kinetic model for the detailed catalytic reaction. In particular, emphasis is on the main reactions which took place during toluene alkylation with methanol. The kinetic scheme employed therefore showed in details the main reactions as presented in scheme 1:

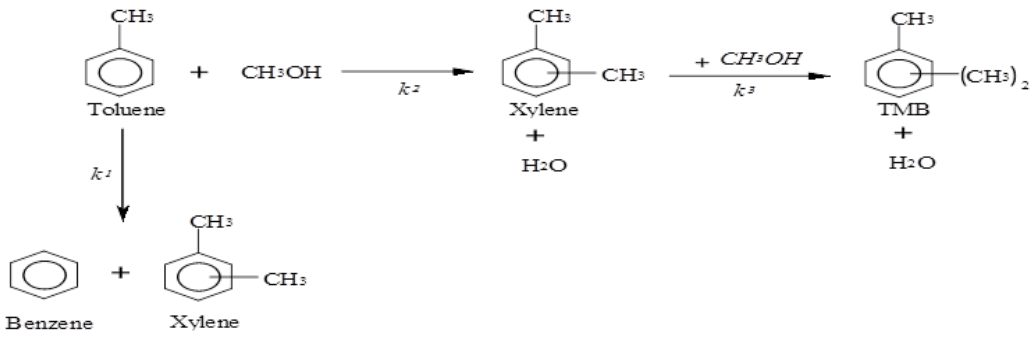

Scheme 1: Reaction network for toluene alkylation with methanol.

Similar reaction scheme have been proposed by Serra et al. [94] when toluene-methanol alkylation reaction was catalyzed by solid acids. For the purpose of developing the kinetic model, experimental data obtained for toluene/MeOH molar ratio of 1:1 is used.

5.6.1 Model Formulation

Power law model has been used to study the kinetics of the observed chemical reactions. The governing equations for the riser simulator are simply material balances for reactants and products of the chemical reaction similar to batch reactor. In general, for each independent reacting species, the material balance equation can be written as:

$$\frac{V}{W_c}\frac{dC_i}{dt} = r_i\varphi \tag{5.1}$$

where r_i and C_i are the reaction rate and mole concentration of each species in the system, V is the volume of the reactor, W_c is the mass of the catalyst, t is time in seconds, while φ is the deactivation function to account for catalytic activity loss. The rate equations for the elementary reactions can then be written as:

$$r_1 = -2k_1C_T^2 \tag{5.2}$$

$$r_2 = -k_2C_TC_M \tag{5.3}$$

$$r_3 = -k_3C_XC_M \tag{5.4}$$

Rate constant which is a function of pre-exponential factor and activation energy as defined by Arrhenius equation is expressed to incorporate temperature dependence of the reaction given as:

$$k_i = k_{0i}exp\left[-\frac{E_i}{R}\left(\frac{1}{T}-\frac{1}{T_0}\right)\right] \tag{5.5}$$

where k_{i0} is the pre-exponential factor of reaction *i* and E_i is the energy of activation of the reaction *i*. T_0 is referred to as the centering temperature which is the average of all the temperatures for the experiment. This was introduced to reduce parameter interaction as postulated by Agarwal and Brisk [95]. Reactions involving hydrocarbons inevitably yields coke deposit. Two catalyst deactivation functions were investigated in this study: reaction time (RT) and reactant conversion (RC) expressed as $\varphi_1 = \exp(-\alpha t)$ [96] and $\varphi_2 = \exp\left(-\lambda(1 - y_{reactant})\right)$ [97]; where α and λ are decay constants for their respective deactivation functions and $y_{reactant}$ is the weight fraction of toluene, (y_T).

Expressing concentrations C_i in terms of weight fraction of each species y_i, which are the measurable variables from the chromatographic analysis, we have:

$$C_i = \frac{y_i W_{hc}}{MW_i V} \tag{5.6}$$

where W_{hc} is the weight of feedstock injected into the reactor, MW_i is the molecular weights of the species.

Based on scheme 1, rate of reaction for toluene, benzene, xylene and TMB species can thus be written as:

$$\frac{dy_T}{dt} = -\left(2k_1 y_T^2 \frac{W_{hc}}{MW_T V} + k_2 y_T y_M \frac{W_{hc}}{MW_M V}\right)\frac{W_c}{V}\varphi \tag{5.7}$$

$$\frac{dy_B}{dt} = k_1 y_T^2 \frac{W_{hc} MW_B W_c}{MW_T^2 V^2}\varphi \tag{5.8}$$

$$\frac{dy_X}{dt} = \left(k_1 y_T^2 \frac{W_{hc} MW_X}{MW_T^2 V} + k_2 y_T y_M - k_3 y_X y_M \frac{W_{hc}}{MW_M V}\right)\frac{W_c}{V}\varphi \tag{5.9}$$

$$\frac{dy_{TMB}}{dt} = k_3 y_X y_M \frac{W_{hc} MW_{TMB} W_c}{MW_X MW_M V^2}\varphi \tag{5.10}$$

5.6.2 Model Assumptions

Summarized below are the assumptions taken into consideration for the model formulation:

1. The reactor operates under isothermal condition
2. Toluene disproportionation is considered to have irreversible reaction path and taken to be second order.
3. Effectiveness factor, η, is been taken to be unity. Similar assumption was used in previous works [98,99,56]
4. Isomers of xylene and TMBs are grouped together for a simplistic model evaluation.

5.6.3 Model Parameter Evaluation

Using non-linear regression analysis combined with fourth order Runge-Kutta routine to numerically integrate the rate equations, the kinetic parameters for the toluene-methanol alkylation reaction over the zeolite catalysts under study were evaluated. The developed model provides approximate estimates of all the kinetic parameters which are shown in Tables 5.5 and5. 6. The result of the model parameters were discriminated using the cross-correlation matrix as shown in Table 5. 7 which shows low and moderate level of parameter interaction with only a few exceptions for the parameters estimated with TOS model. Similar correlation values were obtained for RC model but the results are not shown. Also, the R-squared value of the regression is close to unity (0.99) and a parity plot of the weight fractions of the reactive species (Figure 5.8) gave an excellent fit between the predicted and experimental data, indicating the suitability of the proposed model. Extensive studies have been reported on kinetics of toluene alkylation reaction with methanol over ZSM-5 (modified and unmodified). In the present study, activation

energy for HZSM-5 has an approximate value of ~57 kJ/mol for toluene methylation reaction, irrespective of the deactivation model employed. This value is very much comparable with the works of previous authors as shown in Table 5.8. Vinek and Lercher [100] reported an apparent activation energy of 50 – 55 kJ/mol for toluene alkylation with methanol on H-ZSM-5, a value of 68 kJ/mol was reported by Rabiu and Al-Khattaf [99] and most recently, Odedairo et al [56] estimated a value of 47 kJ/mol for similar reaction on ZSM-5. For a modified ZSM-5 with magnesium, Sotelo et al. [101] obtained apparent activation energy of 60 kJ/mol. In general, activation energy for alkylation of toluene with methanol reported by several authors has been summarized by Mirth et. al. [102] to be typically in the range of 50 – 90 kJ/mol.

For both ZM-2 and MOR/ZSM-5, the apparent energy barriers for the reactions are lower than that on HZSM-5. It has been established that apparent activation energy is equivalent to half the summation of both intrinsic and diffusion activation energies [103]. Intrinsic activation energy however is related to acidity of the catalyst; high acid catalysts have low intrinsic energy. HZSM-5 is a two-dimensional channel structure defined by 10 member ring, with a medium pore of ~6 Å. This creates a steric effect on large molecules which imposes diffusional constraint. We can therefore conclude that, the pore structure of HZSM-5 plays more significant role in its reactivity despite having acid sites (Brønsted) of higher concentration and strength than ZM-2. Methylation of toluene on ZM-2 has apparent activation energy of 15 kJ/mol while 21 kJ/mol is calculated for MOR/ZSM-5 using time-on-stream catalyst deactivation model (Table 5.5). On the other hand, toluene disproportionation overcomes energy barrier of 20.3 kJ/mol and 13.1 kJ/mol on ZM-2 and MOR/ZSM-5 respectively. Similar activation energies for both reactions have been estimated with marginal difference (Table 5.6) when catalyst deactivation by

reactant conversion model is used. These kinetic parameter results are quite similar to the experimental observation in which methylation of toluene is best favored on ZM-2. Due to earlier mentioned diffusional limitation which has been assumed to influence the apparent activation energy of HZSM-5, the order of toluene methylation, ZM-2 > MOR/ZSM-5 > HZSM-5 and toluene disproportionation, MOR/ZSM-5 > ZM-2 > HZSM-5 follows a different pattern from the one proposed earlier. Xylene methylation on HZSM-5 has high activation energy of 70 kJ/mol (RT model). This further confirms the effect of diffusion limitation of large molecules within its pores. TMBs are more bulky molecules, larger than both xylene and toluene, hence higher barrier to overcome. While activation energy values of 15.2 kJ/mol and 17.8 kJ/mol are obtained for xylene methylation on MOR/ZSM-5 and ZM-2 respectively (both possessing larger pores).

5.7 Catalyst Deactivation

A gradual loss of catalytic activity of zeolites is due to coke deposition which poisons the active sites. Two simplified correlations have been utilized to determine the amount of carbonaceous deposits. Time-on-stream (TOS) model measures coke formation as a linear function with time and Reactant conversion (RC) model which considers coking to be proportional to hydrocarbon conversion. Values of the decay constants α and λ for TOS and RC models respectively are given in Tables 5.5 and 5.6. The values indicate low coke formation on the catalysts. Acid sites of zeolites play a vital role in coke formation, being severe on strong acid sites which promote condensation of olefins and aromatics which are potential coke precursors [22,103]. MOR/ZSM-5 has the largest amount Brønsted acid site (Table 5.1) which is known to enhance carbonaceous deposits in the pore structure. Also, zeolites of large pores used in toluene methylation reaction were reported to permit the formation of polynuclear aromatics which are coke precursors

[104]. Since mordenite possesses pores of larger diameters, large aromatic compounds are accommodated and trapped within the MOR/ZSM-5 hybrid which later condenses on the active site. Therefore, the geometrical constraints imposed by the channels of HZSM-5 on the reacting molecules are responsible for preventing large amount of coke formation [105].

Table 5.5: Estimated kinetic parameters for toluene-methanol (1:1) reaction over HZSM-5, MOR/ZSM-5 and ZM-2 catalysts using RT model

	k_1 m^6/kgcat.s ($\times 10^2$)	E_1 (kJ/mol)	k_2 m^6/kgcat.s ($\times 10^2$)	E_2 (kJ/mol)	k_3 m^6/kgcat.s ($\times 10^2$)	E_3 (kJ/mol)	α
			HZSM-5				
values	0.66	54.8	4.50	56.7	1.99	70.0	0.0052
95% CL	0.05	4.7	0.18	3.1	1.45	52.7	0.0039
			MOR/ZSM-5				
values	3.50	13.1	5.25	20.8	18.29	15.2	0.04
95% CL	0.26	3.0	0.53	7.8	2.49	10.3	0.008
			ZM-2				
values	0.65	20.3	9.09	14.6	10.29	17.8	0.01
95% CL	0.06	5.9	0.31	2.3	0.16	11.7	0.005

Table5.6: Estimated kinetic parameters for toluene-methanol (1:1) reaction over HZSM-5, MOR/ZSM-5 and ZM-2 catalysts using RC model

	k_1 m^6/kgcat.s ($\times 10^2$)	E_1 (kJ/mol)	k_2 m^6/kgcat.s ($\times 10^2$)	E_2 (kJ/mol)	k_3 m^6/kgcat.s ($\times 10^2$)	E_3 (kJ/mol)	λ
			HZSM-5				
values	0.76	57.4	5.29	57.1	2.48	65.8	0.60
95% CL	0.11	4.9	0.68	3.1	1.66	48.7	0.40
			MOR/ZSM-5				
values	8.45	18.2	12.83	23.3	44.52	19.3	2.84
95% CL	2.15	3.5	2.95	7.7	11.60	10.1	0.06
			ZM-2				
values	1.11	23.8	15.20	17.1	17.08	20.5	1.65
95% CL	0.22	5.7	2.51	2.3	3.68	11.2	0.50

Table 5.7: Correlation Matrix of toluene alkylation with methanol (toluene/MeOH ratio = 1:1) for RT model

	k_1	E_1	k_2	E_2	k_3	E_3	α
			HZSM-5				
k_1	1.0000	-0.6571	-0.4385	0.4715	-0.2676	0.2265	0.5919
E_1	-0.6571	1.0000	0.5436	-0.8305	0.1915	-0.2217	-0.0791
k_2	-0.4385	0.5436	1.0000	-0.5983	0.3725	-0.3300	0.3367
E_2	0.4715	-0.8305	-0.5983	1.0000	-0.3027	0.3836	-0.0032
k_3	-0.2676	0.1915	0.3725	-0.3027	1.0000	-0.9386	-0.1224
E_3	0.2265	-0.2217	-0.3300	0.3836	-0.9386	1.0000	0.0865
α	0.5919	-0.0791	0.3367	-0.0032	-0.1224	0.0865	1.0000
			MOR/ZSM-5				
k_1	1.0000	-0.1028	-0.3531	0.1246	0.0934	0.0666	0.8537
E_1	-0.1028	1.0000	0.1334	-0.7831	0.0374	-0.1985	-0.0591
k_2	-0.3531	0.1334	1.0000	-0.2252	0.4080	-0.1312	0.0628
E_2	0.1246	-0.7831	-0.2252	1.0000	-0.1176	0.4045	0.0604
k_3	0.0934	0.0374	0.4080	-0.1176	1.0000	-0.3739	0.2259
E_3	0.0666	-0.1985	-0.1312	0.4045	-0.3739	1.0000	0.0464
α	0.8537	-0.0591	0.0628	0.0604	0.2259	0.0464	1.0000
			ZM13				
k_1	1.0000	-0.2618	-0.1963	0.2706	-0.1590	0.1699	0.6259
E_1	-0.2618	1.0000	0.1377	-0.8277	0.1219	-0.2430	-0.1119
k_2	-0.1963	0.1377	1.0000	-0.2072	0.3909	-0.1776	0.5427
E_2	0.2706	-0.8277	-0.2072	1.0000	-0.2535	0.4355	0.1297
k_3	-0.1590	0.1219	0.3909	-0.2535	1.0000	-0.7698	0.0375
E_3	0.1699	-0.2430	-0.1776	0.4355	-0.7698	1.0000	0.1040
α	0.6259	-0.1119	0.5427	0.1297	0.0375	0.1040	1.0000

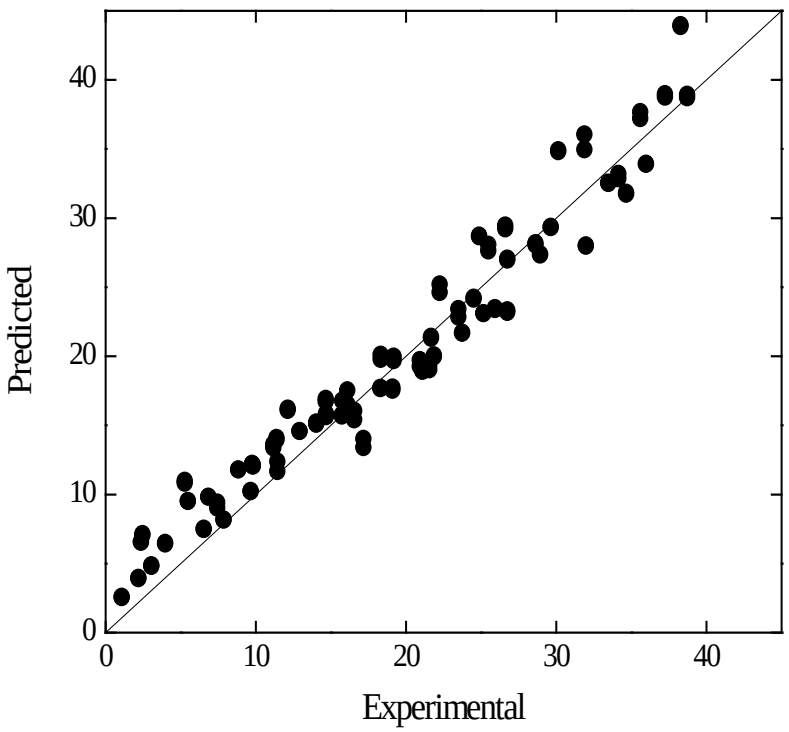

Figure 5.8: Parity plot of toluene conversion for the three zeolite samples

Table 5.8: Activation energies for toluene alkylation with methanol reported in literature.

Author	Catalyst	Temperature range (^{O}C)	Activation Energy(kJ/mol)
Bhat et.al.[107]	HZM-8	400 - 450	61
Sotelo et.al. [102]	Mg- modified ZSM5	460 - 540	60
Vinek et.al. [96]	HZSM-5	300 - 500	50 - 55
Rabiu et .al. [100]	ZSM-5	375 - 450	68
Odedairo et.al.[57]	ZSM-5	300 - 400	47
Present Study	HZSM-5	300 - 400	57

CHAPTER SIX

RESULTS AND DISCUSSION ON BASIC CATALYST

6.1 Catalysts Characterization Results (Physico Chemical properties).

6.1.1 XRD and BET

Figure 6.1shows XRD patterns of Cs-X, ZrB/Cs-X and Cs_2O/Cs-X. All samples retain crystalline structure of FAU, but the intensity of diffraction peaks decreased in the following order; Cs-X> Cs_2O/Cs-X > ZrB/Cs-X.

The BET surface areas are presented in Table 6.1. Since the weight of the zeolite unit cell increased by ion-exchange of Na with Cs and other components were added, the norma lized surface areas as defined below were calculated and included in Table 6.1.

Normalized surface area = (measured surface area) x (unit cell weight of zeolite X containing Cs and borate)/(unit cell weight of Na-X)

The normalized surface area of Cs-X was close to that of Na-X indicating crystalline structure was retained after ion-exchange with Cs. For ZrB/Cs-X addition of the borates followed by calcination at 773 K resulted in a decrease in surface area by about 15 %. Cs_2O loading on Cs-X decreases the normalized surface areas as well; however, crystalline structure seems to be retained for Cs_2O loaded Cs-X. It was reported that all Cs_2O species added to Cs-X were occluded in the zeolite cavities for the catalysts containing less than 2.9 Cs atoms per super cage (14.9 wt% Cs_2O), while parts of Cs_2O

were located on the outer surface of the zeolite crystals for the catalysts containing more than 5.1 Cs atoms per super cage (23.6 wt% Cs_2O) [107]. The Cs_2O contents used in the present study were below 14.9 wt%.

Accordingly, it is suggested that all Cs_2O species were occluded inside the cavities. A marked decrease in surface area for Cs_2O (7.8)/Cs-X is due to the fact that some of the cavities of the Cs_2O (7.8)/Cs-X are full of Cs_2O species.

The decrease in the surface area by modification of Cs-X was in the same order of the decrease in the XRD intensity; Cs-X > Cs_2O/Cs-X >ZrB/Cs-X.

6.1.2 SEM

SEM images (Fig 6.2) shows that Cs-X is composed mostly of crystallites in the range 1 ~ 3 μm, while ZrB/Cs-X is composed of crystallites in the range 1 ~ 3μm and small particles of 0.1 ~ 1 μm attached to the larger crystallites.

The SEM image of Cs_2O/Cs-X is similar to Cs-X. No Cs_2O particles are observed on the surface of Cs-X crystallites, which supports the idea that all Cs_2O species are inside the cavities.

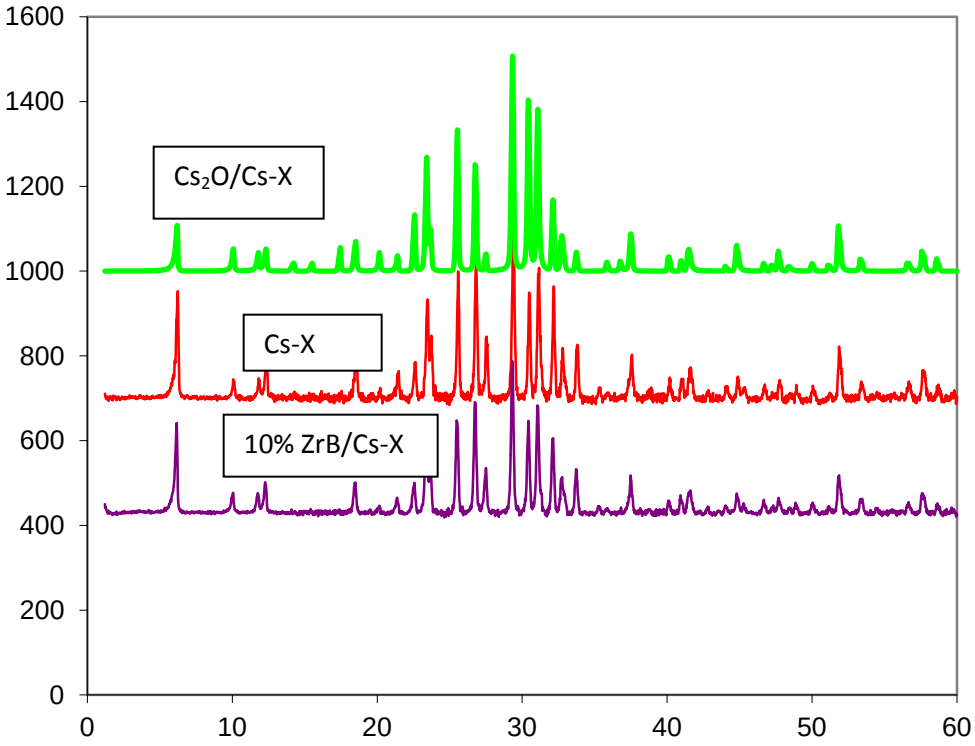

Fig 6.1: XRD Pattern of the Catalysts.

Table 6.1: Surface areas of catalysts

Catalyst	BET surface area	Normalized surface area
	$m^2 g^{-1}$	
Na-X	527	527
Cs-X	373	513
ZrB/Cs-X	286	438
Cs_2O/Cs-X	308	440

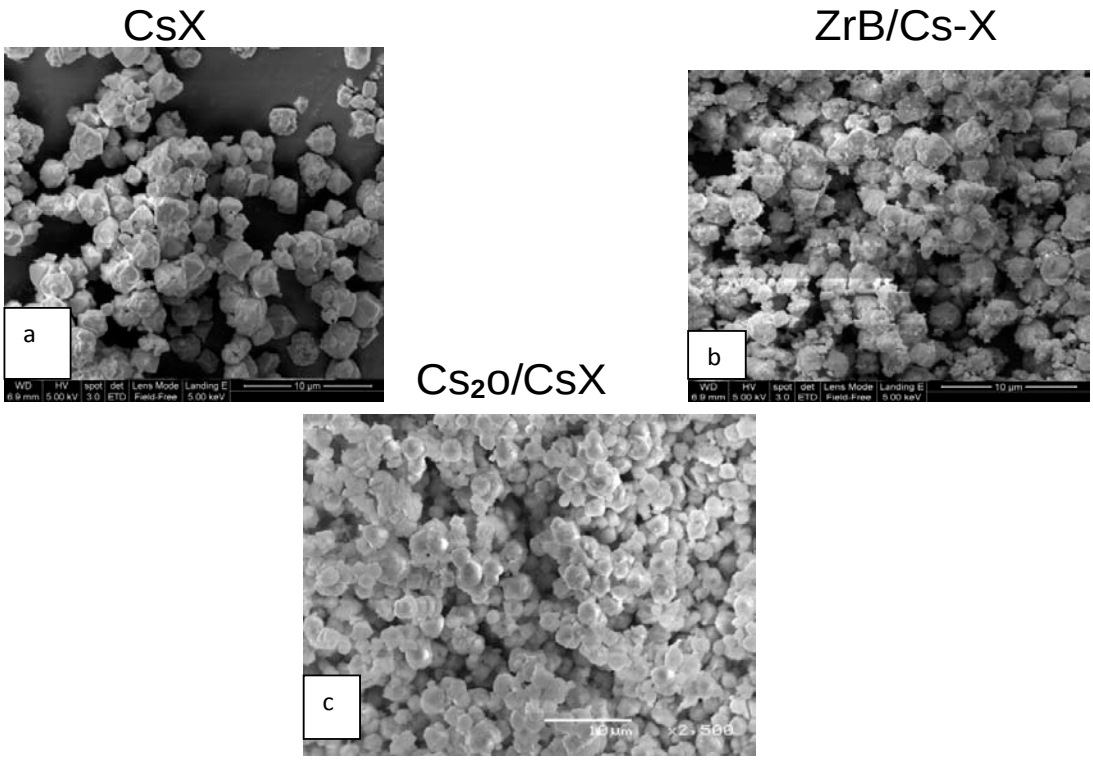

Fig 6.2: SEM diagram of catalysts. a) SEM diagram of Cs-X. b) SEM diagram of ZrB/Cs-X. c) SEM diagram of Cs_2O/Cs-X.

6.1.3 IR Spectra of CO_2

The result of CO_2 IR Spectra of the catalysts are shown in Fig 6.3. The adsorption of CO_2 was done at room temperature and evacuated at 373 and 523K. Two bands at 1480 and 1650 cm^{-1} appeared on Cs-X after evacuation at373 K are assigned to bidentate carbonate. No bands assigned to other carbonates such as unidentate carbonate and bicarbonate were observed after evacuation at 523K. By evacuation at 523 K, these bands were eliminated. The basic sites on Cs-X were in such strength that they cannot retain CO_2 on evacuation at 523 K.

For ZrB/Cs-X, because of strong band below 1500 cm^{-1} due to the presence of B, only one band at 1650 cm^{-1} was observable for ZrB/Cs-X. The band was assigned to bidentate carbonate. The intensity of the band at 1650 cm^{-1} is slightly weaker for ZrB/Cs-X than for Cs-X, the basic sites on Cs-X were slightly weakened by modification with zirconium borate. A small difference in O-H stretching region between Cs-X and ZrB/Cs-X was noted. The intensity of the band at 3740 cm^{-1} was weaker for ZrB/Cs-X than for Cs-X. Zirconium borate may interact with OH groups of Cs-X.

CO_2 was adsorbed much stronger on Cs_2O/Cs-X than on Cs-X. After pretreatment at 723 K, a broad band was observed at about 1400 cm^{-1}. The band is ascribed to ionic carbonate (CO_3^{-1}), and ascribed to Cs_2CO_3. The carbonate formed during preparation partly remained on the surface after the pretreatment. Four bands appeared at 1380, 1440, 1650 and 1680 cm^{-1} after evacuation of the CO_2 adsorbed Cs_2O/Cs-X at 373 K. The two bands at 1380 and 1650 cm^{-1} are the same as observed for Cs-X, and assigned to bidendate carbonate. The band intensity was much higher for Cs_2O/Cs-X than for Cs-X. Two bands at 1440 and 1680 cm^{-1} were observed only for Cs_2O/Cs-X. Since splitting of the bands was 240 cm^{-1}, these bands could be assigned to bicarbonate different from the carbonate

showing bands at 1380 and 1650 cm^{-1}. The bands at 1440 and 1680 cm^{-1} eliminated on evacuation at 523 K. The bands at 1380 and 1650 cm^{-1} remained a little after evacuation at 523 K.

From the results described above, it is suggested that addition of Cs_2O to Cs-X generate both weak basic sites and strong basic sites in addition to mild basic sites present on Cs-X. Some parts of Cs species exist in the form of Cs_2CO_3. It was reported in the literature, that addition of Cs_2O generated strong basic sites, which was confirmed by this study. In addition to the strong basic sites, generation of weak basic sites was observed in the present study, which has not been reported so far.

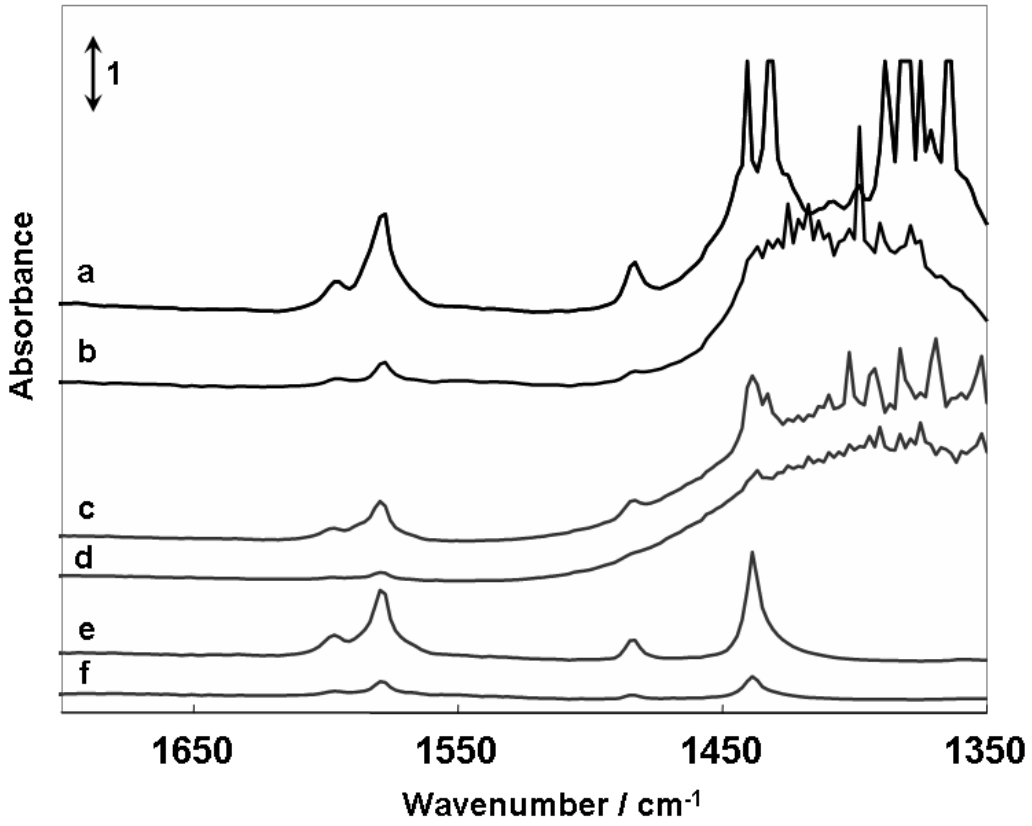

Fig 6.3: CO_2 IR Spectra for Cs-X, ZrB/Cs-X and Cs_2O /Cs-X evacuated at 100 and 250^oC

(a) Cs_2O/Cs-X evacuated at 100^oC.(b) Cs2O/Cs-X evacuated at 250^oC

(c) ZrB/Cs-X evacuated at 100^oC. (d) ZrB/Cs-X evacuated at 250^oC

(e) Cs-X evacuated at 100^oC. (f) Cs-X evacuated at 250^oC

6.1.4 IR Spectra of Pyridine

Figure 6.4 shows IR spectra of pyridine adsorbed on Cs-X, ZrB/Cs-X and Cs_2O /Cs-X evacuated at 473 and 523 K. No bands assigned to pyridinium ion were observed at 1540 cm^{-1} for both Cs-X and ZrB/Cs-X. No protonic acid sites exist on both catalysts. As compared the band intensity at 1580 cm^{-1} which is due to Lewis acid sites, the intensity was weaker for ZrB/Cs-X than for Cs-X. The band position, however, was the same for the two samples.

For Cs_2O/Cs-X, because of a strong band below 1450 cm^{-1} due to carbonate ion species, the band at 1450 cm^{-1} ascribed to pyridine coordinated to Lewis acid site was not observable for Cs_2O/Cs-X. Lack on the band at 1540 cm^{-1} for the catalyst indicated that no Brownsted acid sites are present on the catalyst. The spectral changes with evacuation temperature was the same when compared with Cs-X catalyst, indication that the acid sites were not changed by addition of Cs_2O to Cs-X. It should be noted that the acid sites which can retain pyridine against evacuation at 523 K exist on the surfaces of all the catalysts.

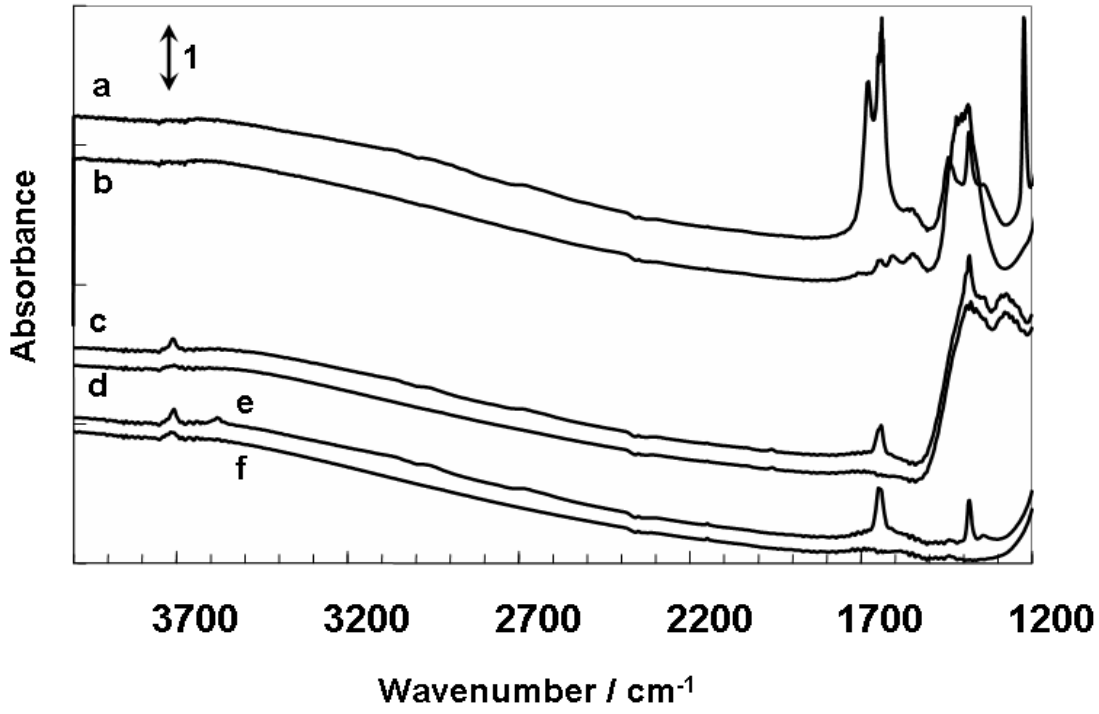

Fig 6.4: IR spectra of pyridine adsorbed on Cs-X, ZrB/Cs-X and Cs_2O /Cs-X evacuated at 200 and 250^oC.

(a) Cs2O/Cs-X evacuated at 200^oC.(b) Cs2O/Cs-X evacuated at 250^oC

(c) ZrB/Cs-X evacuated at 200^oC. (d) ZrB/Cs-X evacuated at 250^oC

(e) Cs-X evacuated at 200^oC. (f) Cs-X evacuated at 250^oC

6.2 Catalytic Activity

The catalytic activities of toluene alkylation with methanol at a temperature of 410^{o}C and molar feed ratio of toluene: methanol (6:1) over the catalysts are shown in Table 6.2.The experimental results showed that styrene and ethyl benzene are the major and main reaction products. Addition of ZrB to Cs-X enhanced both the catalytic activity of Cs-X and also increases the selectivity of styrene ,while the loading of Cs_2O on Cs-X increases the activity the most ,but selective towards ethyl benzene product.

Fig 6.5a and b shows the effect Cs_2O loading on Cs-X and the product selectivity respectively. Addition of Cs_2O to Cs-X enhanced the catalytic activity of Cs-X and reduced the selectivity to styrene as shown in Table 6.2. The optimum amount of Cs_2O addition was 2.1 wt %(Fig 6.5a). The activity of the catalyst containing 2.1 wt% Cs_2O was about twice as high as that of non-added Cs-X catalyst. Addition of 7.8 wt% Cs_2O resulted in a decrease in the activity. Unlike non-added Cs-X, Cs_2O/Cs-X produced much more ethyl benzene than styrene (Fig 6.5b).The higher the amount of loading, the higher the selectivity towards ethyl benzene. This can be attributed to the increase in the basicity of the active site of the catalyst, which facilitates the quick conversion of styrene to ethyl benzene [109, 36, and 109].

The effect of Cs_2O addition to Cs-X on the activity and selectivity observed in the present study were qualitatively similar to those reported in literature. All reported that addition of Cs_2O to Cs-X resulted in an increase in the activity and reduction of styrene selectivity, though no reports described the optimum amount of Cs_2O for the activity enhancement.

Table 6.2: catalytic activities of toluene alkylation with methanol at a temperature of 410^{o}C and molar feed ratio of toluene: methanol (6:1).

Catalyst	Methanol conv. (%)	Toluene conv. (%)	EB selectivity (%)	SM selectivity (%)	SM yield
Cs-X	36.80	1.50	13.80	86.20	1.30
ZrB/Cs-X	45.20	3.10	6.80	93.20	2.90
Cs_2O/Cs-X	65.44	3.41	89.60	10.40	0.36

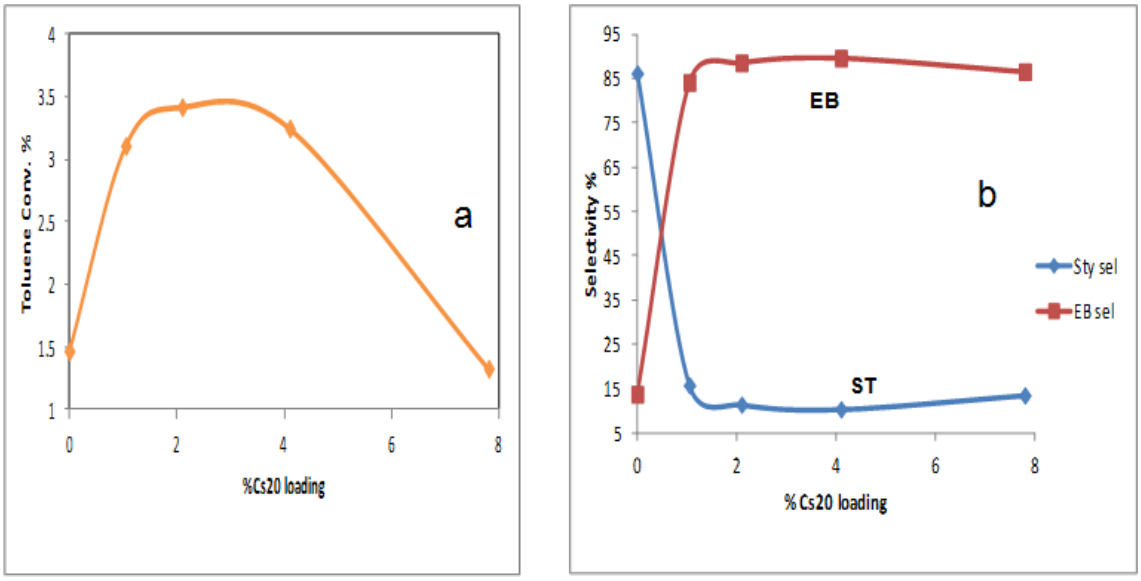

Fig 6.5: Effect of Cs_2O on the activity and product selectivity of Cs-X.a) Effect of Cs_2O loading on Toluene conversion. b) Effect of Cs_2O loading on product selectivity.

The effect of ZrB loading on Cs-X activity and product selectivity is shown in Figure 6.6 a and b.The addition ZrB did not only increases the activity of the catalyst, but also increased the selectivity towards styrene.10% loading of ZrB on Cs-X increases the toluene conversion by 52% (from 1.5% to 3.1%) (Fig 6.6a), above 10% loading the toluene conversion begins to diminish; this can be attributed to the pore blockage of the catalyst as a result of excess loading.

The selectivity of styrene was also increased from 86.2% to 93.2% at 10 % loading of ZrB and above that it begins to diminish (Fig 6.6b), making 10% loading the optimum.

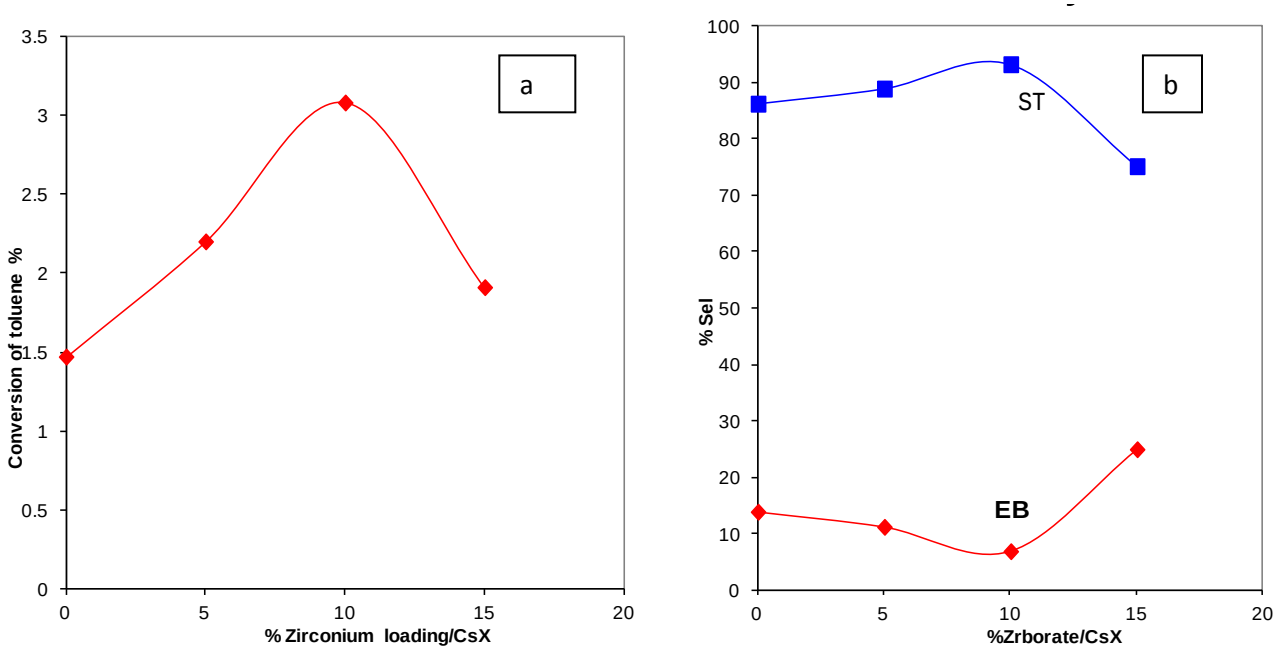

Fig 6.6: Effect of ZrB loading on the activity and products selectivity of Cs-X. (a) Effect of ZrB loading on Toluene conversion. (b) Effect of ZrB loading on product selectivity.

6.3 Effect of Toluene to Methanol Molar Feed Ratio on the Catalysts Activity

The toluene/methanol mole ratio influenced both activity and selectivity. Figures 6.7a and b show the variations of the activity and styrene selectivity, respectively, as a function of mole % of toluene in a feed for Cs_2O (4.1)/Cs-X, ZrB (10)/Cs_2O/Cs-X and Cs-X. The maximum activity was obtained at 33.3 toluene mole %, that is toluene/methanol = 1/2 for all the catalysts. The styrene selectivity, on the other hand, increased monotonically with toluene mole % for all the catalysts.

It should be pointed out that the attainable conversion of toluene does not reach 100% for the reaction with a feed in which toluene/methanol is higher than unity. Toluene should remain unreacted even after all methanol were consumed for the reaction with toluene. The attainable conversions for the feeds of toluene/methanol equal 1, 2, and 6 are 100, 33.3, and 16.7%, respectively.

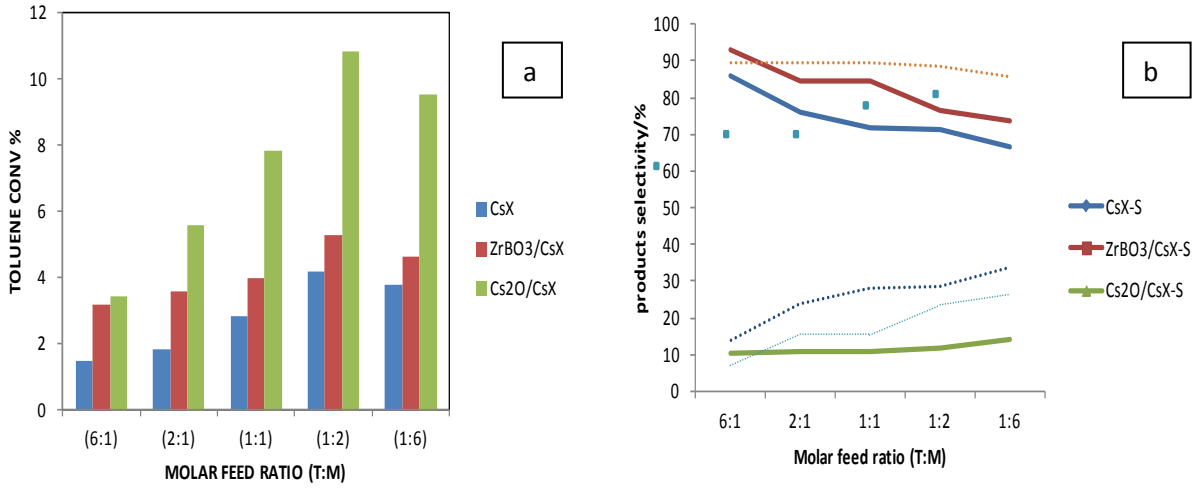

Figure 6.7: Effect of Toluene to Methanol Molar feed on Catalysts activity. Dashed lines represent EB selectivity and thick lines represent SM selectivity.(a) Effect of Molar feed ratio on Toluene conversion.(b) Effect of molar feed ratio on Products selectivity.

6.4 Effect of ZrB addition on the Activity and Products Selectivity of Cs_2O/Cs-X

The addition of ZrB increased the activity and styrene selectivity of Cs_2O/Cs-X. Figure 6.8(a and b) shows the variations of activity and styrene selectivity as a function of ZrB loading under the reaction conditions of toluene: methanol feed ratio of 6:1. The maximum activity was observed at ZrB loading of 10 wt%, while the styrene selectivity increased with the ZrB loading.

The effects of ZrB_2O_5 addition on the activity and selectivity were the same for Cs-X and Cs_2O/Cs-X; both activity and selectivity for styrene were enhanced by addition of proper amount of ZrB_2O_5. The activity of ZrB (10)/Cs_2O/Cs-X was the highest activity under the reaction condition of toluene: methanol feed ratio of 6, though the styrene selectivity was only 40 %. Concerning the styrene yield, the 14% addition of ZrB gave higher yield of styrene (2.4 %) than 10% addition of ZrB (2.1 %). The activity of ZrB added Cs-X was not so high as compared to that of ZrB added Cs-X/Cs_2O, but the styrene selectivity exceeded 90 % under the same reaction conditions. The role of ZrB in the reaction is not certain at present. It was reported that addition of B component suppressed the decomposition of methanol to H_2 and CO [39]. It was also reported that the addition of metal component together with B increased the activity [38]. We reported that the addition of metal components with B using metal borates was an effective way in addition of metal and B components to Cs-X. Among the metal borates, ZrB was most effective in promoting the activity and styrene selectivity for Cs-X based catalysts. Addition of ZrB had never been reported in the literature. In the present study on Cs_2O/Cs-X based catalysts, it was also revealed that ZrB was an efficient additive to Cs_2O/Cs-X.

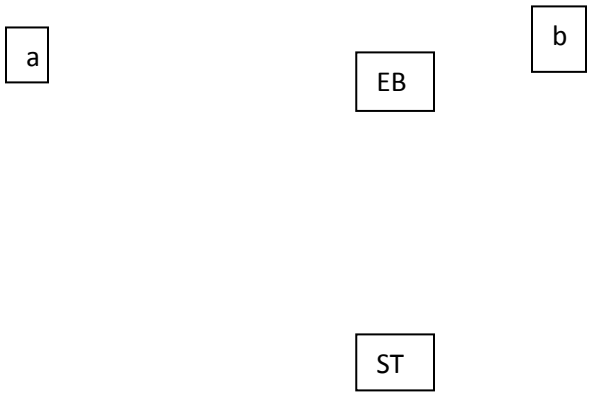

Fig 6.8: Effect of ZrB loading on the catalytic activity of Cs_2O/Cs-X. (a) Effect of ZrB loading on toluene conversion. (b) Effect of ZrB loading on products selectivity.

6.5 Acidity and Basicity of Catalysts

Although it was reported that balanced acidity and basicity are important for an efficient catalyst for side-chain alkylation of toluene, IR studies of adsorbed pyridine and CO_2 could not detect clear differences in acidity and basicity between Cs-X and ZrB/Cs-X. For pyridine adsorption study, only a small decrease in the band intensity was observed without change in the band position for 8a vibration mode (~1580 cm^{-1}). The band position reflected the strength of the interaction between pyridine and Lewis acid sites [110]. No change in the band position for Cs-X and ZrB/Cs-X indicated that the strength of Lewis acid sites is similar for both catalysts. A decrease in the band intensity is suggested to be due to a decrease in the number of Lewis acid sites by the addition of zirconium borate. This idea is consistent with a small decrease in the surface area for ZrB/Cs-X. The same thing can be said about basic sites. CO_2 was adsorbed as bidentate carbonate and the band position was the same for both samples. The only difference between two samples was the band intensity; the intensity was slightly weaker for ZrB/Cs-X than for Cs-X. It is suggested that the strength of basic sites is the same for both catalysts, and the number of basic sites was smaller for ZrB/Cs-X than Cs-X.

It should be noted that the discussion about acidity and basicity described above is applicable only to relatively strong adsorption sites. Because the spectra were measured after evacuation at a high temperature, the species retained on the surface should be adsorbed on strong adsorption sites. Spectra measured after evacuation at such a low temperature as weakly adsorbed species are retained on the surface may contain information about weak acid and base sites. However, distinct information about weak acid and base sites may be difficult to obtain because the band observed after evacuation at the low temperature contains information of all the sites. Isolation of the band due only

to weak sites could not be successful. The possibility cannot be excluded that addition of zirconium borate caused some changes in weak acidic and basic sites.

CHAPTER SEVEN

CONCLUSIONS AND RECOMMENDATIONS

7.1 Conclusions from Acidic Catalyst Methylation Studies

The bi-porous ZSM-5/MCM-41 composites with different porosity were synthesized and investigated for toluene methylation at different feed ratios. The meso porous AlMCM41 and ZM-3 showed overall lower toluene methylation even at optimum feed ratio of 1:1. Whereas composites particularly ZM-2 showed high toluene methylation with high xylenes production due to its optimum L/B ratio and bi-porosity. The formation of larger molecules such as TMBs and TeMB with excess methanol feed ratio can be attributed to the high reactivity of methanol and accessible active sites in the composites.

Kinetic study of toluene alkylation with methanol has been conducted over three different catalysts. The results show that toluene/MeOH molar ratio, pore structure and acidity of the zeolites influence the reaction pathway. Catalytic activity and selectivity towards alkylation of toluene was most significant on ZM-2 which is a composite of MCM-41 and ZSM-5. The reactivity of toluene alkylation is enhanced by the mesopority and medium strength acidity of the catalyst. Detailed kinetic data were obtained employing a fluidized bed reactor (riser simulator) for toluene/MeOH molar ratio 1:1. Power law model was used to evaluate the kinetic parameters based on time-on-stream (TOS) and reactant conversion (RC) catalyst decay function. Similar results were obtained

for both and deactivation due to coke deposit was accounted to be fairly minimal, but not negligible. The apparent activation energies of toluene methylation and disproportionation reactions on HZSM-5 have higher values compared to ZM-2 and MOR/ZSM-5. The order of activation energies for toluene methylation is HZSM-5 (56.1 kJ/mol) > MOR/ZSM-5 (20.8 kJ/mol) > ZM-2 (14.6 kJ/mol) whereas the order of toluene disproportionation is HZSM-5 (54.8) > ZM-2 (20.3) > MOR/ZSM-5 (13.1).

7.2 Conclusions from Basic Catalyst Methylation Studies

Toluene alkylation was studied over a number of combinatorial modified Cs-X catalysts, while ZrB increased both the catalytic yield and styrene selectivity; Cs_2O increased the catalytic activity of Cs-X but reduces the styrene selectivity. Other conclusive points include the following;

- Cs-X modified with zirconium borate showed the highest catalytic activity for styrene formation from toluene and methanol.
- Cs-X modified with metal borates showed a high selectivity for styrene relative to ethyl benzene, which is caused by a selective formation of formaldehyde from methanol.
- Mechanical mixing of Cs-X and metal borates followed by calcination is a good method to prepare Cs-X modified with metallic component and boron.
- The activity of side-chain alkylation of toluene with methanol is enhanced by addition of $Cs_2O$to Cs-X; optimum addition is 2.1wt% Cs_2O.
- The selectivity of ethyl benzene increases on addition of addition of $Cs_2O$to Cs-X.
- The enhancement of the activity and ethyl benzene formation are caused by generation of strong basic sites by Cs_2O addition; strong basic sites facilitate benzyl

anion formation from toluene and hydrogen formation from methanol.

- Addition of ZrB to Cs_2O/Cs-X results in enhancements of the activity and styrene selectivity, optimum loading of ZrB being 10 wt%.

7.3 Recommendations

- Kinetic modeling of the side-chain alkylation should be studied.
- Further mechanistic study should be done on the formation of ethyl benzene during side-chain alkylation of toluene with methanol.

NOMENCLATURE

C_i concentration of specie *i* in the riser simulator (mol/m^3)

CL confidence limit

E_i apparent activation energy of the *i*th reaction (kJ/mol)

k_i apparent rate constant for the *i*th reaction (m^3/kg of catalyst .s)

k_{oi} pre-exponential factor for the *i*th reaction after re-parameterization (m^3/kg of catalyst .s)

MW_i molecular weight of specie *i*

R universal gas constant (kJ/kmol K)

t reaction time (s)

T reaction temperature (K)

T_o average temperature of the experiment

V volume of the riser (45 cm^3)

W_c mass of the catalyst (0.81 g)

W_{hc} total mass of the hydrocarbon injected the riser (0.162 g)

y_i mass fraction of *i*th component

Greek Letters

φ apparent deactivation function

α catalyst deactivation constant (TOS model)

λ catalyst deactivation constant (RC model)

Abbreviations

Conv conversion

Sel. Selectivity

MeOH methanol

RC	reactant conversion
TMB	trimethylbenzene
TOS	time on stream
p-	para
o-	ortho
m-	meta
PS	Polystyrene
EPS	Expandable polystyrene
ABS	Acrylonitrile-butadiene-styrene
SBR	Styrene-butadiene rubber
UPR	Unsaturated polyester resins
SBL	Styrene-butadiene latex
OSD	Other SM related products

REFERENCES

[1] http://wiki.ask.com/Xylene

[2] Journal of Material Processing Tech., 194(2007), 89-92.

[3] http://www.ehow.com/facts_5999368_ortho-xylene-used-for_.html

[4] www.researchandmarkets.com/research/3a42cd/xylenes_global_mar

[5] http://www.yarnsandfibers.com

[6] http://www.tecnon.co.uk

[7] http://www.britannica.com

[8] http://survival-training.info/Library/Chemistry

[9] Hancock, E.G., ed.. Elsevier Scientific Publishing Company. New York, (1982).

[10]SRI International. Chemical Economics Handbook, April (1990).

[11] http://www.freepatentsonline.com

[12] Leonard.F;Thomas.D;Rammy.K;Annika.K;Francisca.M;Senior Design Projects,Department of Chemical and Biomolecular Engineering,University of Pennsylvania(2009).

[13] http://www.styrene forum.org

[14] http://www.chemsystems.com

[15] Tanabe, K; Hölderich, W.F; Appl. Catal. A Gen. 181 (1999) 399-434.

[16] www.dequi.eel.usp.br/~barcza/EstirenoUOP.

[17] Brownstein, A. M.,"Chem. Indus. Ser. 5," Moser, New York, (1981).

[18] Lange, J.P; Mesters, C.M.A.M;. Appl. Catal. A: Gen. 210 (2001) 247-255.

[19] H. Hattori, Heterogeneous basic catalysis. Chem. Rev. 95 (1995) 537-558.

[20] Dessau,Ralph m.(Edison ,NJ)US Patent 4851599,(1989).

[21] Venuto, P. B.; Hamilton, L. A.; Landis, P. S.; Wise, J. J. J. Catal. (1966), 4, 81-98.

[22] Zhu, Chen, Xie ,Yang , Li , , Micro porous and Mesoporous Materials 88 (2006) 16–21.

[23] http://osdir.com/patents/ 07084318,(2006).

[24] Ribeiro, F. R.; Alvarez, F.;Henriques, C.; Lemaos, F.; Lopes, J. M.; Ribeiro, M. F. J. Mol. Catal. A(1995), 96, 245-270.

[25] Martens, J. A.; Perez-Pariente, J.; Sastre, E.; Corma, A.; Jacobs, P. A. Appl. Catal. (1988), 45, 85-101.

[26] Yashima, T.; Ahamed, H.; Yamazaki, K.; Katsuka, M.; Hara, N. J. Catal. (1970), 16, 273-280.

[27] Wang, J. G.; Li, Y. W.; Chen, S. Y.; Peng, S. Y. Zeolites (1995), 15,288-292.

[28] Sidorenko, Y.N.; Galich, P.N.; Gutyrya, V.S.; Il'in, V.G.; Neimark, I.E. *Dokl. Akad. Nauk. SSSR* (1967), *173*, 132.

[29] Shreiber, E.H.; Rhodes, M.D.; Roberts, G.W. *Appl. Catal. B: Environmental (*1999), *23*, 9.

[30] Palomares, A.E.; Eder-Mirth, G.; Lercher, J.A. *J. Catal.* (1997), *168*, 442.

[31] Yashima, T.; Sato, K.; Hayasaka, T.; Hara, N. *J. Catal.* (1972), *26*, 303.

[32] Itoh, H.; Miyamoto, A.; Murakami, Y. *J. Catal.* (1980), *64*, 284.

[33] Kumari Vasanthy, B.; Palanichamy, M.; Krishnasamy, V. *Appl. Catal. A: General* (1996), *148*, 51.

[29] Shreiber, E.H.; Rhodes, M.D.; Roberts, G.W. *Appl. Catal. B: Environmental (*1999), *23*, 9.

[30] Palomares, A.E.; Eder-Mirth, G.; Lercher, J.A. *J. Catal.* (1997), *168*, 442.

[31] Yashima, T.; Sato, K.; Hayasaka, T.; Hara, N. *J. Catal.* (1972), *26*, 303.

[32] Itoh, H.; Miyamoto, A.; Murakami, Y. *J. Catal.* (1980), *64*, 284.

[33] Kumari Vasanthy, B.; Palanichamy, M.; Krishnasamy, V. *Appl. Catal. A: General* (1996), *148*, 51.

[34] Wieland W. S., Davis R. J., Garces J. M., *J. Catal.* (1998) 173, 490.

[35] Wieland W. S., Davis R. J., Garces J. M., *Catal. Today* (1996) 28, 443.

[36] Lacroix.C; Deluzarche.A; Kinnemann .A; Boyer .A; *Zeolites* (1984), 4, 109.

[37] Wang.X; Wang.G; Shen.D; Fu.C; Wei .M; *Zeolites*, (1991), 11, 254.

[38] Uniland M. L., Baker G. E., in *Catalysis in Organic reactions*, W. R. Moser (ed.) Marcel Dekker, New York, Basel, (1981) .

[39] Itoh H.; Hattori T.; Suzuki K.; Miyamoto A.; Mirakami Y.; *J. Catal.*, (1981) 72, 170.

[40] Itoh, H.; Hattori, T.; Suzuki, K.; Mirakami, Y.; *J. Catal.*, (1983) 79, 21-33.

[41] Archier, D.; Coudurier, G.; Naccache, C. In *Proceedings of the 9th International Zeolite Conference*, Montreal; Von Ballmoos, R., Higgins, J.B., and Treacy, M.M.J., Eds.; Butterworth-Heinemann: Boston, (1992) 2, 525-533.

[42] Hathaway, P. E.; Davis, M. E.; *J. Catal.* (1989) 119, 479

[43] Usachev, N. Ya.; Lapidus, A. L.; Usacheva, O. N.; Savel'yev, M. M.; Krasnova, L. L.; Minachev, Kh. M. *Petrol. Chem.* (1993) 33, 291.

[44] Guo, W. G.; Zhang, Z. W.; Liang, J.; Cai, G. Y.; Chen, G. Q. In *Proc. Int. Conf. Pet. Ref.Petrochem. Process* (1991) 3, 1459-1465.

[45] Guo, W. G.; Zhang, Z. W.; Liang, J.; Cai, G. Y.; Chen, G. Q.; Chin. Chem. Lett. (1993) 4, 873.

[46] Das, N. K.; Pramanik, K.; J. Indian Chem. Soc. (1997) 74, 701.

[47] Das, N. K.; Pramanik, K.; J. Indian Chem. Soc. (1997) 74, 705.

[48] Kaeding, W. W.; Chu, C.; Young, L. B.; Weinstein, B.; Butter, S. A. J. Catal. (1981), 76, 159.

[49] Aneke, L. E.; Gerritsen, L. A.; Van den Berg, P. J.; de Jong, W. A. J. Catal. (1979), 59, 2.

[50] Chang, C. D.; Silverstri, A. J. J. Catal. (1977), 47, 24.

[51] Ghosh,Ashim Kumar;US patent 7279608,(2007)

[52] Kaeding, W.W,Chu,C.Y,Weinste ,L.B,Butter ,S.A Journal of Catalysis, Vol. 67, pp. 159-174 (1981).

[53]Aboul-Gheit,K.;Aboul-Fotouh,M. ;Eman, A.;Sahar M. Ahmed, Journal of the Chinese Chemical Society, (2004), 51, 817-826.

[54] I Benito, A del Riego, M Martínez, C Blanco, C Pesquera, F Gonzalez Applied Catalysis A: General Volume 180, Issues 1–2, 19 April (1999), Pages 175–182.

[55] Chang,S.L ;Tae, J. P; Wha,Y.Lee ;Applied Catalysis A: General Volume 96, Issue 2, 26 (1993), Pages 151–161

[56] Odedairo,T; Balasamy,R.J and Al-Khattaf,.S, Ind. Eng. Chem. Res. (2011), 50, 3169–3183

[57] Camara, L.D.T; Rajagopal,K; Aranda, D.A.G;Stud. Surf. Sci.Catal. 139 (2001) 61.

[58] Ramakrishna, M.; Subhash, B.; Musti, S. R. Catalyst. *Ind. Eng. Chem. Res.* (1991), *30*, 281-286.

[59] Minachev, Kh.; Garanin, V. Molecular Sieve Zeolite-11. Adu. Chem. Ser. 1971, 102, 441-450.

[60] Streitwieser, A., J r . ; Reif, L. J .Am. Chem. SOC. (1964),86, 1988-1993.

[61] US Patent No. 7,321,072 B2

[62] Sidorenko, Yu.N.; Galich, P.N. *Petrol Chem.*(1991), *31*, 57.

[63] Rep, M.; Palomares, A.E.; Eder-Mirth, G.; Van Ommen, J.G.; Lercher, J.A. In *Proceedings of the DGMK-conference, Tagungsbericht 9903, Erlangen*; Emig, G.,Rupp, M., and Weitkamp, J., Eds.; DGMK: Hamburg, (1999); pp 279-286.

[64] Izmailova, I.I.; Corma, A. *J. Phys. Chem. B* (1997), *101*, 547.

[65] Blaszkowski, S.R.; Van Santen, R.A. *J. Phys. Chem. B* (1997), *101*, 2292.

[66] Corma, A.; Sastre, G.; Viruela, P. M. *J. Mol. Catal. A: Chem.* (1995), *100*, 75.

[67] Waghmode, S.B.; Bharathi, P.; Sivasanker, S.; Vetrivel, R. *Microporous Mesoporous Mater.* (2000), *38*, 433.

[68] Chang, C.D. In *ACS Symp. Ser.-Perspectives Molecular Sieve Science*; Flank, W.H., and Whyte, Jr., Th.E., Eds.; American Chemical Society: Washington, D.C., 1988; Vol. 368, pp 596-614.

[69] Mirth, G.; Cejka, J.; Lercher, J.A. *J. Catal.* (1993), *139*, 24.

[70] Mirth, G.; Lercher, J.A. *Idem* (1994), *147*, 199.

[71] Phillippou, A.; Anderson, M.W. *J. Am. Chem. Soc.* (1994), *116*, 5774.

[72] Miyamoto, A.; Iwamoto, S.; Agusa, K.; Inui, T. In *Acid-Base Catalysis*; Tanabe, K., Hattori, H., Yamaguchi, T.,and Tanaka, T., Eds.; Verlag Chemie: Weinheim, (1989); pp 497-504.

[73] Borgna, A.; Sepulveda, J.; Magni, S.; Apesteguía, C. In *Proceedings of the 12th International Congress on Catalysis, Granada*; Corma, A., Melo, F.V., Mendioroz, S., and Fierro, J.L.G., Eds.; Elsevier: Amsterdam, (2000); Vol. 130C, pp 2621-2626

[74] King, S.T.; Garces, J. *J. Catal.* (1987), *104*, 59.

[75] Garces, J..M.; Vrieland, G.E.; Bates, S.I.; Scheidt, F.M. *Stud. Surf. Sci. Catal.* (1985), *20*, 67.

[76] Bellat, J.P.; Simonot-Grange, M.-H., *Zeolite*s (1995), *15*, 124.

[77] de L a s a , H. U.S. Patent5,102,628, (1992).

[78] Pruski,J; Pekediz,A ; de Lasa,H; Chem. Eng. Sci. 51 (1996) 1799-1806.

[79] Kraemer,D.W ; Sedran,U ; de Lasa,H.I; riser Chem. Eng. Sci. 45 (1990) 2447–2452.

[80] Beck, J.S ; Vartuli, J.C ; Roth,W.J ; Leonowicz, M.E ; Kresge, C.T ; Schmitt, K.D ; Chu, C.T.U ; Olsen, D.H ; Sheppard, E.W ; McCullen, S.B ; Higgins, J.B ; Schlenker, J.L ; J.Am. Chem. Soc. 114 (1992) 10834.

[81] Song, C.M; Yan, Z.F; Asia-Pac. J. Chem. Eng. 3(2008) 275.

[82] Xia, Y.D; Mokaya, R.J; Mater. Chem. 14 (2004) 3427.

[83] Kleitz,F; Schmidt,W; Schuth, F; Micropor. Mesopor. Mater. 65 (2003) 1.

[84] Guisnet,M; Gnep,N.S; Morin, S; Patarin,J; Loggia,F; Solinas,V; Stud. Surf. Sci. Catal. 117 (1998) 591.

[85] Venuto, P.B; Landis, P.S;. Adv. Catal. 18 (1968) 259.

[86] Parry, E.P; *J. Catal.*, **2** (1963), p. 371

[87]Védrine, J.C; Auroux, A; Bolis, V;Dejaifve, P; Naccache, C; Wierzchowski, P; Derouane, E.G; Nagy, J.B; Gilson, J.P; van Hooff, J.H.C; van den Berg, J.P; Wolthuizen,J; J. Catal. 59 (1979) 248.

[88] Maijanen, A; Derouane, E.G; Nagy, J.B; Appl. Surf. Sci. 75 (1994) 204.

[89]Oliveira, A.C; Essayem, N; Tuel, A; Clacens, J.M; Tâarit, Y.B; Journal of Molecular Catalysis A: Chemical 293 (2008) 31–38

[90] Emeis, C.A; , J. Catal.141 (1993) 347–354.

[91] Baduraig, A; Odedairo,T ; Al-Khattaf, S;Top. Catal. 53 (2010) 1446-1456

[92] Jacobs, P. A. *Carboniogenic Activity of Zeolites*; Elsevier Sci. Publ. Co.: Amserdam, 1977.

[93] Mikkelsen, O; Ronning, P.O; Kolbo, S; Micro. Mesopor. Mater. (2000), 40**,** 95-113

[94] Serra, J.M.; Corma, A.; Farrusseng, D.; Baumes, L.; Mirodatos, C.; Flego, C.; Perego, C. Catal. Today, (2003), 81, 425 – 436.

[95] Agarwal, A. K; Brisk, M. L. *Ind. Eng. Chem. Process Des. Dev*. (1985), *24*, 203.

[96] Weekman, V. W. *Ind. Eng. Chem. Process Des. Dev*. (1968), *7*, 90-95.

[97] Al-Khattaf, S.S.; de Lasa, H.I.. Ind. Eng. Chem. Res, 2001, 40, 5398.

[98]Al-Khattaf S, Rabiu S, Tukur NM, Alnaizy R (2008) Chem Eng J 139:622

[99] Rabiu.S and Al-Khattaf.S; *Ind. Eng. Chem. Res.* (2008), *47*, 39-47

[100] Vinek, H.; Lercher, J. *J. Mol. Catal.* (1991), *64*, 23–39.

[101] Sotelo, J. L.; Uguina, M. A.; Valverde, J. L.; Serrano, D. P.. *Ind. Eng. Chem. Res.*(1993), *32*, 2548-2554.

[102] Mirth, G.; Lercher, J. A. J. Catal.1991, 132, 244–252

[103] Levenspiel, O. Chemical Reaction Engineering, 3rd ed.; John Wiley & Sons: New York, 1999.

[104] Zhu, Z; Chen, Q; Yang, D; Chen, W; Yu, G; Stud. Surf. Sci. Catal.138 (2001) 259.

[105] Walsh. D. E.; Rollmann, L. D. ***.J.*** *Catal*. (1979), 56, 195.

[106] Bhat, Y. S.; Halgeri, A. B.; Prasada Rao, T. S. R. *Ind. Eng. Chem. Res.* **1989**, *28*, 890-894

[107] Yagi, F.; Hattori, H. *Microporous Mater.* (1997), *9*, 247.

[108] Engelhardt.J; Szanyi.J; Valyon .J; J. Catal (1987),107,296

[109] Hathaway,P.E and Davis,M.E; J. Catal 1989,119,497

[110] Busca .G;Phys. Chem 1(1999)723-736.

VITAE

NAME: **Alabi, Wahab Olaiya**

NATIONALITY: **Nigerian**

DATE OF BIRTH: **December 2, 1982**

PLACE OF BIRTH: **Lagos State, Nigeria**

EDUCATION: **ND Electrical Electronics Engineering**

(Distinction)Osun State Polytechnic.

Iree, Nigeria. March, 2003.

B.Sc. Chemical Engineering

(2nd Class Upper Division).

Obafemi Awolowo University (O.A.U),

Ile-Ife, Osun State, Nigeria, 2008.

M.Sc.Chemical Engineering (Distinction)

King Fahd University of Petroleum and

Minerals, Dhahran, Kingdom of Saudi

Arabia, May 2012.

EMAIL ADDRESS: gistawo33@yahoo.com

wahabalabi@yahoo.com

CONTACT ADDRESS: 49, Olusesi Street, Ejigbo, Lagos State, Nigeria.

PHONE NUMBER: +966559129243.